The indosinian orogeny: A perspective from sedimentary archives of north Vietnam

Camille Rossignol, Sylvie Bourquin, Erwan Hallot, Marc Poujol, Marie-Pierre Dabard, Rossana Martini, Michel Villeneuve, Jean-Jacques Cornee, Arnaud Brayard, Françoise Roger

The indosinian orogeny: A perspective from sedimentary archives of north Vietnam

Camille Rossignol, Sylvie Bourquin, Erwan Hallot, Marc Poujol, Marie-Pierre Dabard, Rossana Martini, Michel Villeneuve, Jean-Jacques Cornée, Arnaud Brayard, Françoise Roger

PII: S1367-9120(18)30090-7
DOI: https://doi.org/10.1016/j.jseaes.2018.03.009
Reference: JAES 3438

To appear in: *Journal of Asian Earth Sciences*

Received Date: 8 September 2017
Revised Date: 9 March 2018
Accepted Date: 10 March 2018

Please cite this article as: Rossignol, C., Bourquin, S., Hallot, E., Poujol, M., Dabard, M-P., Martini, R., Villeneuve, M., Cornée, J-J., Brayard, A., Roger, F., The indosinian orogeny: A perspective from sedimentary archives of north Vietnam, *Journal of Asian Earth Sciences* (2018), doi: https://doi.org/10.1016/j.jseaes.2018.03.009

THE INDOSINIAN OROGENY: A PERSPECTIVE FROM SEDIMENTARY ARCHIVES OF NORTH VIETNAM

Camille Rossignol[a,b,*], Sylvie Bourquin[a], Erwan Hallot[a], Marc Poujol[a], Marie-Pierre Dabard[a,†], Rossana Martini[c], Michel Villeneuve[d], Jean-Jacques Cornée[e,f], Arnaud Brayard[g], Françoise Roger[e].

[a]*Univ Rennes, CNRS, Géosciences Rennes - UMR 6118, F-35000 Rennes, France*

[b]*Applied Isotope Research Group, Departamento de Geologia, Universidade Federal de Ouro Preto, MG 35400000, Brazil*

[c]*University of Geneva, Department of Earth Sciences, 13 rue des Maraîchers, 1205 Genève, Switzerland*

[d]*Centre Européen de Recherche et d'Enseignement des Géosciences et de l'Environnement, AMU, Centre St Charles, case 67, 3, Place Victor Hugo, 13331, Marseille, Cedex 03, France*

[e]*Géosciences Montpellier, Université de Montpellier, Place Eugène Bataillon, 34095 Montpellier Cedex 05, France*

[f]*Université des Antilles, Département de géologie, Campus de Fouillole, 97159 Pointe à Pitre Cedex Guadeloupe (FWI)*

[g]*Biogéosciences UMR6282, CNRS, Université Bourgogne Franche-Comté, 6 Boulevard Gabriel, 21000 Dijon, France*

[†]*Deceased*

camil.rossignol@gmail.com; sylvie.bourquin@univ-rennes1.fr; erwan.hallot@univ-rennes1.fr; marc.poujol@univ-rennes1.fr; rossana.martini@unige.ch; villeneuve@cerege.fr; jean-jacques.cornee@gm.univ-montp2.fr; arnaud.brayard@u-bourgogne.fr francoise.roger@gm.univ-montp2.fr.

**Corresponding author: Camille ROSSIGNOL*

Applied Isotope Research Group, Escola de Minas, Departamento de Geologia, Universidade Federal de Ouro Preto, Rua Diogo de Vasconcelos, 122 - Campus Morro do Cuzeiro, Ouro Preto 35400000, Minas Gerais, Brazil

E-mail: camil.rossignol@gmail.com

Abstract

The Triassic stratigraphic framework for the Song Da and the Sam Nua basins, north Vietnam, suffers important discrepancies regarding both the depositional environments and ages of the main formations they contain. Using sedimentological analyses and dating (foraminifer biostratigraphy and U-Pb dating on detrital zircon), we provide an improved stratigraphic framework for both basins. A striking feature in the Song Da Basin, located on the southern margin of the South China Block, is the diachronous deposition, over a basal unconformity, of terrestrial and marine deposits. The sedimentary succession of the Song Da Basin points to a foreland setting during the late Early to the Middle Triassic, which contrasts with the commonly interpreted rift setting. On the northern margin of the Indochina Block, the Sam Nua Basin recorded the activity of a proximal magmatic arc during the late Permian up to the Anisian. This arc resulted

from the subduction of a southward dipping oceanic slab that separated the South China block from the Indochina block. During the Middle to the Late Triassic, the Song Da and Sam Nua basins underwent erosion that led to the formation of a major unconformity, resulting from the erosion of the Middle Triassic Indosinian mountain belt, built after an ongoing continental collision between the South China and the Indochina blocks. Later, during the Late Triassic, as syn- to post-orogenic foreland basins in a terrestrial setting, the Song Da and Sam Nua basins experienced the deposition of very coarse detrital material representing products of the mountain belt erosion.

Keywords

Indochina Block; South China Block; Foreland basin; Foraminifers; Song Da Basin; Sam Nua Basin

1. Introduction

The present-day South-East Asia (SEA, Fig. 1A) comprises a collage of disparate continental blocks (i.e., mostly the South China, Indochina, Simao and Sibumasu blocks) and volcanic arcs (e.g., Ridd, 1971; Burrett, 1974; Metcalfe, 1988, 2011; Lepvrier et al., 2004; Ferrari et al., 2008; Faure et al., 2014; 2016; Burrett et al., 2014; Halpin et al., 2015). These blocks and arcs were mainly amalgamated together during the late Paleozoic – early Mesozoic, contributing to build up the present-day configuration of SEA.

Despite numerous recent studies focused on the SEA geodynamics (e.g., Carter and Clift, 2008; Cai J.-X. and Zhang K.-J., 2009; Metcalfe, 2011, 2013; Liu J. et al., 2012; Cocks and Torsvik, 2013; Burrett et al., 2014; Lai C.-K. et al., 2014; Halpin et al., 2015

and references therein), many aspects of the late Paleozoic – early Mesozoic SEA evolution remain debated. Among others, some controversies focus on the Indochina Block and the South China Block (SCB) that represent two major continental units of SEA. The divergences of opinion relate to the actual location of the ophiolitic boundary between these blocks, the timing of the initiation of the oceanic closure, the polarity of the involved subduction and the timing of the subsequent continental collision.

In northern Vietnam (Fig. 1B), a relative consensus prevails considering that the Song Ma Ophiolitic Suture Zone (SMOSZ) represents a segment of the boundary between the SCB and the Indochina Block (e.g., Ridd, 1971; Metcalfe, 1988, 2011; Lepvrier et al., 2008; Vuong et al., 2013; Faure et al., 2014; 2016, and references therein). The SMOSZ has been proposed to extend westward (Fig. 1A), up to the Ailaoshan Ophiolitic Suture Zone (e.g., Fan W. et al., 2010; Lai C.-K. et al., 2014; Roger et al., 2014; Faure et al., 2016) and to the Song Chay Ophiolitic Suture Zone (Lepvrier et al., 2011; Faure et al., 2014, 2016) before these distinct suture zones were offset by Cenozoic strike-slip sinistral displacements along the Ailaoshan - Red River Shear Zone (e.g., Leloup et al., 1995). A contrasting scenario, also involving sinistral displacements along the Ailaoshan - Red River Shear Zone, proposes an eastward prolongation of the SMOSZ up to the Dian-Qiong - Song Hien Suture Zone (Fig. 1A; Cai J.-X. and Zhang K.-J., 2009; Halpin et al., 2015).

A major debate about the geodynamic evolution of northern Vietnam concerns the closure of the oceanic domain that once separated the SCB from the Indochina Block and the continental collision that ultimately resulted from the closure. A Silurian-Devonian age has been suggested (Thanh et al., 1996; Findlay and Trinh, 1997; Thanh et al., 2011), but younger ages are also put forward. The collision has been thought to occur during the Carboniferous (e.g., Metcalfe, 2011, 2012). A diachronous collision, beginning

during the late Permian to the east and occurring during the Early to Middle Triassic to the west (present-day coordinates) has been suggested by Halpin et al. (2015). The collision has also been proposed to occur during the Early Triassic (e.g., Lepvrier et al., 2004, 2008; Kamvong et al., 2014), the Middle Triassic (e.g., Zhang R.Y. et al., 2013; Faure et al., 2014) or the Late Triassic (Liu J. et al., 2012; Roger et al., 2014). In addition, Carter et al. (2001) and Carter and Clift (2008) proposed that a Triassic thermo-tectonic event resulting from far field stresses reactivated an older suture zone between the South China and the Indochina blocks, forming an intracontinental orogen in north Vietnam. An alternative hypothesis, approaching that of an intracontinental orogeny, is favored by Fan W. et al. (2010) who invoked the closure of a continental back-arc basin that initially separated the SCB from the Simao-Indochina Block.

The vergence of the oceanic subduction that preceded the closure is also a matter of debate. Relative to the present-day coordinates, a northward-directed subduction of a slab attached to the Indochina plate has been proposed (e.g., Lepvrier, 2004, 2008; Nakano et al., 2010; Yan Q. et al., 2017). Alternatively, a slab attached to the South China plate and plunging southward beneath Indochina, is generally favored (e.g., Lepvrier et al., 2011; Liu J. et al., 2012; Vuong et al., 2013; Roger et al., 2014; Faure et al., 2014, 2016; Lai C.-K. et al., 2014; Shi M.-F. et al., 2015). All these contrasted interpretations bear important implications for the paleogeography of the east Tethyan domain during the late Paleozoic – early Mesozoic. It concerns notably the existence and the extent of an oceanic domain separating the SCB from the Indochina Block at that time.

The collision between the Indochina Block and the SCB, here referred to as the Indosinian orogeny, has been originally identified as a tectonic event marked by folds and nappes, sealed by an unconformity (e.g., Deprat, 1915, 1916; Blondel, 1929; Fromaget, 1929, 1934a) called the “Indosinian unconformity” (see Lacassin et al., 1998;

and Lepvrier et al., 2004, for a concise review). Sediments sealing this unconformity have been first attributed to the late Carboniferous ("Uralian" in the terminology used during the beginning of the XXth century; Deprat, 1915, 1916) but were later reattributed to the Late Triassic (e.g., Fromaget, 1929, 1934a). Additionally, at least two different Upper Triassic unconformities (a Norian and a Rhaetian one) were recognized during these pioneering works (e.g., Fromaget, 1934a). Then, an increasing number of late Paleozoic – early Mesozoic unconformities have been reported in northern Vietnam (Thanh, 2007). For instance, two Permian and four Triassic unconformities, excluding the one separating the Upper Triassic from the Lower Jurassic deposits, are evidenced in the Dien Bien Phu area (e.g., Tuyet et al., 2005b). Despite the importance of these unconformities as a record of the Indosinian orogeny, they remain poorly documented (Thanh, 2007). Particularly, the ages of these unconformities are not well constrained, because most of the sealing sedimentary rocks lack stratigraphic fossils (as noticed by Fromaget in 1934a). Therefore, the dating of these unconformities generally relies on the identification of reworked material in the sediments sealing the unconformities (e.g., Fromaget, 1934a) or on lithostratigraphic correlations. Such methods inescapably lead to doubtful dating and/or to large uncertainties on the ages of the unconformities (e.g., "upper Triassic to upper Cretaceous" was proposed for the Indosinian unconformity by Lacassin et al., 1998).

Besides the actual difficulty to obtain reliable age constraints, sedimentary basins are known to record the geodynamic evolution of their adjacent areas. The present study provides an updated Triassic stratigraphic framework for the Song Da and the Sam Nua basins, in order to discuss the overall geodynamic evolution for the Indochina Block and the SCB, as well as the Indosinian orogeny that resulted from their collision.

2. Geological setting

2.1. Regional setting

The Song Da and the Sam Nua basins are located to the south and the north, respectively, of the Nam Co – Song Ma Units (Fig. 1). The Song Ma Zone is composed by an ophiolitic mélange comprising lenses of serpentinized peridotite, gabbro, plagiogranite, diabase and basalt enclosed within metasedimentary rocks (e.g., Hutchison, 1975; Trung et al., 2006; Thanh et al., 2011; Liu J. et al., 2012; Vuong et al., 2013; Zhang R.Y. et al., 2014; Faure et al., 2014). Geochemical analyses indicate normal to enriched MORB affinities (e.g., Trung et al., 2006; Zhang R.Y. et al., 2013, 2014) or supra-subduction zone ophiolite affinities (Thanh et al., 2011) for the mafic rocks, attesting that the Song Ma Zone contains relics of an oceanic paleolithosphere. The age of the mafic protolith (i.e., the age of the oceanic crust) is contentious, but several radiometric results consistently point toward Carboniferous ages (Table 1; Vuong et al., 2013; Zhang R.Y. et al., 2013, 2014).

To the south of the Song Da Fault (Fig. 1B), the Nam Co Unit mainly comprises metasedimentary rocks metamorphosed under greenschist to amphibolite facies conditions (e.g., Zhang R.Y. et al., 2013; Faure et al., 2014) and exhibiting a NW-SE trending foliation (e.g., Findlay and Trinh, 1997; Lepvrier et al., 1997). Towards the southwest, both the Nam Co Unit and the Song Ma Zone experienced eclogite and high-pressure granulite facies metamorphism (Nakano et al., 2008, 2010; Zhang R.Y. et al., 2013) that formed during the Middle to the Late Triassic (Table 1). The metamorphic grade thus increases southwestward (Lepvrier et al., 1997; Faure et al., 2014). Structural evidences point to a top to the northeast shearing (Faure et al., 2014).

The Nam Co – Song Ma Units thus represent the internal zones of an orogen that developed as a result of the collision between the Indochina Block and the SCB (e.g., Faure et al., 2014). The ophiolites of the Song Ma Zone mark the boundary between the Indochina Block to the south and the SCB to the north. The Sam Nua Basin is consequently located on the northern margin of the Indochina Block, while the Song Da Basin belongs to the SCB.

2.2. Song Da Basin

2.2.1. Tectonic setting

The Song Da Basin, as defined by Tri and Khuc (2011), is an elongated, NW-SE trending basin, delineated by the Song Da Fault to the south, the Song Chay Fault to the north and the Dien Bien Phu Fault to the west (Fig. 1B). The western termination of the basin is masked by Quaternary alluvial deposits from the Red River (e.g., Thanh and Khuc, 2012). The present-day fault boundaries do not reflect the initial geometry of the basin but correspond to Cenozoic, mostly strike-slip faults that reactivated Triassic structures (e.g., Lepvrier et al., 2011; Roger et al., 2014).

The basement of the Song Da Basin is heterogeneous and includes various Archean (Lan C.-Y. et al., 2001) to Permian (e.g., Tri and Khuc, 2011; Thanh and Khuc, 2012) metamorphic and sedimentary rocks. The Song Da Basin is classically interpreted as a continental rift, sometimes referred to as the Song Da – Tu Le Rift (e.g., Shi G.R. and Shen S.-Z., 1998; Golotov et al., 2001; Balykin 2010; Anh et al., 2011; Tri and Khuc, 2011; Metcalfe, 2012; Hieu et al., 2013, 2017; Tran et al., 2015). The extension of the

lithosphere associated with the rift formation has been proposed to evolve up to the formation of an oceanic lithosphere within the Song Da Basin (Liu J. et al., 2012).

The interpretation of a rift setting for the Song Da Basin mostly relies on the occurrence of alkaline basalts (e.g., Golotov et al., 2001) and granitoids (e.g., Hieu et al., 2013), typical of the early stages of development of continental rifts. Alkaline basalts are frequently interbedded within the late Permian carbonate and terrigenous sediments corresponding to the Cam Thuy, Vien Nam and Yen Duyet formations (e.g., Thanh and Khuc, 2012; Fig. 2). The geochemical characteristics of these volcanic rocks (e.g., Hanski et al., 2004; Balykin et al., 2010; Rossignol, 2015) relate them to the Emeishan Large Igneous Province (ELIP). Accordingly, the rift is commonly regarded as a local manifestation of the intracontinental emplacement of the ELIP (e.g., Shellnutt et al., 2008; Hoa et al., 2008; Tran et al., 2015). Alternatively, upper Permian to Lower Triassic peralkaline and peraluminous granitoids, located to the north of the Song Da Basin (Fig. 1; Table 1), have been interpreted as intraplate magmatism in a back-arc setting (Zelazniewicz et al., 2013).

2.2.2. Stratigraphic framework

The Cam Thuy and Vien Nam formations (Fig. 2) rest unconformably on the basement of the Song Da Basin. These formations mainly comprise volcanic rocks related to the ELIP (Rossignol, 2015), volcaniclastic rocks and limestone lenses. A marine fauna, including foraminifers (Appendix 1; Fig. S1), has been found in the limestone layers and indicates a marine depositional environment during the Wuchiapingian (Tri and Khuc, 2011; Thanh and Khuc, 2012; Fig. 2). This age is relatively coeval with the emplacement age of the ELIP (e.g., Shellnutt et al., 2012).

The Yen Duyet Fm. (Fig. 2) overlies conformably the Cam Thuy Fm. and is composed of different sedimentary rocks including limestone, shale, volcaniclastic rocks, siltstone, sandstone, coal and paleosoils (Shi G.R. and Shen S.-Z., 1998). The latter suggests a terrestrial depositional environment. However, the formation also yielded a rich marine fauna, (Shi G.R. and Shen S.-Z., 1998; Tri and Khuc, 2011; Metcalfe, 2012; Thanh and Khuc, 2012; Appendix 1), indicating a marine setting during the Changhsingian.

The Co Noi Fm. (Fig. 2) overlies, probably unconformably, older formations (Thanh and Khuc, 2012). However, its exact stratigraphic relationship with the underlying formations remains unclear (Tri and Khuc, 2011 – see the section 4.2. of this study). The Co Noi Fm. comprises terrigenous detrital sediments, with a minor amount of carbonates and volcaniclastic material (Tri and Khuc, 2011; Thanh and Khuc, 2012). Various fossils, including bivalves, ammonoids, gastropods and echinoderm remains indicate deposition during the Early Triassic in a marine environment. More precise depositional environment is contentious. The Co Noi Fm. is indeed supposed to correspond to turbiditic series (Faure et al., 2014), while Huyen et al. (2004) favor estuarine series followed by increasing marine influences in the upper part.

The Co Noi Fm. is conformably overlain by the Dong Giao Fm. (Fig. 2), which comprises limestones containing brachiopods, bivalves, ammonoids (Tri and Khuc, 2011; Thanh and Khuc, 2012; Appendix 1), foraminifers and stromatolites (Martini et al., 1998). These fossils indicate a shallow marine environment during the Anisian (Martini et al., 1998; Tri and Khuc, 2011; Thanh and Khuc, 2012). However, foraminifer biostratigraphy suggests that the deposition of the Dong Giao Fm. may have initiated as early as the Early Triassic (Martini et al., 1998).

The hemipelagic marls, siltstones and claystones of the Nam Tham Fm. (Fig. 2) overlie the Dong Giao Fm. (Tri and Khuc, 2011; Thanh and Khuc, 2012; Appendix 1). The Nam Tham Fm. also comprises subordinate limestones and sandstones, and contains bivalves and ammonoids indicating a Ladinian age (Tri and Khuc, 2011; Thanh and Khuc, 2012; Appendix 1).

The Song Boi Fm. (Fig. 2) contains a basal conglomerate resting unconformably on the older formations, followed by sandstones, siltstones and shales (Tri and Khuc, 2011; Thanh and Khuc, 2012). Bivalves (Thanh and Khuc, 2012) and ammonoid fossils (Tri and Khuc, 2011) indicate a marine depositional environment and an early Norian age, (this work, Appendix 1; Fig. S1).

Above, the unconformable Suoi Bang Fm. (Fig. 2) comprises a basal part consisting mainly in detrital terrigenous sediments and containing bivalves, brachiopods and ammonoids (Son et al., 2005; Tri and Khuc, 2011; Thanh and Khuc, 2012; Appendix 1). The upper part of the formation is composed of sandstones and siltstones interbedded with coal seams and containing brackish-water bivalves and plant fossils, to which a “sub-continental” depositional environment is attributed (Tri and Khuc, 2011; Thanh and Khuc, 2012). On the basis of its paleontological content, structural relationships with other dated units and regional lithostratigraphic correlations, this formation is regarded as Norian - Rhaetian (Son et al., 2005) or as late Norian - Rhaetian in age (Tri and Khuc, 2011; Thanh and Khuc, 2012; Appendix 1). The plant fossil assemblage described from this formation (Tri and Khuc, 2011; Thanh and Khuc, 2012) suggests that the deposition occurred, at least in part, during the Rhaetian and/or the Early Jurassic (this work, Appendix 1; Table S1).

2.3. Sam Nua Basin

2.3.1. Tectonic setting

The Sam Nua Basin (Fig. 1) is delimited to the south by the Song Ca Fault, to the north by the Song Ma Fault and to the west by the Dien Bien Phu Fault, constituting an elongated NW-SE trending basin. As for the Song Da Basin, the present-day boundaries do not reflect the initial geometry of the basin, but correspond to younger deformations along strike-slip faults (e.g., Jolivet et al., 1999; Roger et al., 2014; Wen S. et al., 2015) offsetting the Permian and Triassic structures.

The basement of the Sam Nua Basin comprises Neoproterozoic to late Cambrian metasedimentary rocks that underwent high-grade metamorphism, and of late Silurian to Early Devonian metasedimentary rocks of lower grades, although strongly deformed (e.g., Tri and Khuc, 2011). Two contrasted interpretations are proposed to explain the formation of the Sam Nua Basin, both relying on the geochemical characteristics of calk-alkaline volcanic rocks interbedded with the sedimentary rocks infilling the basin.

The calk-alkaline volcanism is classically attributed to a late orogenic magmatic activity, and thus points toward a late orogenic extensional setting (e.g., Lepvrier et al., 2004; Hoa et al., 2008; Tri and Khuc, 2011). More recently, the same calk-alkaline magmatic rocks have been interpreted as being emplaced in an arc setting (Liu J. et al., 2012; Faure et al., 2014; Shi M.-F. et al., 2015). In such a case, the Sam Nua Basin represent a foreland basin, located above an active subduction zone, in a convergent setting.

2.3.2. Stratigraphic framework

Deposition in the Sam Nua basin initiated with the Dong Trau Fm. (Fig. 3; Son et al., 2005; Tri and Khuc, 2011; Thanh and Khuc, 2012), that rests unconformably on a Proterozoic basement (Son et al., 2005). The Dong Trau Fm. is mainly composed of volcaniclastic material (Tri and Khuc, 2011; Thanh and Khuc, 2012) with interbedded calk-alkaline volcanic rocks (Trung et al., 2007; Shi M.-F. et al., 2015; Rossignol, 2015). The depositional environment is poorly constrained as both marine (ammonoids, bivalves, brachiopods; e.g., Son et al., 2005) and terrestrial (plant remains; Thanh and Khuc, 2012) fossils have been described in the formation. Based on its paleontological content, an Anisian age (247.2 to 242 Ma) is attributed to the Dong Trau Fm. (Son et al., 2005; Tri and Khuc, 2011; Thanh and Khuc, 2012; Appendix 1, section 2). However, Rb-Sr radiometric dating (whole rock isochron method) of altered volcanic rocks yielded a date of 218 ± 10 Ma (Trung et al., 2007; Fig. 3), which is inconsistent with the index fossils found in this formation. As the Rb-Sr isotopic system is prone to resetting during alteration, this age must be considered with caution. Also in contradiction with an Anisian age, a rhyolite collected in the southeastern part of the Sam Nua Basin (Fig. 1A), yielded a late Permian to Early Triassic age (251.9 ± 1.7 Ma, U-Pb dating on zircon, Shi M.-F. et al., 2015; Fig. 3). Furthermore, the Dong Trau Fm. is crosscut by the Song Ma Granite (Son et al., 2005), emplaced between 263 ± 5 Ma and 239 ± 6 Ma (Hieu et al., 2017). The oldest intrusion age, at 263 ± 5 Ma (Fig. 3), indicates that the deposition of the Dong Trau Fm. could have actually started before 263 ± 5 Ma, during the middle to the late Permian (Fig. 3). There are therefore important discrepancies between the Anisian biostratigraphic age inferred from the fossil content of the Dong Trau Fm. (Son et al., 2005; Tri and Khuc, 2011; Thanh and Khuc, 2012; Appendix 1) and ages obtained from structural and geochronological evidences (Fig. 3).

Above the Dong Trau Fm., the Hoang Mai Fm. (Fig. 3) is composed of limestones containing a marine fauna. These fossils give an Anisian age for this formation (Tri and Khuc, 2011; Thanh and Khuc, 2012; Appendix 1). Both formations are unconformably overlain by the Suoi Bang Fm., which also occurs in the Song Da Basin.

3. Methodology

3.1. Field investigations and sampling

We surveyed 4 areas in the Song Da Basin, including, from the southeast to the northeast: the Ninh Binh (Fig. 4A), Muong Khen (Fig. 4B), Mai Son (Fig. 4C) and Banh Hinh (Fig. 1B) areas, and the Sop Cop area (Fig. 5) in the northern part of the Sam Nua Basin. Field investigations were undertaken with two main objectives: (*i*) reconstruction of the depositional environments and (*ii*) sampling (see Appendix 2 for coordinates) for dating purposes using biostratigraphy (foraminifers) or U-Pb detrital zircon geochronology of sedimentary rocks to get maximum depositional ages.

Where feasible, sedimentological sections were described at the scale of 1:100. Interpretation of raw sedimentological data was undertaken using sedimentological analysis (facies analysis, petrographic study, paleontological content description, etc.). The results were then integrated in order to reconstruct each individual depositional environment.

Limestone samples have been collected from the best-preserved portions of the outcrops avoiding, as much as possible, recrystallized and fractured lithologies. The microfacies and biostratigraphic analyses in this work rely on the observation of more than a hundred thin sections under transmitted light. Some samples were also observed

using catholuminescence (CL) microscopy to reveal both specific sedimentological features and microfossils invisible in transmitted light (Appendix 3). The microfacies were determined according to the sedimentary components and textures using the classification of Dunham (1962), supplemented by Embry and Klovan (1971).

3.2. U-Pb zircon geochronology

3.2.1. Analytical methods

The zircon grains were extracted following a classical mineral separation procedure. They were handpicked under a binocular microscope to produce the most representative sampling, with the aim to avoid intentional bias (see, however, Slama and Kosler, 2012 and Malusa et al., 2013, and references therein). Zircon grains were then imaged by CL prior to be analyzed by Laser Ablation – Inductively Coupled Plasma – Mass Spectrometry (LA-ICP-MS) in the Géosciences Rennes laboratory (see Appendix 3 for more information).

3.2.2. Data filtering, maximum age calculations and detection limits

A two-step procedure has been applied to derive maximum depositional ages from sedimentary rock samples. The first step consisted in filtering the data based on their probability of concordance (Ludwig, 1998; Nemchin and Cawood, 2005), calculated using the relevant function in Isoplot/Ex 3.00 (Ludwig, 2012) and including decay constant errors. The cut-off level applied to filter the data was 10% (e.g., Nemchin and Cawood, 2005; Rossignol et al., 2016). Hereafter, concordant analyses refer to those exhibiting a probability of concordance ≥ 10%.

Concordant analyses were kept for the second step that consists in calculating the maximum depositional age using the youngest cluster of at least 3 grains overlapping in age at 2 σ (standard deviation), as proposed by Dickinson and Gehrels (2009), to ensure a statistically robust estimate of the maximum depositional age. Maximum depositional ages were calculated as the concordia age (Ludwig, 1998) of these youngest clusters using Isoplot/Ex 3.00 (Ludwig, 2012) and are provided with 95% confidence limits. Hereafter quoted dates are concordia ages.

To assess the representativeness of the filtered data sets, the detection limits (i.e., the relative proportions, expressed as the percentages of the largest population of zircon grains that are likely to remain undetected at a given confidence level; Andersen, 2005) are provided. Detections limits, calculated following Andersen (2005) and Rossignol et al. (2016), are provided for 1 grain and 3 grains at the 50% and 95% confidence levels.

4. Stratigraphy of the Song Da Basin

4.2. Co Noi Formation

4.2.1. Sedimentological analyses

Description. In the Ban Hinh area (Fig. 1B), the formation shows a clear unconformable relationship with the underlying volcaniclastic rocks of the Cam Thuy Fm. (Fig. 6A to C). The outcrop exposure was large enough to realize a sedimentological section for the basal beds of the Co Noi Fm. (Fig. 7).

Three main facies occur in the Co Noi Fm. at the Ban Hinh locality (Fig. 6A to C and Fig. 7), including two conglomerate facies (Gt, Gh; Table 2) and one sandstone facies (Sh; Table 2). The Gt facies, at the base of the formation, is mainly made up of large (up to 20 cm in diameter), well-rounded boulders displaying a large range of volcanic lithology, with mainly basaltic boulders and subordinate andesitic to rhyolitic pebbles. The Gh and Sh facies are composed of clasts displaying finer grain-sizes, ranging from gravel to pebble (Gh facies) and sand (Sh facies), showing similar lithologies to those exhibited by the clasts within the Gt conglomerates. Occurrence of quartz and epidote veins (Fig. 6A and 6B) indicates that these rocks underwent a greenschist facies metamorphism in this area.

In the other studied localities, the outcrop exposures were too limited to make sedimentological section. Alternating siltstone and fine-grained, bioturbated, sandstone layers with ripple marks crop out in the area of Mai Son (red circled capital letter C in Fig. 1B; Fig. 4C). In the Muong Khen area (red circled capital letter B in Fig. 1B; Fig. 4B), the Co Noi Fm. consists of sandstones exhibiting trough cross-stratification (facies St, Table 2). Unidentifiable plant remains were also found in fine sandstone to siltstone deposits of the Muong Khen area.

Petrographic investigations (Fig. 6D, E and F and Table 3) indicate that the Sh facies sandstones are lithic arenites, mainly made up of poorly sorted, sub-angular to sub-rounded rock fragments. These fragments originate from the reworking of magmatic (granular, microgranular and weathered microlitic textures) and sedimentary rocks (sparitic limestone, siltstone). From one locality to another, the sandstones present variable feldspar contents, the feldspar being commonly weathered with a sub-angular shape. In some localities, these sandstones classify as feldspathic arenites.

Monocrystalline quartz grains, generally well-rounded, opaque minerals, chlorite, epidote and zircon also occur in these arenites.

Interpretation. The depositional environment of the Co Noi Fm. corresponds to a distal braided plain with megaripple migration (Gt, St) and unconfined flow (i.e., sheetflood tabular bed, Sh, Gh). At stratigraphically higher positions (localities of Mai Son and Muong Khen), the deposits of the Co Noi Fm. are indicative of more distal and less energetic depositional environments such as flood plain or lacustrine settings.

The Early Triassic age attributed to the Co Noi Fm. (Tri and Khuc, 2011; Thanh and Khuc, 2012) is mainly based on marine fossils (e.g., ammonoids, Appendix 1). However, our results from the sedimentological analysis indicate a terrestrial paleoenvironment, implying that marine fossils cannot provide a reliable depositional age for theses terrestrial deposits.

4.2.2. Geochronological analyses

Sample VN 12-14. The sample is a lithic arenite from the Muong Khen locality (Fig. 4B). It yielded a large number of zircon crystals that are mainly sub-rounded to sub-angular, with a few euhedral grains. In reflected light, the grains display a pale pinkish color and show very contrasted brightness in CL, some grains having a strong CL intensity while others are nearly non-luminescent. A total of 110 analyses on 104 grains were performed (Fig. 8A). Thirty-three grains (34 analyses) are concordant, resulting in detection limits ranging from 2.1% for the $DL_{1(pL=0.5)}$ to 17.9% for the $DL_{3(pL=0.95)}$ (Table 4). The Th/U ratios, ranging from 0.40 to 5.24, are compatible with a magmatic origin (e.g., Rubatto et al., 2002).

The youngest cluster of grains from this sample gives a concordia date of 243.1 ± 2.3 Ma (n=6, MSWD=0.86, probability=0.58), which is interpreted as the maximum depositional age for this lithic arenite (Fig. 8B). Most of the other concordant dates spread continuously from the maximum depositional age up to 274.0 ± 6.5 Ma (Fig. 8A), and the age distribution of this sample is centered on ca. 255 Ma (Fig. 9A). A unique grain yielded a concordant date of 219.8 ± 6.5 Ma that is younger than the retained maximum depositional age, suggesting that the deposition of the sediment could be younger (Fig. 8A and Fig. 9A). However, as only one grain gives a date of ca. 220 Ma (that possibly results from a Pb loss) and as no separate aliquot have been analyzed to test reproducibility, the statistical requirements are not met to confidently consider this date as a maximum depositional age for the sample.

Sample VN 12-22. It is a feldspathic arenite from the Mai Son locality (Fig. 4C). A large number of zircon grains, displaying rounded to euhedral shapes, were extracted from this sample. In CL, most of the grains have a very faint brightness, and a few grains show patchy luminescence. A total of 103 analyses from 102 grains were performed. Thirty-one grains are concordant (Fig. 8C), resulting in relatively low detection limits, ranging from 2.2% for the $DL_{1(pL=0.5)}$ to 19.0% for the $DL_{3(pL=0.95)}$ (Table 4). The Th/U ratios, ranging from 0.30 to 1.67, suggest a magmatic origin for these grains.

The youngest cluster from this sample gives a concordia date of 237.3 ± 2.4 Ma (n=5, MSWD=1.12, probability=0.35), interpreted as the maximum depositional age (Fig. 8D). The other concordant dates are older and spread from the maximum depositional age up to 273.2 ± 6.3 Ma (Fig. 9B). The age distribution of this sample is unimodal and centered on ca. 250 Ma (Fig. 9B).

Sample VN 12-51. This lithic arenite was sampled at the Ban Hinh locality (Fig. 1B), ca. 10 m above the unconformity with the Cam Thuy Fm. (Fig. 7). A very limited number of zircon grains (4), showing patchy luminescence brightness in CL, were extracted from the sample and only two are concordant, resulting in very high detection limits ($DL_{1(pL=0.5)}$ = 29.3%; $DL_{1(pL=0.95)}$ = 77.6%; Table 4). The Th/U ratios, ranging from 0.54 to 0.93, suggest a magmatic origin for these grains.

Repeated analyses on the grains extracted from this sample (Fig. 8E) allowed to obtain 2 concordant analyses on 2 grains, defining a concordia date of 242.6 ± 4.1 Ma (MSWD=0.74, probability=0.53). This date is interpreted as the maximum depositional age for this sample (Fig. 8F and Fig. 9C), although the statistical requirement of minimum 3 grains in the cluster is not met. However, despite relying on only two grains, this age is equivalent to the maximum depositional ages obtained from the other samples of the Co Noi Fm.

4.3. Dong Giao Formation

4.3.1. Sedimentological analyses

Description. The Dong Giao Fm. includes the main limestone rocks resting upon the aforementioned Co Noi deposits. The limestones are very thick and underwent moderate deformation in the Ninh Binh area (Fig. 4A). The sedimentary succession begins with 350 m of bioclastic black micrites, covered by 150 to 200m of grey carbonate rocks containing oncoids and 50m of white bioclastic limestone. This succession is in turn capped by a 150m thick grey to black limestone with ripple and sole marks (Fig. 10).

A detailed investigation allowed to define six members (*a*, *b*, *c*, *d*, *e* and *f*; Fig. 10) within the Dong Giao Fm. in the Ninh Binh area. To the base, the member *a* consists of finely laminated black mudstone showing, locally, bioturbations and microbialitic structures (Martini et al. 1998). Ghosts of small benthic foraminifers also occur as well as gastropod lumachelles. The overlying member *b* comprises homogeneous black mudstone characterized by remnants of Dasycladacean algae (*Teutloporella*?), strongly recrystallized. The member *c* contains gray to dark gray homogeneous mudstone. Subordinate are wakestone to packstone and packstone to grainstone with abundant peloids, oncoids and various organisms, such as gastropods, bivalves, ostracods and foraminifers. Member *d* is represented by gray grainstone with oncoids and peloids. Less abundant are ostracods, fragments of algae and foraminifers. Member *e* is dominated by white to grey bioclastic packstone, subordinately wackestone and grainstone. Skeletal grains are foraminifers, remnants of echinoderms, bivalves and ostracods. The uppermost member of the formation, member *f*, comprises boundstone to rudstone limestones. The boundstone displays either a thrombolytic facies, in which only some badly preserved foraminifers occur, or micropeloidal facies rich in foraminifers. The rudstone is composed by large ossicles of echinoderms, serpulids, bryozoans, algae, as well as fragments of sponges, bivalves and ostracods, in a micropeloidal matrix.

Interpretation. The lithological characteristics and microfacies of the examined samples indicate that the limestones originated on a wide shallow water carbonate shelf, under low energy conditions. The presence of rudstone and boundstone facies, together with the absence of reefal builder organisms (e.g., corals and sponges), suggests deposition on a carbonate ramp located in a marginal basin that underwent a rapid subsidence,

where algal buildups locally developed. An evolution from intertidal, rarely supratidal, to subtidal conditions is observed from the base to the top of the Dong Giao Fm.

4.3.2. Foraminifers

In the Dong Giao Fm., the foraminifers are mainly present in the upper part of the succession. They have been found in packstone and grainstone facies but also occur in boundstones. The generally well-preserved foraminiferal association is of low diversity, and characteristic of all the studied outcrops in the Song Da area, where limestones crop out.

Among the porcelaneous forms, *Citaella dinarica* (former *Meandrospira*) is the most distinctive and abundant species (samples V95; Fig. 11A and 11B) whereas *Postcladella* sp. (former *Cornuspira*) (samples V140; V143; Fig. 11C, 11D and 11E) and *Hoyenella* gr. *H. sinensis* (sample V144) are rare. The association also contains *Endotriada tyrrhenica* (sample V78; Fig. 11F and 11G), a species with an agglutinated wall. This foraminiferal association confirms the Anisian age already proposed by Martini et al. (1998). Particularly, *Citaella dinarica* is indicative of the Middle Anisian (Pelsonian – ca. 244.3 Ma to ca. 243.1 Ma; Li M. et al., 2018) as reported by many authors in the Tethyan domain (Rettori 1995; Kobayashi et al. 2006 and references herein), as well as in east and southeast Asia: Malaysia Peninsula (Gazdzicki and Smit, 1977; Vachard and Fontaine 1988); north Vietnam (Martini et al. 1998); south China (Lin, J. X. and Zheng Y.M, 1978; He Y., 1984) and in Japan (Kobayashi 1996; Kobayashi et al., 2005, 2006). The Dong Giao Fm., older than ca. 243 Ma, conformably overlies the Co Noi Fm. (e.g., Tri and Khuc, 2011; Thanh and Khuc, 2012; Fig. 2), which gave maximum

depositional age of 237.3 ± 2.4 Ma, resulting in a deposition age contradiction (see discussion).

5. Stratigraphy of the Sam Nua Basin

5.1. Dong Trau Formation

5.1.1. Sedimentological analyses

Description. The Dong Trau Fm. unconformably lies on a high-grade metamorphic basement that is crosscut by doleritic dykes (Fig. 12A), as previously reported by Fromaget (1934b). The Dong Trau Fm. is strongly deformed (faulted and folded, Fig. 12B). The main facies were identified, but no reliable sedimentological log can be provided. The formation is mainly composed of fine-grained siltstones, sometimes intercalated with marls and coarse-grained volcaniclastic sandstones. The siltstones display planar stratifications, which may locally be disturbed by decimetric volcanic bombs (Fig. 12C), and contain a few unidentified plants remains and bivalves. Sometimes, the coarser volcaniclastic sandstones and wackes exhibit asymmetric current ripple indicative of unidirectional currents. Some coarse levels contain several cephalopod remains (ammonoids and orthoconic nautiloids), the preservation degree of which does not allow for a firm taxonomic determination.

The petrographical study reveals that the siltstones comprise rare rounded quartz grains and angular, elongated to needle shaped and cryptocrystalline elements that are interpreted as volcanic shards embedded within a silty matrix (Table 3). The coarser layers enclose numerous lithic fragments, commonly rounded to sub-rounded

weathered rock fragments, displaying various igneous textures ranging from granular to microlitic. Monocrystalline particles are mainly angular to sub-angular, slightly weathered feldspar grains (Fig. 12D), among which plagioclase is frequent. These volcaniclastic sandstones and wackes also contain zircon grains and numerous corroded quartz crystals with embayments (Fig. 12E), suggesting that they derive from felsic volcanic rocks. The matrix is rich in fine-grained quartz and chlorite.

The Dong Trau Fm. also includes rhyolites (Rossignol, 2015). The rocks display porphyritic textures with feldspar and quartz phenocrysts (Fig. 12F and 12G). The quartz phenocrysts are commonly corroded, showing embayments against the groundmass (Fig. 12F), typical for quartz crystals partly destabilized as the pressure dropped during magma ascent. The feldspar phenocrysts consist of sericitized plagioclase and perthitic orthoclase resulting from sanidine recrystallizations. The groundmass is locally spherolitic to microgranular, suggestting that the rocks underwent solid-state recrystallization. The accessory minerals are mainly opaque, euhedral microphenocrysts and zircon (Table 3).

Interpretation. The Dong Trau Fm. corresponds to marine environments, as evidenced by the presence of numerous marine organisms, such as ammonoids. Highly fragmented and poorly preserved plant remains attest that these fossils are allochtonous. They however indicate the relative proximity of a coastline, consistent with a rather shallow marine setting. The occurrences of volcanic bombs and interbedded rhyolitic lava flows, as well as rhyolitic quartz grains (i.e., quartz crystals with embayments), angular feldspar fragments and volcanic shards clearly evidence that a proximal effusive to explosive volcanism was coeval with sedimentation.

5.1.2. Geochronological analyses

Sample VN 12-38. Ninety-nine grains were analysed for this volcaniclastic wacke. Thirteen grains yielded concordant dates, implying high detection limits (Table 4), ranging between 5.2% for the $DL_{1(pL=0.5)}$ and 41.1% for the $DL_{3(pL=0.95)}$. Most of the grains are euhedral to sub-euhedral and display a pinkish color. Most of the grains are euhedral to sub-euhedral and display a pinkish color while a few rounded to sub-rounded grains are ranging from yellow to orange. Internal structures imaged by CL are diverse: patchy to well-defined oscillatory zoning. The Th/U ratios range between 0.31 and 2.38, suggesting a magmatic origin for all these grains.

Except a single grain giving a date of 1052.7 ± 12.7 Ma (Fig. 13A), the concordant grains yielded dates ranging from 272.0 ± 6.4 Ma to 231.7 ± 5.7 Ma. Six analyses define the youngest concordant cluster at 246.4 ± 2.4 Ma (MSWD = 1.5; Fig. 13B). This date is interpreted as the maximum depositional age for this wacke. The main population, defined by 12 grains, exhibits an unimodal age distribution centered on ca. 246 Ma (Fig. 14A).

Samples VN 12-27 and VN 12-41 (rhyolites). As these samples display similar characteristics regarding their zircon contents, they are presented together. Fifty analyses and 59 analyses were performed for samples VN 12-27 (Fig. 15A) and VN 12-41 (Fig. 15C), respectively. Most of the grains are slightly pinkish to translucent and have an elongated euhedral shape, while a few grains are prismatic. In CL, the internal structure is characterized by faint oscillatory or patchy zoning. A few zircon grains show small inherited cores (not analyzed). All the grains have Th/U ratios higher than 0.1 (ranging between 0.27 and 1.39), suggesting a magmatic origin.

Plotted in Tera-Wasserburg diagrams, the analyses spread along the concordia line (Fig. 15A and 15C) following Pb loss trends. The observed spreading of the analyses is thus interpreted as the consequence of variable lead loss. The main cluster of concordant grains yield concordia dates of 248.3 ± 1.6 Ma (VN 12-27; n = 15; MSWD = 1.3; Fig. 15B) and 246.7 ± 1.9 Ma (VN 12-41; n = 9; MSWD = 1.4; Fig. 15D). These dates are interpreted as the emplacement ages for the rhyolites interbedded in the Dong Trau sediments. Additionally, sample VN 12-41 also contains a concordant grain at 264.5±6.4 Ma interpreted as a xenocryst.

5.2. Suoi Bang Formation

5.2.1. Sedimentological analyses

Description. The Suoi Bang Fm. unconformably overlies the deposits of the Dong Trau Fm. (Fig. 16A) and comprises 9 main facies (Fig. 16, Table 2), among which conglomerate facies are dominant (Fig. 16B and 17). Two main facies associations were identified along a 200m thick section: the A1 (Gmm, Gh, Gt and Sm, Table 2) and the A2 (Gt, St, Sm, Fm and Fc, Table 2) facies associations.

In the A1 facies association, the Gmm and Gh facies represent debris flow and upper flow regime deposits (Miall, 1996), respectively, typical of proximal alluvial fan settings. The Gt facies is characteristic of 3D megaripples migration (Miall, 1996), while the interbedded Sm facies corresponds to hyper-concentrated flows (e.g., Mulder and Alexander, 2001) in which sand deposition is too rapid for bedforms to develop. Such alternations are characteristic of distal alluvial fans (Blair, 1999; 2000; Nalpas et al.,

2008) where channelized deposits progressively become prominent over unconfined or poorly confined sheetflood deposits.

In the A2 facies association, the Gt and St facies correspond to sinuous crested 3D megaripples, indicative of channelized deposits in braided rivers (Miall, 1996). In the section, associated alluvial plains are mainly represented by the Fc or Fm facies, which correspond to low energy suspension deposits, and Sm facies, attributed to overbanks and waning floods. Fc facies generally contains organic matter. Toward the top of the section, the reduction of the pebble sizes in the Gt facies, as well as the increasing frequency of the finer-grained facies, illustrate that the depositional environment became more distal (Fig. 17).

The petrographical analysis (Table 3) shows that the massive sandstones (Sm) are mainly constituted by fine- to coarse-grained lithic arenites, with commonly sub-rounded fragments displaying microlitic and microgranular textures (Fig. 16C). These lithic arenites also contain isolated, commonly angular but also sub-rounded, quartz grains. Rare isolated feldspars, white mica, chlorite, rutile, zircon and opaque minerals are also present. The cross-bedded sandstones (St) and conglomerate matrix (Gt) comprise well sorted, sub-rounded to sub-angular coarse isolated quartz grains and a few rounded lithic fragments displaying microcrystalline textures (Fig. 16D). Accessory minerals comprise rounded to euhedral zircon and rutile.

Interpretation. The Suoi Bang Fm. corresponds to an alluvial fan depositional environment (A1 facies association) evolving to a braided alluvial plain (A2 facies association), in which the sediment supply decreased with time. Thus, the deposition of the Suoi Bang Fm. unambiguously took place in a terrestrial setting. Therefore, the

marine fauna described in deposits ascribed to the Suoi Bang Fm. cannot provide a reliable age for the terrestrial deposits evidenced in this work.

5.2.2. Geochronological analyses

Sample VN 12-29. The sample is a lithic arenite sampled 5 m above the unconformity with the Dong Trau Fm. (Fig. 17). It yielded a large number of rounded to euhedral zircon grains ranging from slightly pinkish to nearly red. A total of 198 analyses on 196 grains were performed (Fig. 13C and 13D). Thirty-nine grains give concordant dates, resulting in detection limits ranging from 1.8% for the $DL_{1(pL=0.5)}$ to 15.3% for the $DL_{3(pL=0.95)}$ (Table 5). In CL, the internal structures vary from typical oscillatory zoning to core-rim structure or lack any particular structure. The Th/U ratios, ranging from 0.14 to 2.50, are compatible with a magmatic origin, except one discordant grain exhibiting a Th/U ratio of 0.06, which is possibly metamorphic.

The youngest cluster gives a concordia date of 226.1 ± 3.0 (n = 3, MSWD = 1.03), interpreted as the maximum depositional age of the basal beds from the Suoi Bang Fm. (Fig. 13E) while most of the other concordant dates spread up to 260.0 ± 6.2 Ma. The main population (37 grains) is characterized by an unimodal age distribution, centered on ca. 240 Ma (Fig. 14B). Only two grains yield older concordant dates (Fig. 14B).

Sample VN 12-31. This sample is a quartz arenite, the exact stratigraphic position of which is unknown but is significantly higher in the Suoi Bang pile than the unconformity and the VN-12-29 sample. It also yielded a significant amount of zircon grains characterized by various sizes, shapes (from euhedral to well-rounded), colors (various pinkish shades, brownish, violet, yellow, red and translucent), and CL internal structures

(various brightness, inherited core with one to several overgrowths, or typical magmatic oscillatory zoning), suggesting diverse origins. Most of the grains have high Th/U ratios consistent with a magmatic origin, ranging between 0.1 and 6.0, although 3 grains (among which 2 are concordant and display 644.4 ± 11.0 Ma and 1159.4 ± 9.2 Ma dates) with ratios ranging between 0.03 and 0.09 could be metamorphic in origin.

Thirty-six out of the 116 analyzed grains (120 analyses; Fig 13F and 13G) yield concordant dates, implying low detection limits with a $DL_{1(pL=0.5)}$ of 1.9% and a $DL_{3(pL=0.95)}$ of 16.5% (Table 5). The concordant dates range from the late Permian (258.6 ± 6.2 Ma) to the Neoarchean (2700.1 ± 12.0 Ma), and define a polymodal age distribution (Fig. 14C). The youngest cluster of 3 grains gives a concordia date of 266.5 ± 3.7 Ma (n = 3, MSWD = 2.1), interpreted as the best estimate of the maximum depositional age for this sample (Fig 13G).

6. Discussion

6.1. Stratigraphic evolution of the Song Da Basin and tectonic implications

6.1.1. Depositional environments and age of the Triassic formations

The sedimentary succession of the Co Noi Fm. investigated during this study corresponds to terrestrial depositional environments, ranging from distal braided plain to flood plain or lacustrine settings (Fig. 18A). These environments contrast sharply with both the turbiditic environment suggested by Faure et al. (2014) and the marine setting suggested by the occurrence of various marine fossils within deposits from other localities assigned to the same formation (Tri and Khuc, 2011; Thanh and Khuc, 2012;

Fig. 18B). The very contrasted depositional environments of the various deposits attributed to the Co Noi Fm. highlight the need to reconsider its status as a single formation (e.g., Huyen et al., 2004). As the dating of the Co Noi Fm. previously relied on marine fossils (Tri and Khuc, 2011; Thanh and Khuc, 2012), the depositional age of the terrestrial deposits from this study remains to be established.

The geochronological results obtained on the sandstones from the Co Noi Fm. provide 3 maximum depositional ages of 243.1 ± 2.3 Ma, 237.3 ± 2.4 Ma and 242.6 ± 4.1 Ma for this formation. Even if some localities underwent a greenschist facies metamorphism, that could have enhanced Pb loss, the age density distribution for the sample VN 12-22 is not skewed toward young ages (Fig. 9B), suggesting it provides a reliable maximum depositional age, unaffected by Pb loss (Spencer et al., 2016). This maximum depositional age (237.3 ± 2.4 Ma) indicates a Ladinian-Carnian or younger depositional age for the terrestrial deposits of the Co Noi Fm.

The depositional environments for the Dong Giao Fm. correspond to a wide shallow water carbonate shelf. Its deposition could have initiated as early as the Early Triassic and resumed up to the Middle Anisian (Martini et al., 1998; Tri and Khuc, 2011; Thanh and Khuc, 2012 and new biostratigraphic data presented in this study). As the Dong Giao Fm. conformably overlies the Co Noi Fm. (Fig. 2 and Fig. 4), implying the Dong Giao Fm. is younger than the Co Noi Fm. The youngest maximum depositional age for the Co Noi Fm. (237.3 ± 2.4 Ma) is thus in contradiction with an Early Triassic to Middle Anisian (i.e., older than 243 Ma) age for the Dong Giao Fm.

To overcome this inconsistency, there are two possibilites. Because of deformation, the observed superposition (Fig. 2) could result, at least locally, from tectonics that led to the formation of reverse series. Such an interpretation, which could lead to reconsider the assumed stratigraphic superposition, is supported by the intense

deformation that affects, at least locally, the basin, as attested by, recumbent folds in the Son La area (Faure et al., 2014). However, structural and sedimentological analyses clearly evidence at several locations that the Dong Giao Fm. conformably overlies the Co Noi Fm. (e.g., Mong et al., 2004; Bao et al., 2004; Son et al., 2005, and Tuyet et al., 2005b; Tri and Khuc, 2011; Thanh and Khuc, 2012). Consequently, we interpret the apparent age paradox as resulting from the diachronous depositions of both the Co Noi and the Dong Giao formations. This is consistent with the suggestion that the deposition of the Dong Giao could have initiated as early as the Early Triassic (Martini et al., 1998) and resumed at least up to the Anisian (Fig. 18A). It also implies that the Co Noi and the Dong Giao sediments deposited coevally at different places, and corollary, diachronously at a given place (Fig. 18A), which is consistent with the observation that the two formations seal the unconformity at different places (e.g., Mong et al., 2004; Bao et al., 2004; Son et al., 2005, and Tuyet et al., 2005b). As the analysis of the regional maps also shows that most of the Dong Giao deposits postdate the deposition of the Co Noi Fm., the hypothesis that the Dong Giao Fm. also contains deposits that were emplaced after the Middle Triassic cannot be discarded (Fig. 18A). It follows that the duration of the stratigraphic gap sealed by both the Dong Gia and the Co Noi formations differ from place to place. Some area might have been subjected to a short stratigraphic gap, while other areas could have encountered a protracted stratigraphic gap that encompassed both the Early and the Middle Triassic (Fig. 18A).

6.1.2. The Song Da Basin: a foreland basin

The distinctive feature of the Song Da Basin is the deposition of strongly diachronous formations (both the Co Noi and the Dong Giao) over a basal unconformity (Fig. 18A).

The diachronous sealing of a basal unconformity by mostly terrestrial deposits is common in foreland basins, where the forebulge region undergoes weathering, soil formation and erosion of the basement (e.g., DeCelles and Giles, 1996; Sinclair, 1997; Caravaca et al., in press). The sealing of a basal unconformity by well-developed, purely terrestrial deposits, nevertheless departs from the usual initial deposition of shallow marine to tidal sediments, as observed in most foreland basins worldwide (e.g., Sinclair, 1997). However, it is worth mentioning that the only Lower Triassic deposits known in the Song Da Basin are marine sediments, as evidenced by the occurrence of foraminifers (Martini et al., 1998) and ammonoids (e.g., Tri and Khuc, 2011; Thanh and Khuc, 2012; Appendix 1). Nonetheless, purely terrestrial deposits have also been evidenced at the early stages of foreland basin infilling (e.g., Houseknecht, 1986; Catuneanu, 2004; Caravaca et al., in press).

In the Song Da Basin, assuming that the basal unconformity and associated gap mark the transition from a passive margin to a foreland basin setting (Fig. 19A), this major geodynamic change could have been initiated as early as the Changhsingian (latest Permian). This is corroborated by the report of terrestrial deposits and paleosols in the Yen Duyet Fm. (Shi G.R. and Shen S.-Z., 1998). Such timing is consistent with the earliest (i.e., between ca. 266 and ca. 237 Ma; Lepvrier et al., 1997) syn-tectonic metamorphic event experienced by the rocks constituting the internal part of the orogen (Faure et al., 2014). In addition, at least two other younger unconformities are documented in the Song Da Basin (Mong et al., 2004; Bao et al., 2004; Son et al., 2005; Tuyet et al., 2005b; Tri and Khuc, 2011; Thanh and Khuc, 2012; Appendix 1). These unconformities potentially witness protracted tectonic deformations affecting the Song Da Basin during the Triassic.

Assuming a proarc (i.e., localized in front of the orogenic belt, on the subducting South China plate, see below) foreland setting, the main sourcing area for the Co Noi sandstones would have been located on the SCB (Fig. 19B). The latter experienced important volcanic activities associated with the Emeishan Large Igneous Province (ELIP) event between ca. 260 Ma and 240 Ma (Shellnutt et al., 2008). The peak of the volcanic activity occured between ca. 260 and 257 Ma (e.g., Shellnutt et al., 2012). This is in agreement with the age distribution of sandstone samples collected in the Co Noi Fm., which are unimodal and centered on ca. 255 Ma and ca. 250 Ma (Fig. 9). The grain Th/U ratios, as well as the occurrence of numerous reworked and weathered volcaniclasts in these sandstones, suggest that these grains mainly originated from volcanic rocks.

The carbonate sedimentation (Dong Giao Fm.), directly sealing the basal unconformity (Mong et al., 2004; Bao et al., 2004; Son et al., 2005, and Tuyet et al., 2005b) or conformably overlying the Co Noi Fm. (Tri and Khuc, 2011; Thanh and Khuc, 2012), attests for the progressive drowning of the basin below sea level. Although eustatism may account for relative sea level changes, it is likely that in the Song Da Basin the drowning resulted, at least in part, from an increased flexural subsidence related the topographic load exerted by the adjacent thrust belt that was building at that time (e.g., Lepvrier et al., 1997; 2004; Nakano et al., 2008, 2010; Liu J. et al., 2012; Faure et al., 2014; Roger et al., 2014; Zhang R.Y. et al., 2013, 2014). This thrust belt results from the collision between the SCB and the Indochina Block and corresponds to the Indosinian orogen. Diachronous carbonate deposits, spanning from the Early Triassic up to the Ladinian-Carnian in different locations of the Song Da Basin, constitute a common stratigraphic signature of forebulge and back-bulge depozones in foreland basins located in the tropical or sub-tropical climatic belts (e.g., DeCelles and Giles, 1996; Sinclair, 1997; Maurizot, 2014; Caravaca et al., in press). These were the climatic

conditions underwent by the Song Da Basin as it was located at tropical latitudes during the Triassic (e.g., Li P. et al., 2004; Gilder et al., 2008).

From the Early to the Late Triassic, the Song Da Basin experienced progressive and pronounced lithological changes. These modifications are marked by an increasing siliciclastic input, partly constituted by immature sandstones made up of feldspar and volcaniclastic particles (Thanh and Khuc, 2012). This progressive lithological shift from calcareous to siliciclastic sedimentation initiated as soon as the Anisian in the upper part of the Dong Giao Fm. (Thanh and Khuc, 2012) and continued throughout the Ladinian and the Late Triassic (Nam Tham and Suoi Bang formations; Fig. 19C; Appendix 1). This shift suggests a change in the lithology of the hinterland that sourced the basin, and/or an increasing proximity with respect to the source area of siliciclastic detrital particles. These siliciclastic inputs are interpreted to derive from the erosion of the thrust wedge, as classically evidenced in a number of other foreland basins (e.g., Sinclair, 1997).

Finally, a large number of the discrepancies in the equivocal stratigraphic framework that was in use for the Song Da Basin (Appendix 1) were probably rooted in the significant diachronous deposition of the main formations constituting the basin (Fig. 18A). The dating of the terrestrial formations that lack preserved fossils for biostratigraphic dating, as well as a reevaluation of the age of the main marine deposits from published data (Appendix 1) and newly collected samples provided new support to overcome these initial stratigraphic discrepancies.

6.2. Stratigraphic evolution of the Sam Nua Basin and tectonic implications

6.2.1. Depositional environments and ages of the Triassic formations

Dong Trau Fm. Numerous marine organisms, such as ammonoids, found within the volcaniclastic sediments of the Dong Trau Fm., attest a deposition in a marine setting (Fig. 20A). The volcaniclastic deposits comprise rhyolitic quartz grains (i.e., quartz crystals with embayments), angular feldspar fragments and volcanic shards, along with volcanic bombs and interbedded rhyolitic lava flows. These evidences indicate that proximal effusive to explosive volcanism was coeval with sedimentation.

The emplacement of the rhyolites from the Sop Cop area, northern part of the Sam Nua Basin, occurred during the Early to the Middle Triassic, at 248.3 ± 1.6 Ma and 246.7 ± 1.9 Ma. This is consistent with the maximum depositional age obtained on the volcaniclastic wacke collected in the Dong Trau Fm. (246.4 ± 2.4 Ma). These results are also consistent with a rhyolite from the southeastern part of the Sam Nua Basin, which gave an age of 251.9 ± 1.7 Ma (Shi M.-F. et al., 2015). The depositional age of the Dong Trau Fm. is thus consistent with the biostratigraphic age inferred from the ammonoid content (Tri and Khuc, 2011; Thanh and Khuc, 2012, Fig. 2; Appendix 1). This is furthermore consistent with the 239 ± 6 Ma age obtained on the Song Ma Granite (Hieu et al., 2017), intrusive within the Dong Trau Fm. (Son et al., 2005).

The interpretation of the tectonic setting of the Sam Nua Basin during the Early to Middle Triassic critically relies on the geochemical signature of calk-alkaline rocks, among which the rhyolites interbedded within the Dong Trau Fm. (Lepvrier et al., 2004; Hoa et al., 2008; Tri and Khuc, 2011). These geochemical signatures are however ambiguous (e.g., Morris et al., 2000; Hoa et al., 2008), resulting in opposite views about the tectonic setting for the Sam Nua Basin at that time, some studies pointing to a late orogenic basin (Lepvrier et al., 2004; Hoa et al., 2008; Tri and Khuc, 2011) while other favor a foreland basin (Liu J. et al., 2012; Faure et al., 2014, 2016; Shi M.-F. et al., 2015).

Three independent observations made during this work allow to decipher between these contrasted hypotheses.

First, the marine depositional environments of the Dong Trau Fm. are plausibly expected to occur in the vicinity of volcanic arcs, while terrestrial deposits more likely accumulate during the late orogenic stages of continental collisions. The marine deposits of the Dong Trau Fm., which were coeval with a very proximal calk-alkaline magmatic activity, are thus compatible with an arc related setting.

Second, the Dong Trau rhyolites and associated volcaniclastic rocks are strongly deformed (Fig. 12B), as attested by the numerous folds and faults crosscutting the whole formation. Thus, the Dong Trau Fm. underwent significant deformations that occurred after its deposition, suggesting that the Dong Trau deposits were involved in at least one orogenic cycle. This is in agreement with arc-related basins that formed before major collisions. In contrast, intra-mountain late orogenic basins are expected to undergo only minor deformations.

Third, the Dong Trau Fm. is stratigraphically located below the angular unconformity with the Suoi Bang Fm., which also proves that the volcanism in the Dong Trau Fm. was emplaced before the major tectonic event responsible for the unconformity. These evidences indicate that the Sam Nua Basin was probably located in the immediate vicinity of a subduction related magmatic arc during the Early to the Middle Triassic, as already suggested in various studies (Liu J. et al., 2012; Faure et al., 2014, 2016; Shi M.-F. et al., 2015; Hieu et al., 2017). A late orogenic setting (Lepvrier et al., 2004; Hoa et al., 2008; Tri and Khuc, 2011) appears unlikely.

The occurrence of arc related magmatic rocks implies that a slab constituted by an oceanic lithosphere was subducting to generate the calk-alkaline magmatism. This requires that an oceanic domain, constituted by an oceanic lithosphere, separated the

SCB from the Indochina Block, and was not totally consumed by subduction processes when the calk-alkaline volcanoes were active, i.e., during the Early to the Middle Triassic. Hypotheses proposing that the SCB and the Indochina Block were separated by a continental rift (e.g., Metcalfe, 2012), by a back-arc basin that developed over a thinned continental crust (Fan W. et al., 2010), or that these blocks were already amalgamated (e.g., Carter et al., 2001; Carter and Clift, 2008), do not explain the occurrence of voluminous Early to Middle calk-alkaline magmatic rocks in the Sam Nua Basin; consequently, these hypotheses are improbable.

The occurrence of arc related rocks in the Sam Nua Basin, to the south of the Song Ma Ophiolitic Suture Zone, implies that the Triassic subduction was dipping toward the southwest (present-day coordinates), beneath the Indochina block, as sugested by several authors (e.g., Liu J. et al., 2012; Vuong et al., 2013; Roger et al., 2014; Faure et al., 2014, 2016; Shi M.-F. et al., 2015; Hieu et al., 2017). Corollary, this precludes the hypothesis of a northward dipping slab beneath the SCB, as it has been advocated (e.g., Lepvrier et al., 2004; 2008; Nakano et al., 2010; Yan Q. et al., 2017).

Suoi Bang Fm. The sedimentary succession of the Suoi Bang Fm. investigated during this study exhibits terrestrial depositional environments, ranging from alluvial fan to a braided alluvial plain (Fig. 20A). These environments contrast with the marine setting suggested by the occurrence of various marine fossils within deposits from other localities that are also assigned to the same formation (Tri and Khuc, 2011; Thanh and Khuc, 2012; Appendix 1). However, this is in agreement with the report of coal seams, brackish-water bivalves and plant fossils in the upper part of the formation (Tri and Khuc, 2011; Thanh and Khuc, 2012).

The maximum depositional age for the Suoi Bang Fm. (226.1 ± 3.0 Ma) is consistent with a Late Triassic to Early Jurassic depositional age, which is indicated by the plant remains that occur in the Suoi Bang Fm. (Appendix 1; section 2; Table S1). Additionally, this also agrees with available structural relationships with dated magmatic rocks (Fig. 2; see, however, discussion in Appendix 1).

6.2.2. Age and significance of the major unconformity separating the Dong Trau from the Suoi Bang formations

In the Sop Cop area (Fig. 5), the angular unconformity between the Dong Trau and the Suoi Bang formations (Fig. 16A) formed between the Ladinian (Middle Triassic), and the late Norian. The formation of the unconformity is therefore coeval with high-pressure granulite facies metamorphic rocks (ca. 240 to 230 Ma; Table 1; Nakano et al., 2010; Zhang R.Y. et al., 2013, 2014) cropping out in the Nam Co Unit, to the north of the Sam Nua Basin.

The Suoi Bang sediments sealing the So Cop unconformity are particularly coarse (up to 1m in diameter; Table 2), display angular shapes and are made up of the material composing the underlying Dong Trau Fm. These features suggest that the detrital particles were of local provenance and hint for sharp topographic gradients in the adjacent watersheds of the Sam Nua Basin. The main population of detrital zircon grains from the sandstone collected immediately above the unconformity (Fig. 17; sample VN 12-29) is characterized by an unimodal age distribution, centered at ca. 242 Ma (Fig. 14B). As this sandstone is volcaniclast-rich (Fig. 16C, Table 3), the grains likely derive from the reworking of volcanic and volcaniclastic rocks comparable to those from the Dong Trau Fm., located immediately below the unconformity, sustaining the hypothesis

of proximal sources. In contrast, the zircon grains extracted from the sandstone (sample VN 12-31) collected higher in the stratigraphic pile display a completely different age distribution (Fig. 14C). This implies that the zircon populations originate from different sources, which were, in addition, different from that of sample VN 12-29. Along with the observed lithological dissimilarities in the Suoi Bang sediments, significant changes in the lithologies composing the detrital sources that fed the Suoi Bang layers must be inferred. A large number of factors may account for such changes, including varying zircon fertility in the source rocks (e.g., Amidon et al., 2005; Moecher and Samson, 2006), the reorganization of the drainage network (e.g., Thomas, 2011), changes of the erosion rates (Amidon et al., 2005) and/or changes of the hydrodynamic sorting conditions of the grains (e.g., Lawrence et al., 2011). Nothing indicates which of these factors were prominent in the present case, but all involve significant evolutions of landscapes and associated topographies that could result from tectonic events.

From the gap duration, the structural and sedimentological characteristics exhibited by the Suoi Bang Fm., we conclude that the So Cop unconformity should be considered as a major unconformity in northern Vietnam. Overall, the above lines of evidence suggest that the angular unconformity that separate the Dong Trau from the Suoi Bang formations resulted from a major tectonic event that occurred after the construction of a magmatic arc, while coeval ductile deformation and high-grade metamorphic rocks formed (Lepvrier et al., 1997, 2004; Carter et al., 2001; Nakano et al., 2008, 2010; Zhang R.Y. et al., 2013). We thus argue that the So Cop unconformity is a segment of the Indosinian unconformity that developed following the erosion of the Indosinian mountain range.

6.3. Comparison between the stratigraphic evolution of the Song Da and the Sam Nua basins and implications for the Indosinian orogeny

From the late Permian (Fig. 21 and Fig. 22A) up to the Middle Triassic, the Sam Nua Basin experienced the deposition of the volcaniclastic rocks of the Dong Trau Fm., as well as rhyolites with subduction-related geochemical characteristics (Shi M.-F et al., 2015; Rossignol, 2015). The Sam Nua Basin was, at that time, separated from the Song Da Basin to the north by an oceanic domain, the remnants of which crop out in the SMOSZ (Hutchison, 1975; Trung et al., 2006; Thanh et al., 2011; Vuong et al., 2013; Zhang R.Y. et al., 2014; Faure et al., 2014). This oceanic domain probably existed since the Carboniferous (Table 1; Vuong et al., 2013; Zhang R.Y. et al., 2013, 2014). Its exact size remains unknown although regional to world scale paleogeographic models suggest it was no more than a few hundred kilometers wide (Li P. et al., 2004; Ferrari et al., 2008; Cocks and Torsvik, 2013; Domeier and Torsvick, 2014). This ocean, sometimes referred to as the Song Ma Ocean (e.g., Ferrari et al., 2008; Lai et al., 2014b), has been attributed to a branch of the Paleotethys (e.g., Faure et al., 2014) but may also represent an independent ocean, named the “Paleoasian ocean” by Domeier and Torsvick (2014). These distinct interpretations illustrate the numerous, ongoing debates about the paleogeography of the SEA during the late Paleozoic and early Mesozoic. The subduction of this oceanic domain under the northern active continental margin of the Indochina Block probably began as early as the end of the Cisuralian (early Permian), as shown by the emplacement of magmatic rocks displaying subduction related geochemical signatures in the Truong Song Belt (e.g., Liu et al., 2012; Hieu et al., 2017). In our studied area, magmatic activity associated with this subduction occurred continuously from the late Permian up to the Anisian (Middle Triassic), as evidenced by the intrusions that compose the Song Ma Granite (e.g., Hieu et al., 2017; Table 1) and the associated

volcanic activity preserved in the Dong Trau Fm. To the north, the Song Da Basin experienced the emplacement of a variety of magmatic rocks related to the Emeishan Large Igneous Province (e.g., Hanski et al., 2004; Balykin et al., 2010) during the late Permian.

During the Early to the Middle Triassic (Anisian, Fig. 21 and Fig. 22B), the Sam Nua Basin was opened to oceanic influences as attested by the occurrence of marine fossils preserved in the Dong Trau Fm. It was also related to a magmatic arc at the active continental margin of the Indochina plate, since the Dong Trau deposits and associated rhyolites witness a subduction that was active up to the Anisian. As a consequence the basin plausibly occupied a forearc position with respect to the mountain belt. Further north, the Song Da Basin experienced the deposition, over a basal unconformity, of the Dong Giao and the Co Noi formations, corresponding, respectively, to platform limestone (Martini et al., 1998) and terrestrial deposits. These formations, deposited diachronously in a foreland basin originated from the flexural response of the lithosphere related to the building of the southward Indosinian orogen (Fig. 19). At the end of the Middle Triassic, the oceanic domain that previously separated the Indochina from the South China blocks was probably almost completely subducted (Fig. 22B). Nonetheless, the closure of this oceanic domain could have occurred diachronously (Halpin et al., 2015).

From the Ladinian to the early Norian (ca. 240 to 220 Ma; Fig. 21 and Fig. 22C) the northern part of the Sam Nua Basin, and probably most of the present-day northern Vietnam, including the Song Da Basin, underwent deformation and erosion that led to the formation of the Indosinian collisional orogen. This erosional event led to the formation of the Indosinian unconformity that developed coevally with high-grade metamorphic rocks (Lepvrier et al., 1997; Nakano et al., 2010; Zhang R.Y. et al., 2013) in

the Song Ma and the Nam Co units. Magmatic activity associated with the continental collision occurred as early as the late Middle Triassic and continued throughout the Norian (Table 1 and references therein, see also Appendix 1).

During the late Norian to the Rhaetian (Fig. 21 and Fig. 22D), the Sam Nua and Song Da basins became syn- to post-orogenic foreland basin. These basins then experienced the deposition of coarse, terrestrial deposits, constituting the Suoi Bang Fm. that resulted from the erosion of the Indosinian mountain belt. The stratigraphic frameworks of both the Sam Nua and the Song Da basins are thus in agreement with most of the geological evidences attesting that the collision between the Indochina and the South China blocks occurred during the Middle to the Late Triassic.

7. Conclusions

A revised stratigraphic framework has been established for the Song Da and the Sam Nua basins, based on sedimentological and dating (U-Pb geochronology on zircon and foraminifer biostratigraphy) analyses, This new stratigraphic framework has important implications regarding the tectonic settings for both basins and allows us to reconstruct the regional geodynamic evolution of the South China Block, where the Song Da Basin is located, and the Indochina Block, where the Sam Nua basin developed. The major outcomes of this revised stratigraphic framework are:

1. Strongly diachronous deposits of terrestrial (Co Noi Fm.) and marine (Dong Giao Fm.) deposits over a basal unconformity occurred in the Song Da Basin during the Early to the Middle Triassic. Such a sedimentary fill of the Song Da Basin is in accordance with a foreland setting, and at odds with the commonly interpreted rift setting for this basin during the Triassic. A proarc foreland setting on the

southern margin of the SCB is furthermore consistent with the coeval development of the Indosinian thrust belt to the south of the basin.

2. Discordant over a metamorphic basement, the late Permian to Middle (ca. 260-242 Ma) Triassic deposits (Dong Trau Fm.) contains a significant amount of volcaniclasts and interbedded rhyolites. The proximal volcanic activity was related to an active magmatic arc at that time, located on the northern margin of the Indochina plate. This shows that an oceanic domain was separating the Indochina Block from South China Block before their collision. It also implies that the subducting oceanic slab was dipping to the south, beneath the Indochina plate. A forearc setting is inferred from the marine influences attested by fossils such as ammonoids
3. The late Middle Triassic (Ladinian) to Late Triassic (Norian) is characterized by an erosional event that resulted in the Indosinian unconformity, which is ultimately related to the collision between the South China and the Indochina blocks, due to the closure of an oceanic domain.
4. During the Late Triassic, the Song Da and the Sam Nua basins encountered deposition of coarse, terrestrial sediments (Suoi Bang Fm.) originating from the erosion of the Indosinian mountain belt. These deposits in the foreland of the belt remain poorly dated, as terrestrial fossils preserved within this formation have a limited stratigraphic resolution, and as only one maximum depositional age at ca. 226 Ma is available.

Acknowledgements

Sadly, our colleague Marie-Pierre Dabard passed away in December 2017, before the completion of this manuscript. We dedicate this paper to her. The geochronological analyses were supported by the Observatoire des Sciences de l'Univers de Rennes (OSUR). X. Le Coz, Y. Lepagnot, A. Lauqué (OSUR) and C. Astoury (Geosciences Montpellier) are acknowledged for thin section preparation, rock crushing and assistance for mineral separation, respectively. We express our gratitude to J. Broutin (Université Pierre et Marie Curie, France) for his help to review plant content in the different formations investigated in this study. We also thank H. Maluski (Geosciences Montpellier) for his help during fieldwork and insights on the geodynamics of Vietnam. This work also benefited from field assistance and fruitful discussions with Nhat Truong Doan and Nguyen Dinh Huu (Hanoi University of Science, Vietnam), to whom we are very grateful, despite they do not fully share the ideas developed in this paper. We appreciated the help and assistance of To Ti Sam (Hanoi University of Science, Vietnam) during a field mission. Vu Van Tich and Nguyen Van Vuong (Hanoi University of Science, Vietnam) are acknowledged for logistic assistance. This research was supported by the INSU/CNRS (TELLUS - SYSTER program, coordinated by F. Roger), the Swiss NSF project 200020_156422 (to R.M.) and the ANR project AFTER (ANR-13-JS06-0001-01; to A.B.). The financial support of the CNPq (projeto 433761/2016-4 to C.R.) was essential for the completion of this manuscript. The authors thank Ian Metcalfe and an anonymous reviewer for their insightful reviews.

References

Amidon, W.H., Burbank, D.W., Gehrels, G.E., 2005. Construction of detrital mineral populations: insights from mixing of U-Pb zircon ages in Himalayan rivers. Basin Research 17, 463–485. doi:10.1111/j.1365-2117.2005.00279.x

Andersen, T., 2005. Detrital zircons as tracers of sedimentary provenance: limiting conditions from statistics and numerical simulation. Chemical Geology 216, 249–270.

Anh, T.V., Pang, K.-N., Chung, S.-L., Lin, H.-M., Hoa, T.T., Anh, T.T., Yang, H.-J., 2011. The Song Da magmatic suite revisited: A petrologic, geochemical and Sr–Nd isotopic study on picrites, flood basalts and silicic volcanic rocks. Journal of Asian Earth Sciences 42, 1341–1355. doi:10.1016/j.jseaes.2011.07.020

Ballouard, C., Boulvais, P., Poujol, M., Gapais, D., Yamato, P., Tartèse, R., Cuney, M., 2015. Tectonic record, magmatic history and hydrothermal alteration in the Hercynian Guérande leucogranite, Armorican Massif, France. Lithos 220-223, 1–22.

Balykin, P.A., Polyakov, G.V., Izokh, A.E., Trong, T., Thi, N., Quoc, T., Petrova, T.E., 2010. Geochemistry and petrogenesis of Permian ultramafic-mafic complexes of the Jinping – Song Da rift (southeastern Asia). Russian Geology and Geophysics 51, 611–624. doi:10.1016/j.rgg.2010.0

Bao, N.X., Thuc, D.D., Dung, H.T., Bac, N.V., Lam, N.N., Ty, N.V., 2004. Geology and mineral resources of Van Yen sheet (F-48-XXVII), department of geology and minerals of Vietnam, Ha Noi.

Blair, T.C., 1999. Sedimentology of the debris‐flow‐dominated Warm Spring Canyon alluvial fan, Death Valley, California. Sedimentology 46, 941–965.

Blair, T.C., 2000. Sedimentology and progressive tectonic unconformities of the sheetflood-dominated Hell's Gate alluvial fan, Death Valley, California. Sedimentary Geology 132, 233–262. doi:10.1016/S0037-0738(00)00010-5

Blondel, F., 1929, Etat de nos connaissances en 1929 sur la géologie de l'Indochine française: Bulletin du Service Géologique de l'Indochine 18, 2–17 (in French).

Bureau of Geology and Mineral Resources of Yunnan Province, 1990. Geological map of Yunnan Province. Geological Publishing House, Beijing.

Burrett, C.F., 1974. Plate tectonics and the fusion of Asia. Earth and Planetary Science Letters. 21, 181–189.

Burrett, C.F., Meffre, S., Lai, C.-K., Khositanont, S., Chaodumrong, P., Udchachon, M., Ekins, S., Halpin, J.A., 2014. The configuration of Greater Gondwana—Evidence from LA ICPMS, U–Pb geochronology of detrital zircons from the Palaeozoic and Mesozoic of Southeast Asia and China. Gondwana Research 26, 31–51. doi:10.1016/j.gr.2013.05.020

Cai, J.-X., Zhang, K.-J., 2009. A new model for the Indochina and South China collision during the Late Permian to the Middle Triassic. Tectonophysics 467, 35–43. doi:10.1016/j.tecto.2008.12.003

Caravaca, G., Brayard, A., Vennin, E., Guiraud, M., Le Pouriet, L., Grosjean, A.-S., Thomazo, C., Olivier, N., Fara, E., Escarguel, G., Bylund, K.G., Jenks, J.F., Stephen, D.A., in press. Controlling factors for differential subsidence in the Sonoma Foreland Basin (Early Triassic, western USA). Geological Magazine 0, 1–25. doi:10.1017/S0016756817000164

Carter, A., Roques, D., Bristow, C., Kinny, P., 2001. Understanding Mesozoic accretion in Southeast Asia: Significance of Triassic thermotectonism (Indosinian orogeny) in Vietnam. Geology 29, 211–214. doi:10.1130/0091-7613(2001)029<0211:UMAISA>2.0.CO;2

Carter, A., Clift, P.D., 2008. Was the Indosinian orogeny a Triassic mountain building or a thermotectonic reactivation event? Comptes Rendus Geoscience. 340, 83–93. doi:10.1016/j.crte.2007.08.011

Catuneanu, O., 2004. Retroarc foreland systems-evolution through time. Journal of African Earth Sciences 38, 225–242. doi:10.1016/j.jafrearsci.2004.01.004

Chen, Z., Lin, W., Faure, M., Lepvrier, C., Vuong, N.V., Tich, V.V., 2014. Geochronology and isotope analysis of the Late Paleozoic to Mesozoic granitoids from northeastern Vietnam and implications for the evolution of the South China block. Journal of Asian Earth Sciences 86, 131–150. doi:10.1016/j.jseaes.2013.07.039

Cocks, L.R.M., Torsvik, T.H., 2013. The dynamic evolution of the Palaeozoic geography of eastern Asia. Earth-Science Reviews 117, 40–79. doi:10.1016/j.earscirev.2012.12.001

Cohen, K.M., Finney, S.C., Gibbard, P.L., Fan, J.-X., 2013 (updated, v2017/02). The ICS International Chronostratigraphic Chart. Episodes 36, 199-204.

Deprat, J., 1915. Les zones plissées intermédiaires entre le Yunnan et le Haut-Tonkin. Comptes Rendus l'Académie des Sciences 160, 640–642 (in French).

Deprat, J., 1916. Sur la structure de la zone interne des nappes préyunnanaises et sur l'existence de charriages antéouraliens dans le nord du Tonkin. Comptes Rendus l'Académie des Sciences 162, 637–639 (in French).

Dickinson, W.R., Gehrels, G.E., 2009. Use of U–Pb ages of detrital zircons to infer maximum depositional ages of strata: A test against a Colorado Plateau Mesozoic database. Earth and Planetary Science Letters 288, 115–125.

DeCelles, P.G., Giles, K.A., 1996. Foreland basin systems. Basin Research 8, 105–123. doi:10.1046/j.1365-2117.1996.01491.x

Domeier, M., Torsvik, T.H., 2014. Plate tectonics in the late Paleozoic. Geoscience Frontiers 5, 303–350. doi:10.1016/j.gsf.2014.01.002

Dunham, R.J., 1962. Classification of carbonate rocks according to depositional textures. In: American Association of Petroleum Geologists Memoir, v. 1. AAPG special volumes, pp 108–121.

Embry, A.F. and Klovan, J.E., 1971. A Late Devonian reef tract on northeastern Banks Island, NWT. Bulletin of Canadian Petroleum Geology 19, 730–781.

Fan, W., Wang, Y., Zhang, A., Zhang, F., Zhang, Y., 2010. Permian arc–back-arc basin development along the Ailaoshan tectonic zone: Geochemical, isotopic and geochronological evidence from the Mojiang volcanic rocks, Southwest China. Lithos 119, 553–568. doi:10.1016/j.lithos.2010.08.010

Faure, M., Lepvrier, C., Nguyen, V.V., Vu, T.V., Lin, W., Chen, Z., 2014. The South China block-Indochina collision: where, when, and how? Journal of Asian Earth Sciences 79, 260–274. doi:10.1016/j.jseaes.2013.09.022

Faure, M., Lin, W., Chu, Y., Lepvrier, C., 2016a. Triassic tectonics of the southern margin of the South China Block. Comptes Rendus - Geoscience 348, 5–14. doi:10.1016/j.crte.2015.06.012

Ferrari, O.M., Hochard, C., Stampfli, G.M., 2008. An alternative plate tectonic model for the Palaeozoic–Early Mesozoic Palaeotethyan evolution of Southeast Asia (Northern Thailand–Burma). Tectonophysics 451, 346–365.

Findlay, R.H., Trinh, P.T., 1997. The Structural Setting of the Song Ma Region, Vietnam and the Indochina-South China Plate Boundary Problem. Gondwana Research 1, 11–33. doi:10.1016/S1342-937X(05)70003-4

Fromaget, J. 1929, Note préliminaire sur la stratigraphie des formations secondaires et sur l'âge des mouvements majeurs en Indochine: Bulletin du service géologique de l'Indochine 18, 2-34 (in French).

Fromaget, J., 1934a. Observations et réflexions sur la géologie stratigraphique et structurale de l'Indochine. Bulletin de la Société Géologique de France 1-3, 101–164 (in French).

Fromaget, J., 1934b. Le Trias dans la partie Nord-Ouest du Synclinal de Sam Neua (Tonkin et Laos). Comptes Rendus Hebdomadaires de l'Académie des Sciences de Paris 199, 962–964 (in French).

Gazdzicki, A., Smit, O.E., 1977. Triassic foraminifers from the Malay Peninsula. Acta Geologica Polonica 27, 319–342.

Geological map of Lao People's Democratic Republic, 1: 1 500 000, 1990. United Nation publication.

Gilder, S.A., Tan, X., Bucher, H., Kuang, G., Yin, J., 2008. Optimization of apparent polar wander paths: An example from the South China plate. Physics of the Earth and Planetary Interior 169, 166–177. doi:10.1016/j.pepi.2008.07.016

Gilley, L.D., Harrison, M., Leloup, P.H., Ryerson, F.J., Lovera, O.M., Wang, J.-H., 2003. Direct dating of left-lateral deformation along the Red River shear zone, China and Vietnam. Journal of Geophysical Research. 108, 2127. doi:10.1029/2001JB001726

Glotov, A.I., Polyakov, G. V, Hoa, T.T., Balykin, P.A., Akimtsev, V.A., Krivenko, A.P., Tolstykh, N.D., Phuong, N.T., Thanh, H.H., Hung, T.Q., Petrova, T.E., 2001. The Ban Phuc Ni-Cu-PGE deposit related to the Phanerozoic komatiite-basalt association in the Song Da Rift, northwestern Vietnam. The Canadian Mineralogist 39, 573–589. doi:10.2113/gscanmin.39.2.573

Halpin, J.A., Tran, H.T., Lai, C.-K., Meffre, S., Crawford, A.J., Zaw, K., 2015. U–Pb zircon geochronology and geochemistry from NE Vietnam: A "tectonically disputed" territory between the Indochina and South China blocks. Gondwana Research. doi:10.1016/j.gr.2015.04.005

Hanski, E., Walker, R.J., Huhma, H., Polyakov, G.V., Balykin, P.A., Hoa, T.T., Phuong, N.T., 2004. Origin of the Permian-Triassic komatiites, northwestern Vietnam. Contributions to Mineralogy and Petrology 147, 453–469. doi:10.1007/s00410-004-0567-1

He, Y., 1984. Middle Triassic foraminifera from central and southern Guizhou, China. Acta Palaeontlogica Sinica 23, 420–431.

Hieu, P.T., Chen, F.-K., Thuy, N.T.B., Cuong, N.Q., Li, S.-Q., 2013. Geochemistry and zircon U–Pb ages and Hf isotopic composition of Permian alkali granitoids of the Phan Si Pan zone in northwestern Vietnam. Journal of Geodynamics 69, 106–121. doi:10.1016/j.jog.2012.03.002

Hieu, P.T., Li, S.-Q., Yu, Y., Thanh, N.X., Dung, L.T., Tu, V.L., Siebel, W., Chen, F., 2017. Stages of late Paleozoic to early Mesozoic magmatism in the Song Ma belt, NW Vietnam: evidence from zircon U–Pb geochronology and Hf isotope composition. International Journal of Earth Sciences 106. doi:10.1007/s00531-016-1337-9

Hoa, T.T., Izokh, A.E., Polyakov, G.V., Borisenko, A.S., Anh, T.T., Balykin, P.A., Phuong, N.T., Rudnev, S.N., Van, V.V., Nien, B.A., 2008. Permo-Triassic magmatism and metallogeny of Northern Vietnam in relation to the Emeishan plume. Russian Geology and Geophysics 49, 480–491. doi:10.1016/j.rgg.2008.06.005

Houseknecht, D.H., 1986. Evolution from passive margin to foreland basin: the Atoka Formation of the Arkoma Basin, south-central U.S.A., in: Allen, A.P., Homewood, P. (Eds.), Foreland Basins. International Association of Sedimentologists Special Publication, pp. 327–347. doi:10.1002/9781444303810

Hutchison, C.S., 1975. Ophiolite in Southeast Asia. Geological Society of America Bulletin 86, 797–806.

Huyen, D.T., Huu, N.D., Hung, N.H., Truong, D.N., Ngoc, N.L., 2004, Tai lieu moi ve dia tang va co sinh cac tram yich Trias ha o Tay Bac Bo (New data on stratigraphy and palaeontology of Lower Triassic sediments in West Bac Bo): TC Dia chat, A/283, p. 1-9 (in Vietnamese with English abstract).

Jackson, S.E., Pearson, N.J., Griffin, W.L., Belousova, E.A., 2004. The application of laser ablation-inductively coupled plasma-mass spectrometry to in situ U–Pb zircon geochronology. Chemical Geology 211, 47–69.

Jolivet, L., Maluski, H., Beyssac, O., Goffé, B., Lepvrier, C., Thi, P.T., Vuong, N.V., 1999. Oligocene-Miocene Bu Khang extensional gneiss dome in Vietnam: Geodynamic implications. Geology 27, 67–70. doi:10.1130/0091-7613(1999)027<0067:OMBKEG>2.3.CO;2

Kamvong, T., Meffre, S., Maas, R., Stein, H., Lai, C.-K., 2014. Adakites in the Truong Son and Loei fold belts, Thailand and Laos: Genesis and implications for geodynamics and metallogeny. Gondwana Research 26, 165–184.

Kobayashi, F., 1996. Middle Triassic (Anisian) foraminifers from Kaizawa Formation, southern Kanto Mountains, Japan. Transactions and Proceedings of the Palaeontological Society of Japan, New Series 183, 528–539.

Kobayashi, F., Martini, R., Zaninetti, L., 2005. Anisian foraminifers from allochthonous limestones of the Tanoura formation (Kurosegawa Terrane, West Kyushu, Japan). Geobios, 38, 751-763.

Kobayashi, F., Martini, R., Rettori, R., Zaninetti, L., Ratanasthien, B., Saegusa, H., Nakaya, H., 2006. Triassic foraminifers of the Lampang Group (Northern Thailand). Journal of Asian Earth Sciences, 27, 312-325.

Lacassin, R., Leloup, P.H., Trinh, P.T., Tapponnier, P., 1998. Unconformity of red sandstones in north Vietnam: field evidence for Indosinian orogeny in northern Indochina? Terra Nova 10, 106–111.

Lai, C.-K., Meffre, S., Crawford, A.J., Zaw, K., Xue, C.-D., Halpin, J.A., 2014. The Western Ailaoshan Volcanic Belts and their SE Asia connection: A new tectonic model for the Eastern Indochina Block. Gondwana Research 26, 52–74. doi:10.1016/j.gr.2013.03.003

Lan, C.-Y., Chung, S.-L., Lo, C.-H., Lee, T.-Y., Wang, P.-L., Li, H., Van Toan, D., 2001. First evidence for Archean continental crust in northern Vietnam and its implications for crustal and tectonic evolution in Southeast Asia. Geology 29, 219–222.

Lawrence, R.L., Cox, R., Mapes, R.W., Coleman, D.S., 2011. Hydrodynamic fractionation of zircon age populations. Geological Society of America Bulletin 123, 295–305. doi:10.1130/B30151.1

Leloup, P.H., Lacassin, R., Tapponnier, P., Schärer, U., Zhong, D., Liu, X., Zhang, L., Ji, S., Trinh, P.T., 1995. The Ailao Shan-Red River shear zone (Yunnan, China), Tertiary transform boundary of Indochina. Tectonophysics 251, 3–84.

Lepvrier, C., Maluski, H., Van Vuong, N., Roques, D., Axente, V., Rangin, C., 1997. Indosinian NW-trending shear zones within the Truong Son belt (Vietnam) ^{40}Ar-^{39}Ar Triassic ages and Cretaceous to Cenozoic overprints. Tectonophysics 283, 105–127.

Lepvrier, C., Maluski, H., Tich, V.V., Leyreloup, A., Thi, P.T., Vuong, N.V., 2004. The Early Triassic Indosinian orogeny in Vietnam (Truong Son Belt and Kontum Massif); implications for the geodynamic evolution of Indochina. Tectonophysics 393, 87–118.

Lepvrier, C., Vuong, N.V., Maluski, H., Thi, P.T., Vu, T.V., 2008. Indosinian tectonics in Vietnam. Comptes Rendus Geosciences 340, 94–111.

Lepvrier, C., Faure, M., Van, V.N., Vu, T.V., Lin, W., Trong, T.T., Hoa, P.T., 2011. North-directed Triassic nappes in Northeastern Vietnam (East Bac Bo). Journal of Asian Earth Sciences 41, 56–68. doi:10.1016/j.jseaes.2011.01.002

Li, M., Huang, C., Hinnov, L., Chen, W., Ogg, J., Tian, W., 2018. Astrochronology of the Anisian stage (Middle Triassic) at the Guandao reference section, South China. Earth and Planetary Science Letters 482, 591–606. doi:10.1016/j.epsl.2017.11.042

Li, P., Rui, G., Junwen, C., Ye, G., 2004. Paleomagnetic analysis of eastern Tibet: implications for the collisional and amalgamation history of the Three Rivers Region, SW China. Journal of Asian Earth Sciences 24, 291–310. doi:10.1016/j.jseaes.2003.12.003

Lin, J.X., Zheng, Y.M., 1978. Triassic foraminifers. In: Hubei Institute of Geological Sciences (Ed.), Paleontological Atlas of Central South China 4 (Microfossils). Geological Publishing House, Beijing, pp. 43–49 (in Chinese).

Liu, J., Tran, M.-D., Tang, Y., Nguyen, Q.-L., Tran, T.-H., Wu, W., Chen, J., Zhang, Z., Zhao, Z., 2012. Permo-Triassic granitoids in the northern part of the Truong Son belt, NW Vietnam: Geochronology, geochemistry and tectonic implications. Gondwana Research. 22, 628–644.

Liu, F., Wang, F., Liu, P., Liu, C., 2013. Multiple metamorphic events revealed by zircons from the Diancang Shan–Ailao Shan metamorphic complex, southeastern Tibetan Plateau. Gondwana Research 24, 429–450. doi:10.1016/j.gr.2012.10.016

Liu, H., Wang, Y., Cawood, P.A., Fan, W., Cai, Y., Xing, X., 2015. Record of Tethyan ocean closure and Indosinian collision along the Ailaoshan suture zone (SW China). Gondwana Research. 27, 1292–1306. doi:10.1016/j.gr.2013.12.013

Lowe, D.R., 1982. Sediment gravity flows: II Depositional models with special reference to the deposits of high-density turbidity currents. Journal of Sedimentary Research 52, 279–297.

Ludwig, K.R., 1998. On the Treatment of Concordant Uranium-Lead Ages. Geochimica and Cosmochimica Acta 62, 665–676.

Ludwig, K.R., 2012. User's Manual for a geochronological toolkit for Microsoft Excel. Berkeley Geochronological Center 75.

Malusa, M.G., Carter, A., Limoncelli, M., Villa, I.M., Garzanti, E., 2013. Bias in detrital zircon geochronology and thermochronometry. Chemical Geology 359, 90–107. doi:10.1016/j.chemgeo.2013.09.016

Martini, R., Zaninetti, L., Cornée, J.-J., Villeneuve, M., Tran, N., Ta, T.T., 1998. Occurrence of Triassic foraminifers in carbonates deposits from the Ninh Binh Area (North Vietnam). Compte Rendus l'Académie des Sciences de Paris, Sciences de la Terre des Planètes 326, 113–119.

Maurizot, P., 2014. Evolution and sedimentation in a forebulge environment: example of the late Eocene Uitoé Limestone, New Caledonia, Southwest Pacific, New Zealand Journal of Geolgy and Geophysic 57, 390–401. doi:10.1080/00288306.2014.938085

Metcalfe, I., 1988, Origin and assembly of south-east Asian continental terranes, *in* Audley-Charles, M.G. and Hallam, A. eds., Gondwana and Tethys, The Geological Society, London, Special Publication 37, 101–118.

Metcalfe, I., 2011. Tectonic framework and Phanerozoic evolution of Sundaland. Gondwana Research 19, 3–21.

Metcalfe, I., 2012. Changhsingian (Late Permian) conodonts from Son La, northwest Vietnam and their stratigraphic and tectonic implications. Journal of Asian Earth Sciences 50, 141–149. doi:10.1016/j.jseaes.2012.01.002

Metcalfe, I., 2013. Gondwana dispersion and Asian accretion: Tectonic and palaeogeographic evolution of eastern Tethys. Journal of Asian Earth Sciences 66, 1–33. doi:10.1016/j.jseaes.2012.12.020

Miall, A.D., 1996. The geology of fluvial deposits. Springer, p. 582

Moecher, D., Samson, S., 2006. Differential zircon fertility of source terranes and natural bias in the detrital zircon record: Implications for sedimentary provenance analysis. Earth and Planetary Science Letters 247, 252–266. doi:10.1016/j.epsl.2006.04.035

Mong, D.M., Canh, L.T., Quang, P.V., Phuc, P.T., Thang, P.X., Lan, U.V., 2004. Geology and mineral resources of Ninh Binh sheet (F-48-XXXIV), department of geology and minerals of Vietnam, Ha Noi.

Mulder, T., Alexander, J., 2001. The physical character of subaqueous sedimentary density flows and their deposits. Sedimentology 48, 269–299.

My, B.P., Hoanh, N.V., Ky, P.V., Tuyet, T.D., 2004. Geology and Mineral Resources of Kim Binh – Lao Cai sheet (F-48-VIII and F-48-XIV), Department of Geology and Minerals of Vietnam, Ha Noi.

Nalpas, T., Dabard, M.-P., Ruffet, G., Vernon, A., Mpodozis, C., Loi, A., Hérail, G., 2008. Sedimentation and preservation of the Miocene Atacama Gravels in the Pedernales–Chanaral Area, Northern Chile: Climatic or tectonic control? Tectonophysics 459, 161–173. doi:10.1016/j.tecto.2007.10.013

Nakano, N., Osanai, Y., Minh, N.T., Miyamoto, T., Hayasaka, Y., Owada, M., 2008. Discovery of high-pressure granulite-facies metamorphism in northern Vietnam: Constraints on the Permo-Triassic Indochinese continental collision tectonics. Comptes Rendus Geoscience 340, 127–138. doi:10.1016/j.crte.2007.10.013

Nakano, N., Osanai, Y., Sajeev, K., Hayasaka, Y., Miyamoto, T., Minh, N.T., Owada, M., Windley, B., 2010. Triassic eclogite from northern Vietnam: inferences and geological

significance. Journal of Metamorphic Geology 28, 59–76. doi:10.1111/j.1525-1314.2009.00853.x

Nemchin, A.A., Cawood, P.A., 2005. Discordance of the U–Pb system in detrital zircons: Implication for provenance studies of sedimentary rocks. Sedimentary Geology 182, 143–162.

Postma, G., 1990. Depositional architecture and facies of river and fan deltas: a synthesis, in: Collela, A., David, B.P. (Eds.), Coarse-Grained Deltas. International Association of Sedimentology Special Publication, p. 13–28.

Rettori R., 1995. Foraminiferi del Trias inferiore e medio della Tetide: revisione tassonomica, stratigraphica ed interpetazione foligenetica. Publications of the Geological and Palaeontological division of the University of Geneva 18, University of Geneva, pp 147.

Ridd, M.F., 1971. South-East Asia as a part of Gondwanaland. Nature 234, 531–533.

Roger, F., Jolivet, M., Maluski, H., Respaut, J.-P., Münch, P., Paquette, J.-L., Tich, V.V., Vuong, N.V., 2014. Emplacement and cooling of the Dien Bien Phu granitic complex: Implications for the tectonic evolution of the Dien Bien Phu Fault (Truong Son Belt, NW Vietnam). Gondwana Research 26, 785–801.

Rossignol, C., 2015. Evolution géodynamique du domaine Est Téthysien (Asie du Sud Est) du Permien supérieur au Trias supérieur: étude des bassins sédimentaires et des séries volcano-sédimentaires associées. Mémoires Géosciences Rennes, p. 417, ISBN: 2-914375-95-6

Rossignol, C., Bourquin, S., Poujol, M., Hallot, E., Dabard, M.-P., Nalpas, T., 2016. The volcaniclastic series from the Luang Prabang Basin, Laos: A witness of a triassic magmatic arc ? Journal of Asian Earth Sciences 120, 159–183. doi:10.1016/j.jseaes.2016.02.001

Rubatto, D., 2002. Zircon trace element geochemistry: partitioning with garnet and the link between U–Pb ages and metamorphism. Chemical Geology 184, 123–138. doi:10.1016/S0009-2541(01)00355-2

Shellnutt, J.G., Zhou, M.-F., Yan, D.-P., Wang, Y., 2008. Longevity of the Permian Emeishan mantle plume (SW China): 1 Ma, 8 Ma or 18 Ma? Geological Magazine 145, 373–388. doi:10.1017/S0016756808004524

Shellnutt, J.G., Denyszyn, S.W., Mundil, R., 2012. Precise age determination of mafic and felsic intrusive rocks from the Permian Emeishan large igneous province (SW China). Gondwana Research 22, 118–126. doi:10.1016/j.gr.2011.10.009

Shi, G.R., Shen, S.Z., 1998. A Changhsingian (Late Permian) brachiopod fauna from Son La, northwest Vietnam. Journal of Asian Earth Sciences 16, 501–511. doi:10.1016/S0743-9547(98)00028-2

Shi, M.-F., Lin, F.-C., Fan, W.-Y., Deng, Q., Cong, F., Tran, M.-D., Zhu, H.-P., Wang, H., 2015. Zircon U–Pb ages and geochemistry of granitoids in the Truong Son terrane, Vietnam: Tectonic and metallogenic implications. Journal of Asian Earth Sciences 101, 101–120. doi:10.1016/j.jseaes.2015.02.001

Sinclair, H.D., 1997. Tectonostratigraphic model for underfilled peripheral foreland basins: An Alpine perspective. Bulletin of the Geological Society of America 109, 324–346. doi:10.1130/0016-7606(1997)109<0324:TMFUPF>2.3.CO;2

Slama, J., Kosler, J., Condon, D.J., Crowley, J.L., Gerdes, A., Hanchar, J.M., Horstwood, M.S.A., Morris, G.A., Nasdala, L., Norberg, N., Schaltegger, U., Schoene, B., Tubrett, M.N., Whitehouse, M.J., 2008. Plesovice zircon — A new natural reference material for U–Pb and Hf isotopic microanalysis. Chemical Geology 249, 1–35. doi:10.1016/j.chemgeo.2007.11.005

Son, P., Thuc, D.D., Thang, N.D., Ty, T.V., 2005. Geology and mineral resources of Muong Kha – Son La sheet (F-48-XXV and F-48-XXVI), department of geology and minerals of Vietnam, Ha Noi.

Spencer, C.J., Kirkland, C.L., Taylor, R.J.M., 2016. Strategies towards statistically robust interpretations of in situ U – Pb zircon geochronology. Geoscience Frontiers 1–9. doi:10.1016/j.gsf.2015.11.006

Thanh, T.-D., Janvier, P., Phuong, T.H., 1996. Fish suggests continental connections between the Indochina and South China blocks in Middle Devonian time. Geology 24, 571–574.

Thanh, T.D., 2007. On some significant unconformities in the Paleozoic and Mesozoic stratigraphy of North Viet Nam. VNU Journal of Science, Earth Sciences 23, 137–146.

Thanh, N.X., Tu, M.T., Itaya, T., Kwon, S., 2011. Chromian-spinel compositions from the Bo Xinh ultramafics, Northern Vietnam: Implications on tectonic evolution of the Indochina block. Journal of Asian Earth Sciences 42, 258–267. doi:10.1016/j.jseaes.2011.02.004

Thanh T.-D., and Khuc, V., 2012, Stratigraphic Units of Vietnam (2nd ed), Vietnam National University Publisher, Hanoi, p. 554

Thomas, W.A., 2011. Detrital-zircon geochronology and sedimentary provenance. Lithosphere 3, 304–308. doi:10.1130/RF.L001.1

Tran, T.H., Lan, C.-Y., Usuki, T., Shellnutt, J.G., Pham, T.D., Tran, T.A., Pham, N.C., Ngoc, T.P., Izokh, A.E., Borisenko, A.S., 2015. Petrogenesis of Late Permian silicic rocks of Tu Le basin and Phan Si Pan uplift (NW Vietnam) and their association with the Emeishan large igneous province. Journal of Asian Earth Sciences 109, 1–19. doi:10.1016/j.jseaes.2015.05.009

Tri T.V., and Khuc V., 2011, Geology and Earth Resources of Vietnam, Publishing House for Science and Technology, Hanoi, p.646

Trung, N.M., Tsujimori, T., Itaya, T., 2006. Honvang serpentinite body of the Song Ma fault zone, Northern Vietnam: A remnant of oceanic lithosphere within the Indochina–South China suture. Gondwana Research 9, 225–230. doi:10.1016/j.gr.2005.06.012

Trung, N.M., Nuong, N.D., Itaya, T., 2007. Rb-Sr Isochron and K-Ar ages of igneous rocks from the Samnua Depression Zone in Northern Vietnam. Journal of Mineralogical and Petrological Sciences 102, 86–92. doi:10.2465/jmps.060628

Tuyet, T.D., Thuy, D.V., Lu, N.D., Than, N.H., Duong, P.V., Hung, T.T., 2005a. Geology and mineral resources of Khi Su – Muong Te sheet (F-48-VII and F-48-XIII), department of geology and minerals of Vietnam, Ha Noi

Tuyet, T.D., Thong, A.V., Hung, N.B., Hoi, N.V., Duong, P.V., 2005b. Geology and mineral resources of Phong Sa Ly – Dien Bien Phu sheet (F-48-XIX and F-48-XX), department of geology and minerals of Vietnam, Ha Noi

Usuki, T., Lan, C.-Y., Tran, T.H., Pham, T.D., Wang, K.-L., Shellnutt, L.G., Chung, S.-L., 2015. Zircon U–Pb ages and Hf isotopic compositions of alkaline silicic magmatic rocks in the Phan Si Pan-Tu Le region, northern Vietnam: Identification of a displaced western extension of the Emeishan Large Igneous Province. Journal of Asian Earth Sciences 97, 102–124. doi:10.1016/j.jseaes.2014.10.016

Vachard, D., Fontaine, H., 1988. Biostratigraphic importance of Triassic foraminifera and algae from South-East Asia. Revue de Paléobiologie, 7, 87–98.

van Achterbergh, E., Ryan, C.G., Jackson, S.E. and Griffin, W.L., 2001. Data reduction software for LA-ICP-MS. In Laser ablation-ICPMS in the earth science. P. Sylvester ed. Mineralogical Association of Canada. 29, 239-243.

Vermeesch, P., 2012. On the visualisation of detrital age distributions. Chemical Geology 312–313, 190–194. doi:10.1016/j.chemgeo.2012.04.021

Vuong, N.V., Hansen, B.T., Wemmer, K., Lepvrier, C., Tích, V.V., Thang, T.T., 2013. U/Pb and Sm/Nd dating on ophiolitic rocks of the Song Ma suture zone (northern Vietnam): Evidence for upper Paleozoic paleotethyan lithospheric remnants. Journal of Geodynamics 69, 140–147. doi:10.1016/j.jog.2012.04.003

Wang, S., Mo, Y., Wang, C., Ye, P., 2016. Paleotethyan evolution of the Indochina Block as deduced from granites in northern Laos. Gondwana Research, in press. doi:10.1016/j.gr.2015.11.011

Wen, S., Yeh, Y.-L., Tang, C.-C., Phong, L.H., Toan, D.V., Chang, W.-Y., Chen, C.-H., 2015. The tectonic structure of the Song Ma fault zone, Vietnam. Journal of Asian Earth Sciences 107, 26–34. doi:10.1016/j.jseaes.2015.03.046

Yan, Q., Metcalfe, I., Shi, X., 2017. U-Pb isotope geochronology and geochemistry of granites from Hainan Island (northern South China Sea margin): Constraints on late Paleozoic-Mesozoic tectonic evolution. Gondwana Research 49, 333–349. doi:10.1016/j.gr.2017.06.007

Zelazniewicz, A., Hoa, T.T., Larionov, A.N., 2013. The significance of geological and zircon age data derived from the wall rocks of the Ailao Shan–Red River Shear Zone, NW Vietnam. Journal of Geodynamics 69, 122–139. doi:10.1016/j.jog.2012.04.002

Zhang, R.Y., Lo, C.-H., Chung, S.-L., Grove, M., Omori, S., Iizuka, Y., Liou, J.G., Tri, T.V., 2013. Origin and Tectonic Implication of Ophiolite and Eclogite in the Song Ma Suture Zone between the South China and Indochina Blocks. Journal of Metamorphic Geology 31, 49–62.

Zhang, R.Y., Lo, C.-H., Li, X.-H., Chung, S.-L., Anh, T.T., Tri, T.V., 2014. U-Pb dating and tectonic implication of ophiolite and metabasite from the Song Ma suture zone,

northern Vietnam. American Journal of Science 314, 649–678. doi:10.2475/02.2014.07

Figures and tables caption

Figures

Figure 1. Simplified geological map of north Vietnam.

A. Tectonic subdivisions of southeast Asia.

The blocks are delimited by suture zones (definite or supposed): AS: Ailaoshan, CM: Changning Menglian, DQ-SH: Dian-Qiong – Song Hien, JH: Jinghong, LP: Luang Prabang; NU: Nan Uttaradit. Major Cenozoic faults: MY: Mae Yuam Fault, RRF: Red River Fault. SCF: Song Chay Fault, SDF: Song Da Fault, SMF: Song Ma Fault. Circled black star: location of a dated rhyolite in the extreme southern part of the Sam Nua Basin (251.9 ± 1.7 Ma; Shi M.-F. et al., 2015). Bold box refers to the area enlarged in Fig. 1B.

B. Simplified geological map of north Vietnam. The numbers refer to Table 1 for the available dating results on igneous and metamorphic rocks.

Areas investigated in this study are denoted with a red-circled capital letter: A: Ninh Binh (Fig. 4A); B: Muong Khen (Fig. 4B); C: Mai Son (Fig. 4C); D: Ban Hinh; E: Sop Cop (Fig. 5). Geological background after 6 geological maps of north Vietnam at the 1: 200 000 scale: Khi Su – Muong Te (Tuyet et al., 2005a); Kim Binh – Lao Cai (My et al., 2004); Muong Kha – Son La (Son et al., 2005); Phong Sa Ly – Dien Bien Phu (Tuyet et al., 2005b); Van Yen (Bao et al., 2004); Ninh Binh (Mong et al., 2004), the geological map of Laos (1: 1 500 000; United Nations publication, 1990) and the geological map of the

Yunnan Province (1: 500 000; Bureau of Geology and Mineral Resources of Yunnan Province, 1990).

Figure 2. Synthetic lithostratigraphic subdivisions of the Song Da Basin.

Compiled and simplified from Tri and Khuc (2011); Thanh and Khuc (2012) and this work (Appendix 1). The early Norian age here assigned to the Song Boi Fm. is revised according to the ammonoid fossil assemblage reported for this formation by Tri and Khuc (2011) and Thanh and Khuc (2012). See Appendix 1 for further details.

The used stratigraphic chart is the International Chronostratigraphic Chart v2017/02 (Cohen et al., 2013, updated). Perm.: Permian, Loping.: Lopingian, Ca.: Capitanian, Wu.: Wuchiapingian, Ch.: Changsingian, In.: Induan, Ole.: Olenekian.

Figure 3. Synthetic lithostratigraphic subdivisions of the Sam Nua Basin.

Compiled and simplified from Tri and Khuc (2011) and Thanh and Khuc (2012), and modified after geochronological constraints obtained by Hieu et al. (2017). The stratigraphic subdivisions were established from regional lithostratigraphic correlations and fossil contents. See text and Appendix 1.

Perm.: Permian, Loping.: Lopingian, Ca.: Capitanian, Wu.: Wuchiapingian, Ch.: Changsingian, In.: Induan, Ole.: Olenekian.

Figure 4. Geological maps and cross-sections of investigated localities in the Song Da Basin.

Letters in this figure correspond to the red-circled capital letters in Fig. 1B.

A. Geological map of the Ninh Binh area.

B. Geological map (B1) and cross section (B2) of the Muong Khen area.

C. Geological map (C1) and cross section (C2) of the Mai Son area.

Geological maps modified from Mong et al., 2004; Bao et al., 2004; Son et al., 2005, and Tuyet et al., 2005b. No geological map available at appropriate scale for the Banh Hinh area.

Figure 5. Geological map and cross-section of the Sop Cop area, northen part of the Sam Nua Basin.

This area corresponds to the red-circled capital letter E in Fig. 1B.

A. Geological map, modified from Son et al. (2005).

B. Cross-section.

Figure 6. Field and thin section photographs of representative outcrops and samples from the Co Noi Formation, Song Da Basin.

A, B. Photographs illustrating the unconformable relationship between the basement (Cam Thuy Fm.) and the Co Noi Fm. at the Ban Hinh locality. B: view from the NE of the outcrop illustrated in A, showing the Gt facies conglomerates (Table 2) of the Co Noi Fm. overlying unconformably the volcaniclastic rocks of the Cam Thuy Fm.

C. Interpretation of A: the volcaniclastic mafic lappilistone of the Cam Thuy Fm. are unconformably overlain by the Co Noi Fm. Pervasive quartz-epidote veins attest that these rocks underwent a greenschist-facies metamorphism. Facies codes: Table 2.

D. Coarse-grained, calcite-cemented, lithic arenite (sample VN 12-51, plane-polarized light) from the Ban Hinh locality, Co Noi Fm. 1: lithic fragment made up of sparitic calcite. 2: sedimentary lithic fragment. 3: silty lithic fragment. 4: calcite-cemented lithic fragment, possibly of intraformational origin.

E. Feldspathic arenite (sample VN 12-22, plane-polarized light) from the Mai Son locality, Co Noi Fm. 1: sub-rounded monocrystalline quartz grain. 2: weathered, sub-angular alkali feldspar grain. 3: rounded volcaniclasts displaying various microlitic textures and weathering.

F. Lithic arenite (sample VN 12-14, plane-polarized light) from the Muong Khen locality, Co Noi Fm. 1: sub-angular weathered feldspar. 2: silty lithic fragment. 3: rounded volcaniclasts displaying various microlitic textures and weathering. 4: polycrystalline quartz grain.

Figure 7. Sedimentological log for the Co Noi Formation.

Sedimentological section of the Co Noi Fm. at the Ban Hinh locality (red circled capital letter D in Fig. 1B) and location of the sample used for petrographic and geochronological (VN 12-51; Fig. 8E and F) analyses. Facies codes: see Table 2. Depositional environments correspond to unequivocal terrestrial environments; here a distal braided plain with megaripple migration and unconfined flow. See text for discussion.

Figure 8. Geochronological diagrams for the sedimentary rocks from the Co Noi Formation.

All the diagrams were generated using Isoplot/Ex 3.00 (Ludwig, 2012).

A, B. Lithic arenite VN 12-14, Muong Khen locality.

C, D. Feldspathic arenite VN 12-22, Mai Son locality.

E, F. Lithic arenite VN 12-51, Ban Hinh locality.

Diagrams on the left (A, C and E) display all the analyses (except the few highly discordant ones plotting out of the boxes). Diagrams on the right (B, D and F) focus on the maximum depositional ages.

Figure 9. Histograms and age probability distribution diagrams for the sedimentary rocks from the Co Noi Formation.

A. Muong Khen area.

B. Mai Son area.

C. Banh Hinh area.

The histograms were generated using an identical bin width. The kernel densities were estimated using an identical bandwith (h) from the concordant detrital ages. The open circles below each diagram denote the individual analyses used to generate the diagrams (using Density Plotter 7.3; Vermeesch, 2012). N_a: number of analyses, N_{zr}: number of zircon grains.

Figure 10. Synthetic lithostratigraphic log for the Dong Giao Formation.

This synthetic log, along with samples used for the biostratigraphic determinations, was derived from extensive investigations in the Ninh Binh area (Fig. 4A). Foraminifers from samples V10 and V12 have already been described and illustrated in Martini et al. (1998). Letters *a* to *f* refer to the members identified in this formation. See text for detailed description.

Figure 11. Representative foraminifers from the Dong Giao Formation.

A, B. *Citaella dinarica* Kochansky-Devide and Pantic, 1966, sample V95. *Citaella dinarica* is indicative of the Middle Anisian (Pelsonian).

C, D, E. *Postcladella* sp., C, E: sample V143; D: sample V140.

F, G. *Endotriada tyrrhenica* Vachard, Martini, Rettori and Zaninetti, 1994, sample V78.

Scale bar is 100 micrometers. Sampling sites: Appendix 2.

Figure 12. Field and thin section photographs of representative outcrops and samples from the Dong Trau Formation, associated rhyolites and Song Ma granite, Sop Cop area, Sam Nua Basin.

A. Mafic dikes crosscutting the high-grade metamorphic basement.

B. Disharmonic folds within the Dong Trau Fm.

C. Volcanic bomb deforming silt layers in the Dong Trau Fm., interpreted as corresponding to an explosive volcanic activity (fall deposit) coeval to the sedimentation. Hammer for scale.

D. Volcaniclastic wacke (sample VN 12-38, plane-polarized light). 1: sub-angular, weathered plagioclase. 2: chlorite. 3: rounded, weathered volcaniclast displaying a microlitic texture.

E. Volcaniclastic wacke (sample VN 12-37, collected ca. 200 m to the south of the sample VN 12-38, cross-polarized light). 1: corroded quartz with embayments. 2: strongly weathered, rounded lithic fragments. 3: matrix comprising quartz and chlorite.

F. Porphyritic rhyolite (sample VN 12-27, cross-polarized light). 1: rhyolitic quartz phenocryst with embayments against the groundmass. 2: crypto- to microcrystalline groundmass, mostly made up of quartz and feldspar (devitrification).

G. Porphyritic rhyolite (sample VN 12-41, cross-polarized light). 1: perthitic orthoclase (recrystallized sanidine) phenocryst. 2: spherulite from the groundmass (devitrification). 3: see F-2. 4: euhedral plagioclase phenocryst. 5: euhedral opaque microphenocryst.

Figure 13. Geochronological diagrams for the sedimentary rocks from the Dong Trau and Suoi Bang formations.

All the diagrams were generated using Isoplot/Ex 3.00 (Ludwig, 2012). Legend: see Fig. 8.

A, B. Volcaniclastic wacke VN 12-38, Dong Trau Fm. The dotted error ellipse corresponds to a concordant analysis which is younger than the maximum depositional age, interpreted as the result of Pb loss.

C, D, E. Lithic arenite VN 12-29, Suoi Bang Fm.

F, G, H. Quartz arenite VN 12-31, Suoi Bang Fm.

The diagrams on the left column (A, C, D, F and G) show all the analyses (except the few highly discordant ones that plot out of the boxes). The diagrams on the right column (B, E and H) focus on the maximum depositional ages.

Figure 14. Histograms and age probability distribution diagrams for the sedimentary rocks from the Dong Trau and Suoi Bang formations.

A. Dong Trau Fm. Inset: histogram and age probability distribution between 200 and 300 Ma.

B. Suoi Bang Fm. Inset: histogram and age probability distribution between 200 and 300 Ma.

C. Suoi Bang Fm.

The histograms were generated with an identical bin width, except for the insets in Fig. 16A and 16B. The kernel densities were estimated using an identical bandwith (h) from the concordant ages. The open circles below each diagram denote the individual analyses used to generate the diagrams (using Density Plotter 7.3; Vermeesch, 2012). N_a: number of analyses, N_{zr}: number of zircon grains.

Figure 15. Geochronological diagrams for the rhyolite samples interbedded within the Dong Trau Fm.

All the diagrams were generated using Isoplot/Ex 3.00 (Ludwig, 2012).

A, B. Dong Trau Rhyolite, sample VN 12-27.

C, D. Dong Trau Rhyolite, sample VN 12-41.

The diagrams on the left column (A and C) show all the analyses (except the few highly discordant ones that plot out of the boxes). The diagrams on the right column (B and D) display only concordant analyses and focus on the emplacement ages of the rhyolites. Dark grey ellipses correspond to the concordant analyses used to calculate the concordia date. Light grey ellipses correspond to concordant analyses not included in the concordia age calculation. Light grey dotted ellipses are interpreted to correspond to analyses that suffered Pb loss. Error ellipses are depicted at the 2 σ level.

Figure 16. Outcrop scale and thin section photographs of representative samples from the Suoi Bang Formation, Sam Nua Basin.

A. Unconformity between the Dong Trau Fm. (here represented by volcanic rocks) and the overlying Suoi Bang Fm.

B. Representative facies of the Suoi Bang Fm. Facies code: see Table 2.

C. Lithic arenite (sample VN 12-29, plane-polarized light). 1: angular, monocrystalline quartz grain. 2: weathered and rounded volcaniclast displaying a microlitic texture. 3: cryptocrystalline lithic fragments.

D. Quartz arenite (sample VN 12-31, cross-polarized light). 1: polycrystalline quartz grain. 2: muscovite flakes. 3: microcrystalline lithic fragment.

Figure 17. Sedimentological log for the Suoi Bang Formation.

Sedimentological section of the Suoi Bang Fm. at the Sop Cop locality with structural dips and sample location (VN 12-29). Here, the A1 facies association is lacking, and the A2 facies association directly overlies the Dong Trau Fm. Facies codes: see Table 2. Deposition unambiguously took place in a terrestrial setting, and the depositional environments, interpreted from facies associations (see text), correspond to alluvial fan depositional evolving to braided alluvial plain.

Figure 18. Revised and current Triassic stratigraphy of the Song Da Basin.

A. Revised stratigraphy. The revisions concern both the depositional environments and the ages of some of the main formations of the basin.

B. For comparison, extracted from Fig. 2, the current lithostratigraphic subdivisions (after Tri and Khuc, 2011; and Thanh and Khuc, 2012). Notice that the Nam Tham Fm., which has not been investigated in this work, does not appear in Fig. 18A.

In.: Induan, Ol.: Olenekian.

Figure 19. Integrated stratigraphic and structural framework for the Song Da Basin during the Early Triassic.

A. Sedimentary fill of the Song Da Basin.

B. Proposed tectonic setting for the Song Da Basin during the Early Triassic.

C. Schematic chronostratigraphic representation of the sedimentary fill of the Song Da Basin.

Figure 20. Revised and current stratigraphy for the Sam Nua Basin.

A. Revised stratigraphy. The revisions concern both depositional environments and the ages of some of the main formations of basin. The depositional age of the Dong Trau Fm. is deduced from interbedded volcanic rocks at 248.3 ± 1.6 Ma and 246.7 ± 1.9 Ma and a maximum depositional age at 246.4 ± 2.4 Ma (this study). As the Dong Trau Fm. is crosscut by the Song Ma Granite, (Son et al., 2005), emplaced as early as 263 ± 5 Ma (Hieu et al., 2017) the deposition of the Dong Trau Fm. might have started during the Guadalupian or before. The Suoi Bang Fm. deposited, at least in part, during the Rhaetian-Early Jurassic (Table S1; Appendix 1). This is consistent with the maximum depositional age of 226.1 ± 3.0 Ma obtained for a sample collected in this formation (this study) and other geochronological and structural constraints (Fig. 3, see however Appendix 1).

B. For comparison, extracted from Fig. 3, the current lithostratigraphic subdivisions (after Tri and Khuc, 2011; and Thanh and Khuc, 2012). Notice that the Hoang Mai Fm., which was not investigated in the present work, does not appear in Fig. 14A.

Perm.: Permian, Loping.: Lopingian, Ca.: Capitanian, Wu.: Wuchiapingian, Ch.: Changsingian, In.: Induan, Ole.: Olenekian.

Figure 21. Summary of the revised stratigraphic subdivisions of the Sam Nua and the Song Da basin.

The letters A to D correspond to the time periods of the schematic cross-sections presented in Fig. 22. Coordinates refer to the present-day datum. Wuchia.: Wuchiapingian, Ch.: Changsingian, In.: Induan, Ole.: Olenekian.

Figure 22. Schematic geodynamic evolution model for northern Vietnam.

Schematic cross-sections showing the possible configuration of the South China and Indochina plates during the late Permian to the Late Triassic.

A. Late Permian. A forearc position is inferred for the Sam Nua Basin as it was opened to marine influences during the Early Triassic.

B. Middle Triassic. The Song Da Basin underwent flexural subsidence related to the developing Indosinian thrust belt.

C. Late Triassic. Culmination of the Indosinian orogeny and formation of high-pressure metamorphic rocks in the internal domains of the chain. The Sam Nua and Song Da basins were subjected to intense erosion that lead to the formation of the Indosinian unconformity (see text for discussion).

D. Latest Triassic (Rhaetian). The Sam Nua and Song Da basins became syn- to post-orogenic foreland basins, mostly receiving the products of the erosion of the Indosinian mountain belt.

Tables

Table 1. Compilation of selected radiometric dates.

Table 2. Description of the main sedimentological facies.

Table 3. Main petrographic features of the analyzed samples.

Table 4. Summary of the geochronological results.

Appendices

Appendix 1. Lithostratigraphic subdivisions and age constraints for the formations of the Song Da and Sam Nua basins.

Appendix 2. Coordinates of analyzed samples.

Appendix 3. Analytical methods.

Appendix 4. Analytical results of LA-ICP-MS U-Pb zircon dating.

Table 1. Compilation of selected radiometric dates.

Symbol in Fig. 1	Rock type	Isotopic system - mineral	Age (Ma)[a]	Reference
Protolith age of oceanic crust material				
i	Metagabbro	Sm-Nd - Amp+Clz+WR	387 ± 56*	Vuong et al., 2013
ii	Metagabbro	Sm-Nd - Amp+Px+WR	338 ± 24*	Vuong et al., 2013
iii	Gabbro	Sm-Nd - Amp+WR	332 ± 45**	Vuong et al., 2013
iv	Plagiogranite	Crystallization age not determined – see below		Vuong et al., 2013
v	Pyroxenite	U-Pb - Zrc	340 ± 29	Zhang R.Y. et al., 2014
vi	Amphibolite	Sm-Nd - Amp+Ttn+WR	315 ± 92	Vuong et al., 2013
vii	Amphibolite	Crystallization age not determined – see below		Vuong et al., 2013
viii	Metagabbro	Sm-Nd - Ttn+WR	313 ± 32*	Vuong et al., 2013
Peak metamorphism age				
a	Amphibolite	U-Pb - Zrc	245.8 ± 1.7	Liu F. et al., 2013
b	HP, HT metamorphic rock	U-Pb - Zrc	245 ± 5	Carter et al., 2001
c	Migmatite	U-Pb - Zrc	267 ± 1 and 260 ± 1	Zelazniewicz et al., 2013
d	Micaschist	Th-U-Pb - Mnz	220.1 ± 3.5	Gilley et al., 2003
e	Migmatite	U-Pb - Zrc	264.4 ± 1.3	Zelazniewicz et al., 2013
f	Eclogite	Th-U-Pb - Mnz	243 ± 4	Nakano et al., 2010
g	Eclogite	Th-U-Pb - Mnz	243 ± 4	Nakano et al., 2010
h	Amphibolite	U-Pb - Zrc	239.3 ± 2.6	Zhang R.Y. et al., 2014
i	HP granulite***		nd	Nakano et al., 2008
j	Amphibolite	U-Pb - Zrc	228.0 ± 2.9	Zhang R.Y. et al., 2014
k	Eclogite	U-Pb - Zrc	230.5 ± 8.2	Zhang R.Y. et al., 2013
iv	Plagiogranite – age of metamorphic resetting	U-Pb - Zrc	222 ± 4	Vuong et al., 2013
vi	Amphibolite	U-Pb - Ttn	265.4 ± 3.7	Vuong et al., 2013
vii	Amphibolite	U-Pb - Zrc	241.3 ± 5.3	Vuong et al., 2013
Crystallization age of magmatic rocks				
1	Monzogranite	U-Pb - Zrc	251.9 ± 1.4	Liu H. et al., 2015
2	Granite	U-Pb - Zrc	252.2 ± 7.7	Usuki et al., 2015
3	Granite	U-Pb - Zrc	259.0 ± 3.5	Usuki et al., 2015
4	Alkali granite	U-Pb - Zrc	260 ± 3	Zelazniewicz et al., 2013
5	Granite	U-Pb - Zrc	253 ± 2	Hieu et al., 2013
6	Granite	U-Pb - Zrc	253 ± 2	Hieu et al., 2013
7	Granite	U-Pb - Zrc	251 ± 2	Hieu et al., 2013
8	Granite	U-Pb - Zrc	253.3 ± 2.6	Usuki et al., 2015
9	Granite	U-Pb - Zrc	257.7 ± 3.7	Usuki et al., 2015
10	Granite	U-Pb - Zrc	248.7 ± 6.9	Usuki et al., 2015
11	Granite	U-Pb - Zrc	256.3 ± 6.0	Usuki et al., 2015
12	Granite	U-Pb - Zrc	253.0 ± 2.4	Usuki et al., 2015
13	Rhyolite	U-Pb - Zrc	253.2 ± 2.5	Usuki et al., 2015
14	Granite	U-Pb - Zrc	252.3 ± 5.2	Usuki et al., 2015
15	Granite	U-Pb - Zrc	253.7 ± 2.5	Usuki et al., 2015
16	Rhyolite	U-Pb - Zrc	251.5 ± 5.0	Usuki et al., 2015
17	Rhyolite	U-Pb - Zrc	261.9 ± 3.5	Usuki et al., 2015
18	Rhyolite	U-Pb - Zrc	257.9 ± 3.3	Usuki et al., 2015
19	Rhyolite	U-Pb - Zrc	258.3 ± 3.2	Usuki et al., 2015
20	Rhyolite	U-Pb - Zrc	259.7 ± 3.1	Usuki et al., 2015
21	Rhyolite	U-Pb - Zrc	259.8 ± 3.1	Usuki et al., 2015
22	Rhyolite	U-Pb - Zrc	259.1 ± 3.2	Usuki et al., 2015
23	Rhyolite	U-Pb - Zrc	254.7 ± 2.6	Usuki et al., 2015
24	Granite	Pb-Pb - Zrc	227.7± 9.6	Chen Z. et al., 2014
25	Rhyodacite	U-Pb - Zrc	248 ± 2	Zelazniewicz et al., 2013
26	Granite	U-Pb - Zrc	242.4 ± 2.2	Hoa et al., 2008
27	Gabbro	U-Pb - Zrc	275.5 ± 4.6	Liu J. et al., 2012
28	Gabbroic diorite	U-Pb - Zrc	248.0 ± 2.0	Liu J. et al., 2012
29	Granodiorite	U-Pb - Zrc	277 ± 2	Roger et al., 2014
30	Granodiorite	U-Pb - Zrc	296 ± 3	Hieu et al., 2017
31	Granodiorite	U-Pb - Zrc	289 ± 5	Hieu et al., 2017
32	Granite	U-Pb - Zrc	230 ± 1	Roger et al., 2014
33	Granodiorite	U-Pb - Zrc	225 ± 3	Roger et al., 2014
34	Granodiorite	U-Pb - Zrc	229.3 ± 3.1	Liu J. et al., 2012
35	Granodiorite	U-Pb - Zrc	242.2 ± 1.3	Shi M.-F. et al., 2015
36	Monzonite	U-Pb - Zrc	201.8 ± 3.6	Liu J. et al., 2012
37	Granodiorite	U-Pb - Zrc	233 ± 4	Hieu et al., 2017
38	Granodiorite	U-Pb - Zrc	231 ± 4	Hieu et al., 2017
39	Granite	U-Pb - Zrc	244 ± 5	Hieu et al., 2017
40	Tonalite	U-Pb - Zrc	256 ± 7	Hieu et al., 2017
41	Granite	U-Pb - Zrc	263 ± 5	Hieu et al., 2017
42	Granite	U-Pb - Zrc	260 ± 5	Hieu et al., 2017
43	Rhyolite	U-Pb - Zrc	248.3 ± 1.6	This study

44	Rhyolite	U-Pb - Zrc	246.7 ± 1.9	This study
45	Granite	U-Pb - Zrc	239 ± 6	Hieu et al., 2017
46	Diorite	U-Pb - Zrc	262 ± 4	Hieu et al., 2017
47	Diorite	U-Pb - Zrc	270.9 ± 3.3	Liu J. et al., 2012
48	Granodiorite - tonalite	U-Pb - Zrc	236.3 ± 3.2	Wang S. et al., 2016
49	Granodiorite - tonalite	U-Pb - Zrc	238.6 ± 3.2	Wang S. et al., 2016
50	Granodiorite - tonalite	U-Pb - Zrc	249.0 ± 1.9	Wang S. et al., 2016

Zrc: zircon; Px: pyroxene; Ttn: titanite; Amp: amphibole; Clz: clinozoisite; Mnz: monazite; WR: whole rock.
[a]: uncertainties are given at the 2σ level
*: isochron based on 2 points only; **: isochron based on 3 points; ***: reworked sample, collected as a pebble in a conglomerate; nd: not determined.

Table 2. Main sedimentary facies of the Song Da and Sam Nua basins.

Code	Lithofacies	Sedimentary structures	Depositional processes
Siltstone and mudstone			
Fm	Relatively homogeneous clay to silt.	Massive.	Deposition from suspension.
Fc	Blue to black clay, rich in organic matter.	Planar lamination.	Deposition from suspension.
Sandstone			
Sm	Fine to coarse sand, relatively well sorted, sub-rounded to rounded grains with various mineralogy and texture (lithic fragments, quartz).	Massive.	Subaerial hyperconcentrated density flow (Lowe, 1982; Mulder and Alexander, 2001); rapid suspension fallout (Postma, 1990).
St	Coarse sand to gravel with sometimes scattered rounded pebbles of quartz and siltstones.	Through cross-stratifications underlined by grain-size variations. Erosive basal boundary.	Tractive current, upper part of the lower flow regime, 3D megaripple migration (Miall, 1996).
Sh	Coarse to very coarse sand, with some scattered pebbles.	Planar or sub-planar.	Tractive current, upper flow regime (Miall, 1996).
Conglomerate			
Gmm	Very poorly sorted (cm to m in diameter) angular to rounded pebbles and boulders, nearly monogenic (rhyolitic clasts with a minor amount of quartz pebbles). Matrix supported, with a coarse-grained matrix.	Erosional basal boundaries.	Debris flow (Miall, 1996).
Gh	Poorly sorted (cm to m in diameter) angular pebbles and boulders, polygenic (quartz, siltstones, basaltic to rhyolitic clasts). Clasts-supported with a sandy to silty matrix.	Crude horizontal stratification. Normally-graded	Upper flow regime (Miall, 1996).
Gt	Sub-angular to rounded pebbles (cm to dm).	Through cross stratification (L = pluri-metric, h = 10 to 80 cm). Normally-graded.	Tractive current, upper part of the lower flow regime (Miall, 1996).

Table 3. Main petrographic features of the analyzed samples.

Sample	Petrography
Song Da Basin	
Co Noi Formation	
VN 12-14	Lithic arenite. Rounded to sub-angular weathered alkali feldspar and plagioclase. Rounded and weathered volcaniclasts displaying microlithic texture. Polycrystalline quartz grains. Monocrystalline and rounded to sub-rounded quartz grains. Microcrystalline lithic fragments. Epidote, chlorite, opaque minerals, zircon grains. Calcite veins.
VN 12-22	Feldsapthic arenite. Well-sorted (ca. 0.1 mm in diameter), sub-rounded to sub-angular elements. Monocrystalline, weathered feldspar (alkali and plagioclase) grains, sub-rounded to sub-angular quartz grains. Lithic fragments of various origins (volcaniclasts, sedimentary rock fragments?). Opaque minerals. Zircon grains.
VN 12-51	Calcite-cemented lithic arenite. Coarse-grained, sub-rounded to sub-angular, poorly sorted lithic fragments. The lithic fragments are strongly weathered and display various texture. When identifiable, some lithic fragments show microlitic or microgranular textures. Silty lithic fragments. Spartic calcite lithic fragments. Opaque minerals. Rare zircon grains.
Sam Nua Basin	
Dong Trau Formation	
VN 12-38	Volcaniclastic wacke. Monocrystalline, slightly weathered feldspar, monocrystalline, rounded to sub-rounded quartz grains, sometimes of rhyolitic type (e.g., with embayment against volcanic groundmass or sedimentary matrix). Weathered, rounded (mm to cm in size) feldspathic lithic fragments with microgranular texture. These lithic fragments sometime contain zircon grains. Calcite (sparitic and micritic forms). Matrix made up of quartz and chlorite. Zircon grains as accessory minerals.
Dong Trau Rhyolites	
VN 12-27	Rhyolite with porphyritic texture. Quartz phenocrysts with embayement against the groundmass. The groundmass contains crystallized area made up of quartz grains showing equilibrated texture. A few opaque minerals. Zircon grains.
VN 12-41	Rhyolite with porphyritic texture. Perthitic orthoclase (recrystallized after sanidine) phenocrysts. The groundmass contains crystallized area made up of quartz grains showing equilibrated texture and spherolites, also indicative of a crystallization of amorphous groundmass. Opaque minerals. Zircons grains.
Suoi Bang Formation	
VN 12-29	Lithic arenite. Well sorted (ca. 0.2 mm in diameter) lithic fragments displaying microcrystalline and microgranular textures. Monocrystalline, mainly angular but sometimes sub-rounded quartz grains. Rounded, slightly weathered alkaline feldspar and rare plagioclase grains. White mica (muscovite) flakes, opaque minerals, chlorite and zircon grains.
VN 12-31	Quartz arenite. Well sorted, coarse (ca. 0.5 mm in diameter), sub-angular to sub-rounded quartz grains. Microgranular and microcrystalline, commonly sub-rounded, lithic fragments. White mica flakes underlining the stratification. Zircon grains displaying various shapes, from euhedral to rounded. Rutile, opaque minerals.

Table 4. Summary of the geochronological results.

Sample	Sedimentary and volcaniclastic rocks											
			Probability of concordance ≥ 10%, decay constants errors included									
	N_a	N_{zr}	N	Detection limits (%)				Maximum depositional age				
				$DL_{1(pL=0.5)}$	$DL_{1(pL=0.95)}$	$DL_{3(pL=0.5)}$	$DL_{1(pL=0.95)}$	Concordia age	± (2σ)	n	MSWD	Probability
Song Da Basin												
Co Noi Formation												
VN 12-14	110	104	33	2.1	8.7	8.1	17.9	243.1	2.3	6	0.86	0.58
VN 12-22	103	102	31	2.2	9.2	8.6	19.0	237.3	2.4	5	1.12	0.35
VN 12-51	10	4	2	29.3	77.6	n.a.	n.a.	242.6	4.1	2	0.74	0.53
Sam Nua Basin												
Dong Trau Formation												
VN 12-38	99	99	13	5.2	20.6	20.1	41.1	246.4	2.4	6	1.50	0.11
Suoi Bang Formation												
VN 12-29	198	196	39	1.8	7.4	6.8	15.3	226.1	3.0	3	1.03	0.40
VN 12-31	120	116	36	1.9	8.0	7.4	16.5	266.5	3.7	3	2.1	0.068
Dong Trau Rhyolites												
	N_a	N_{zr}	Concordia age						± (2σ)	n	MSWD	Probability
VN 12-27	50	47	248.3						1.6	15	1.3	0.10
VN 12-41	59	59	246.7						1.9	9	1.4	0.11

N_a: number of analyses per sample; N_{zr}: number of zircon grain analyzed per sample; N: number of concordant zircon grain; n: number of analyses used to calculate the maximum deposition age (sedimentary rocks) or emplacement age (magmatic rocks); DL_1: detection limit for at least one grain; DL_3: detection limit for at least three grains; $_{pL}$: probability level assigned to the detection limits; MSWD: mean square of weighted deviates. The MSWD and the probability given for the concordia ages are for both concordance and equivalence.

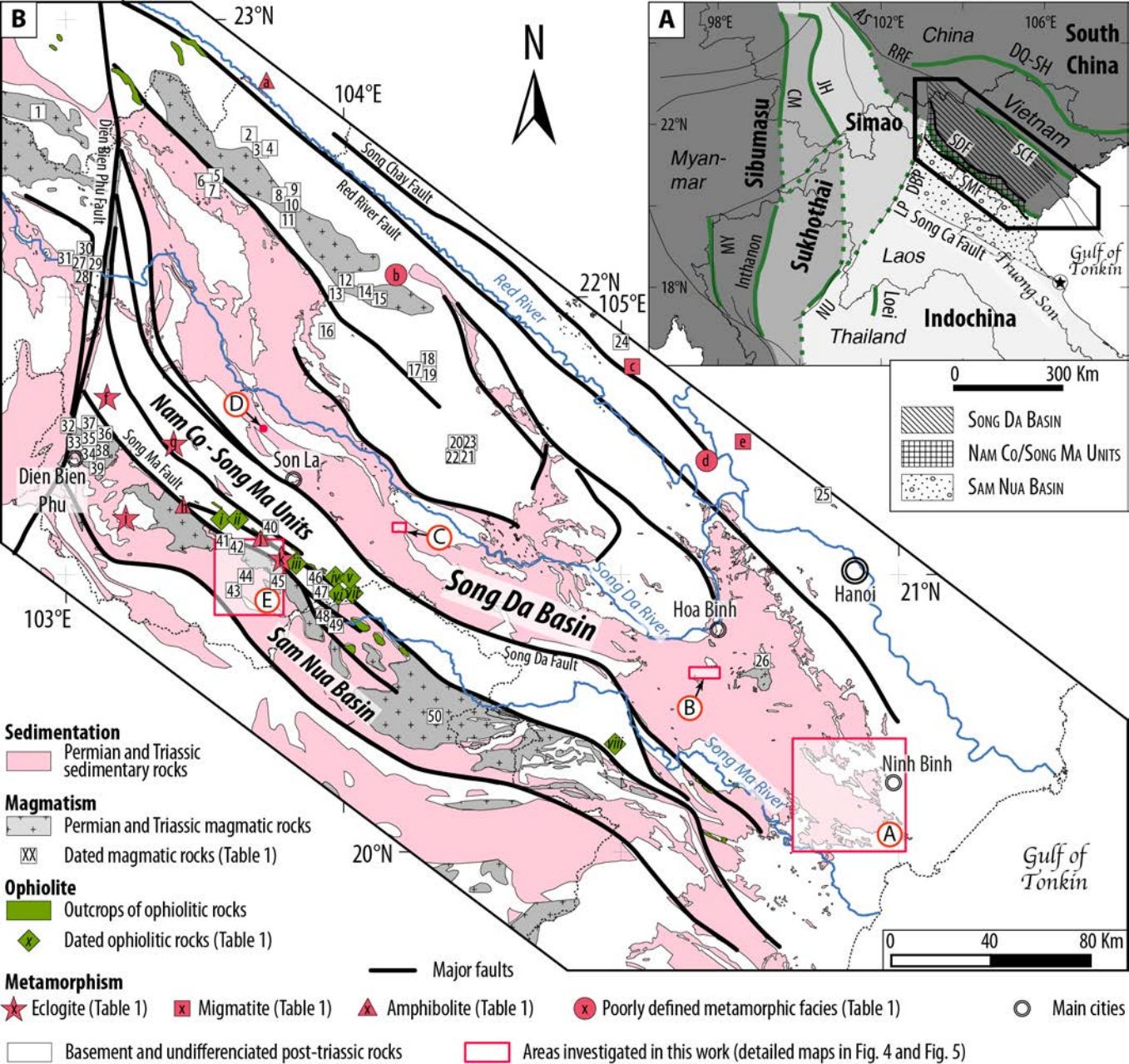
B
A
23°N
104°E
22°N
105°E
21°N
103°E
20°N
N
98°E
102°E
106°E
22°N
18°N
China
South China
Vietnam
Myan-mar
Laos
Thailand
Indochina
Simao
Sibumasu
Sukhothai
Inthanon
Loei
JH
CM
MY
NU
RRF
DQ-SH
AS
SDF
SCF
SMF
DBF
LP
Song Ca Fault
Truong Son
Gulf of Tonkin
0 300 Km
Song Da Basin
Nam Co/Song Ma Units
Sam Nua Basin
Dien Bien Phu Fault
Song Chay Fault
Red River Fault
Red River
Nam Co - Song Ma Units
Song Ma Fault
Son La
Dien Bien Phu
Song Da Basin
Song Da River
Song Da Fault
Sam Nua Basin
Hoa Binh
Hanoi
Ninh Binh
Song Ma River
0 40 80 Km
Sedimentation
Permian and Triassic sedimentary rocks
Magmatism
Permian and Triassic magmatic rocks
XX Dated magmatic rocks (Table 1)
Ophiolite
Outcrops of ophiolitic rocks
x Dated ophiolitic rocks (Table 1)
Major faults
Metamorphism
Eclogite (Table 1)
x Migmatite (Table 1)
x Amphibolite (Table 1)
x Poorly defined metamorphic facies (Table 1)
Main cities
Basement and undifferenciated post-triassic rocks
Areas investigated in this work (detailed maps in Fig. 4 and Fig. 5)

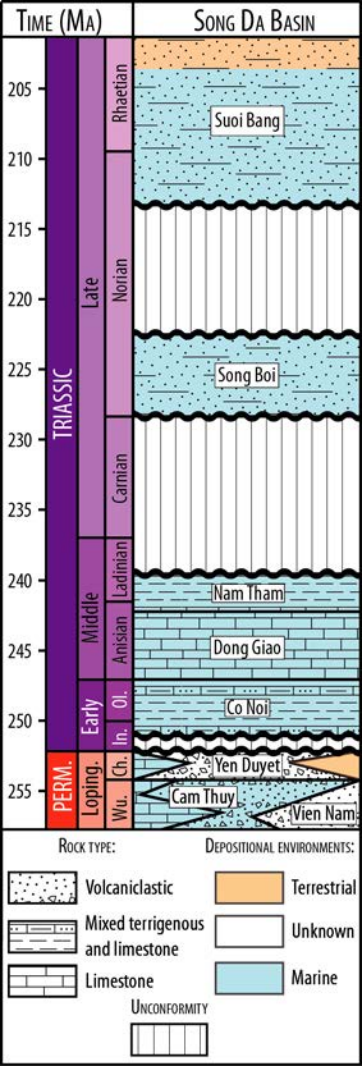
Time (Ma)
Song Da Basin
205
210
215
220
225
230
235
240
245
250
255
TRIASSIC
PERM.
Early
Middle
Late
Loping.
Wu.
Ch.
In.
Ol.
Anisian
Ladinian
Carnian
Norian
Rhaetian
Suoi Bang
Song Boi
Nam Tham
Dong Giao
Co Noi
Yen Duyet
Cam Thuy
Vien Nam
Rock type:
Volcaniclastic
Mixed terrigenous and limestone
Limestone
Unconformity
Depositional environments:
Terrestrial
Unknown
Marine

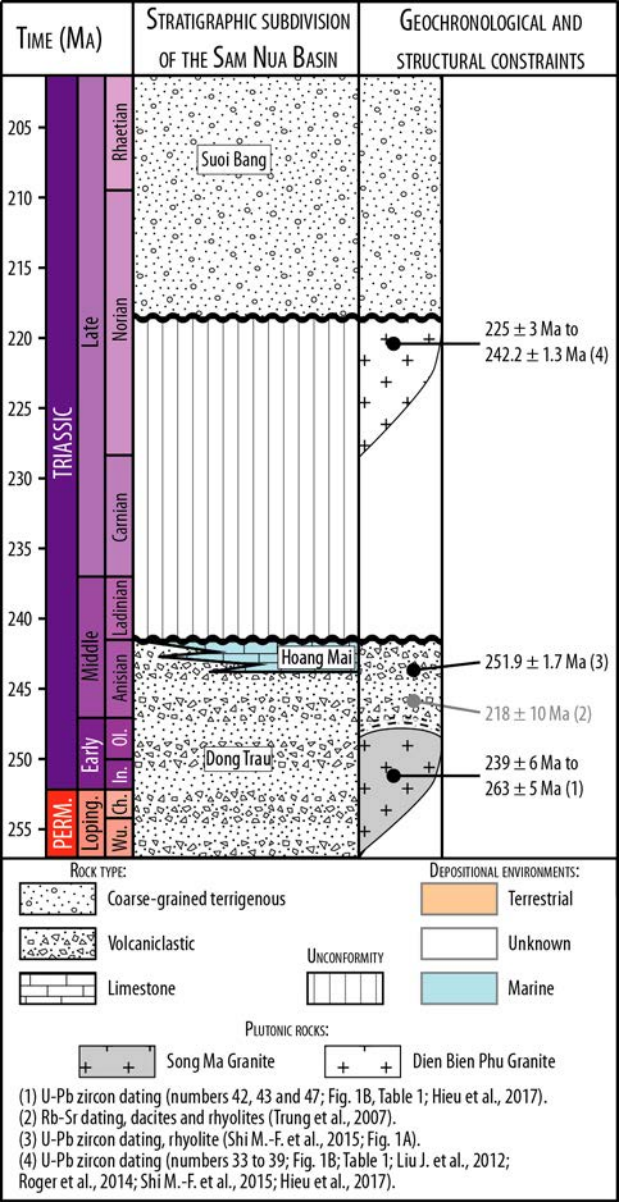

(1) U-Pb zircon dating (numbers 42, 43 and 47; Fig. 1B, Table 1; Hieu et al., 2017).
(2) Rb-Sr dating, dacites and rhyolites (Trung et al., 2007).
(3) U-Pb zircon dating, rhyolite (Shi M.-F. et al., 2015; Fig. 1A).
(4) U-Pb zircon dating (numbers 33 to 39; Fig. 1B; Table 1; Liu J. et al., 2012; Roger et al., 2014; Shi M.-F. et al., 2015; Hieu et al., 2017).

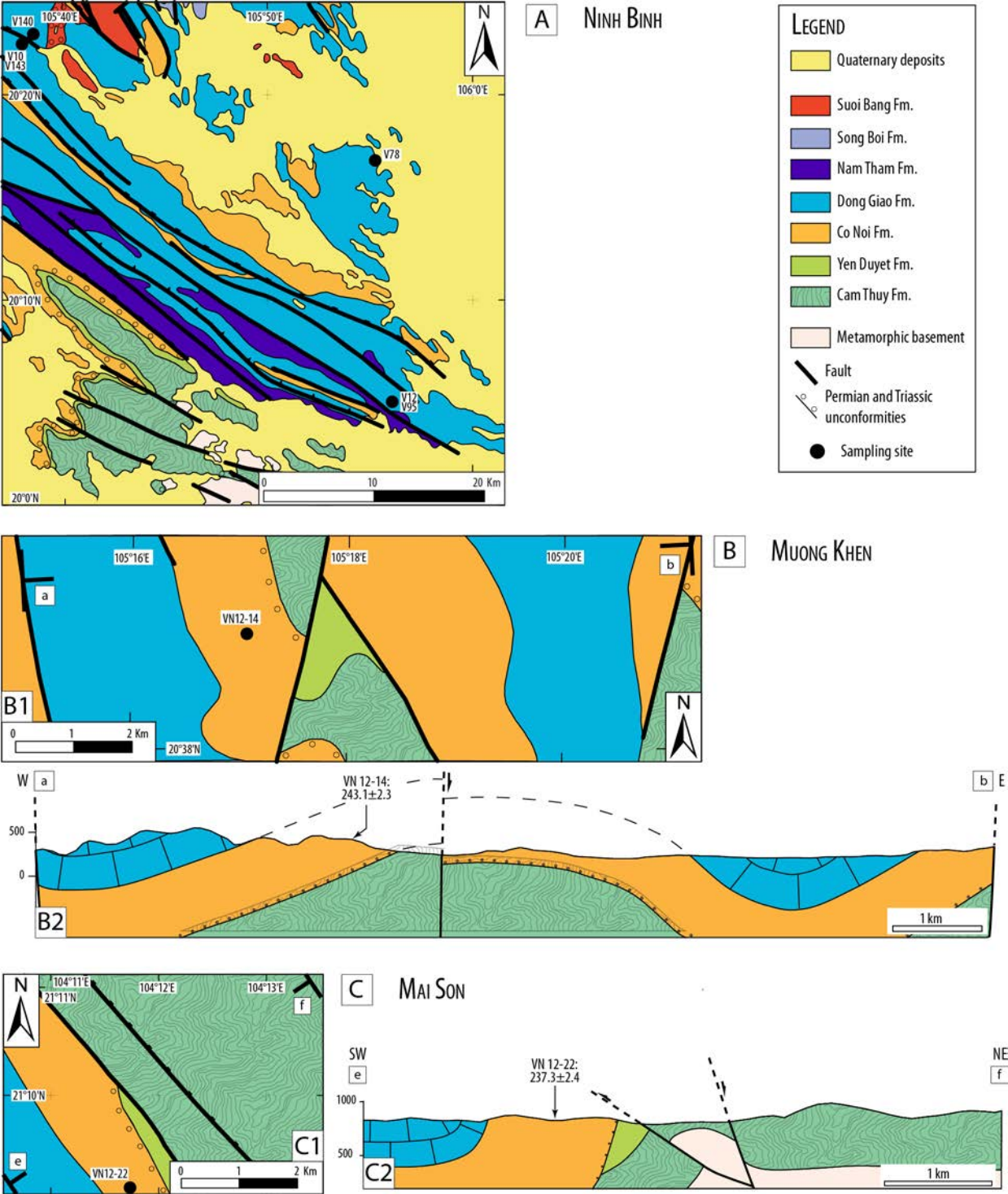
A
Ninh Binh
Legend
Quaternary deposits
Suoi Bang Fm.
Song Boi Fm.
Nam Tham Fm.
Dong Giao Fm.
Co Noi Fm.
Yen Duyet Fm.
Cam Thuy Fm.
Metamorphic basement
Fault
Permian and Triassic unconformities
Sampling site
105°40'E
105°50'E
106°0'E
20°20'N
20°10'N
20°0'N
V140
V10
V143
V78
V12
V95
0
10
20 Km
B
Muong Khen
105°16'E
105°18'E
105°20'E
20°38'N
VN12-14
B1
0
1
2 Km
W
E
VN 12-14:
243.1±2.3
500
0
B2
1 km
C
Mai Son
104°11'E
104°12'E
104°13'E
21°11'N
21°10'N
VN12-22
C1
SW
NE
VN 12-22:
237.3±2.4
1000
500
C2
1 km

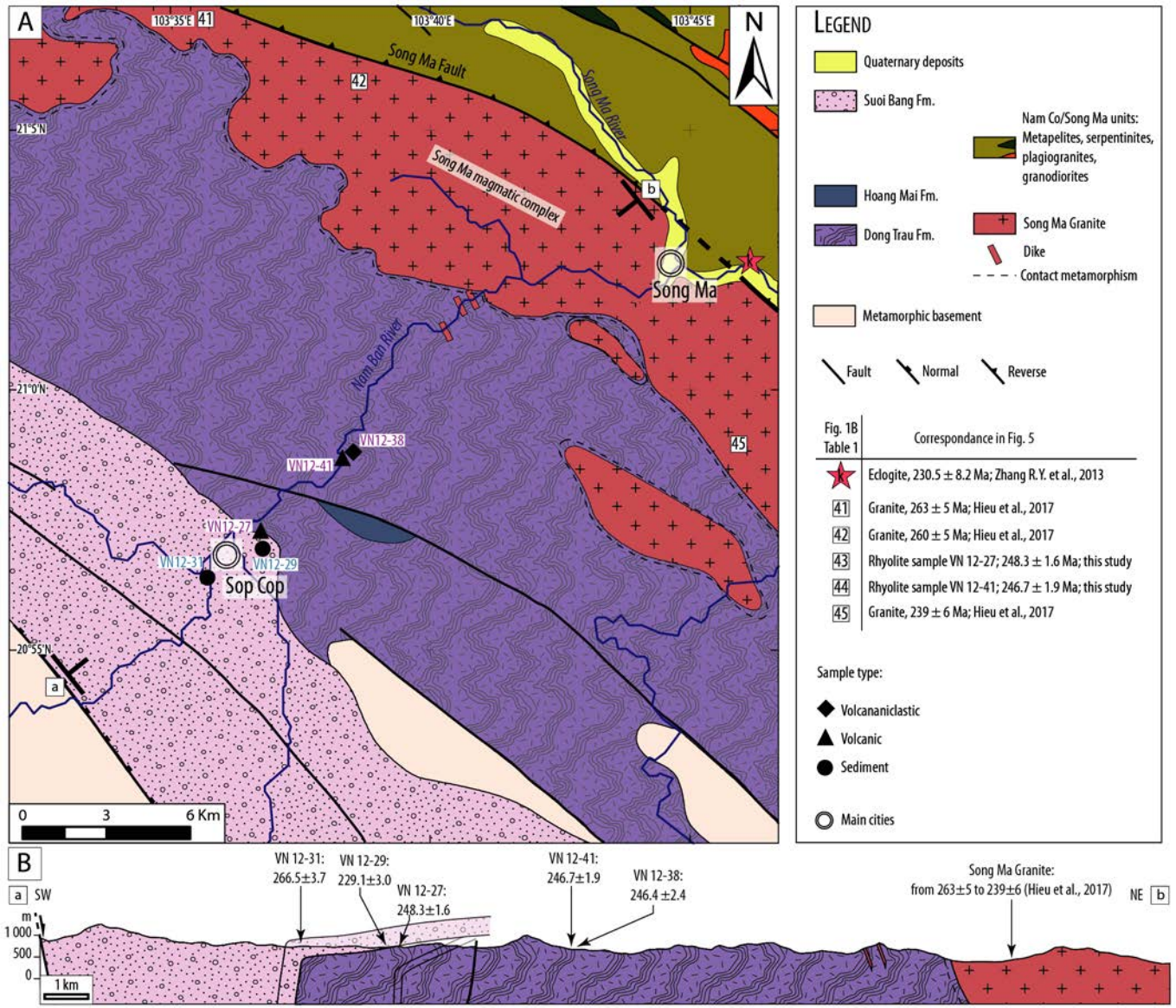
A
103°35'E
103°40'E
103°45'E
21°5'N
21°0'N
20°55'N
41
42
45
Song Ma Fault
Song Ma River
Song Ma magmatic complex
Song Ma
Nam Ban River
VN12-38
VN12-41
VN12-27
VN12-31
VN12-29
Sop Cop
a
b
0
3
6 Km
N
LEGEND
Quaternary deposits
Suoi Bang Fm.
Nam Co/Song Ma units: Metapelites, serpentinites, plagiogranites, granodiorites
Hoang Mai Fm.
Dong Trau Fm.
Song Ma Granite
Dike
Contact metamorphism
Metamorphic basement
Fault
Normal
Reverse
Fig. 1B Table 1
Correspondance in Fig. 5
Eclogite, 230.5 ± 8.2 Ma; Zhang R.Y. et al., 2013
41 Granite, 263 ± 5 Ma; Hieu et al., 2017
42 Granite, 260 ± 5 Ma; Hieu et al., 2017
43 Rhyolite sample VN 12-27; 248.3 ± 1.6 Ma; this study
44 Rhyolite sample VN 12-41; 246.7 ± 1.9 Ma; this study
45 Granite, 239 ± 6 Ma; Hieu et al., 2017
Sample type:
Volcananiclastic
Volcanic
Sediment
Main cities
B
a SW
NE b
m
1 000
500
0
1 km
VN 12-31: 266.5±3.7
VN 12-29: 229.1±3.0
VN 12-27: 248.3±1.6
VN 12-41: 246.7±1.9
VN 12-38: 246.4 ±2.4
Song Ma Granite: from 263±5 to 239±6 (Hieu et al., 2017)

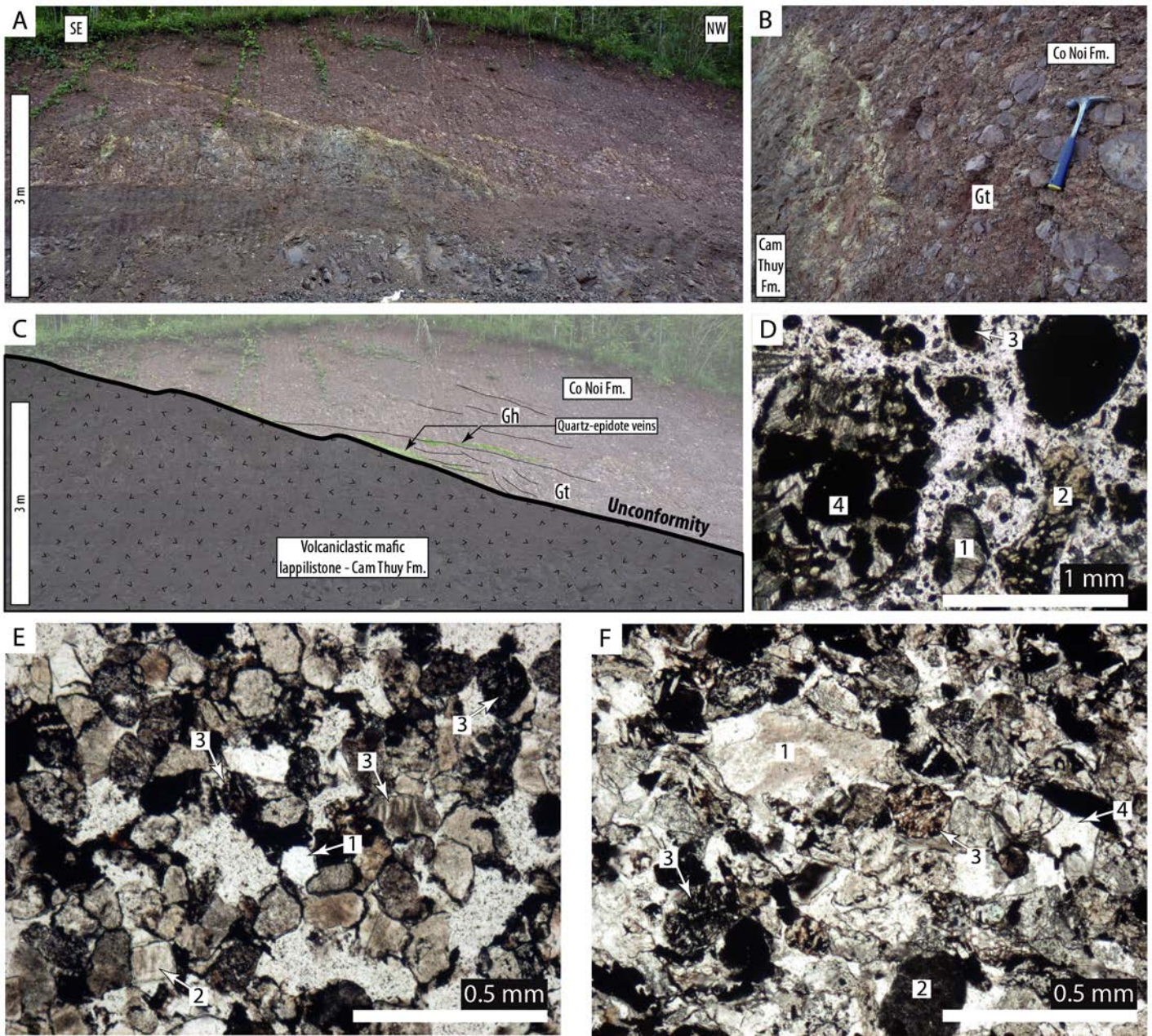
A
SE
NW
3 m
B
Co Noi Fm.
Gt
Cam Thuy Fm.
C
Co Noi Fm.
Gh
Quartz-epidote veins
Gt
Unconformity
Volcaniclastic mafic lappilistone - Cam Thuy Fm.
3 m
D
3
4
2
1
1 mm
E
3
3
3
1
2
0.5 mm
F
1
4
3
3
2
0.5 mm

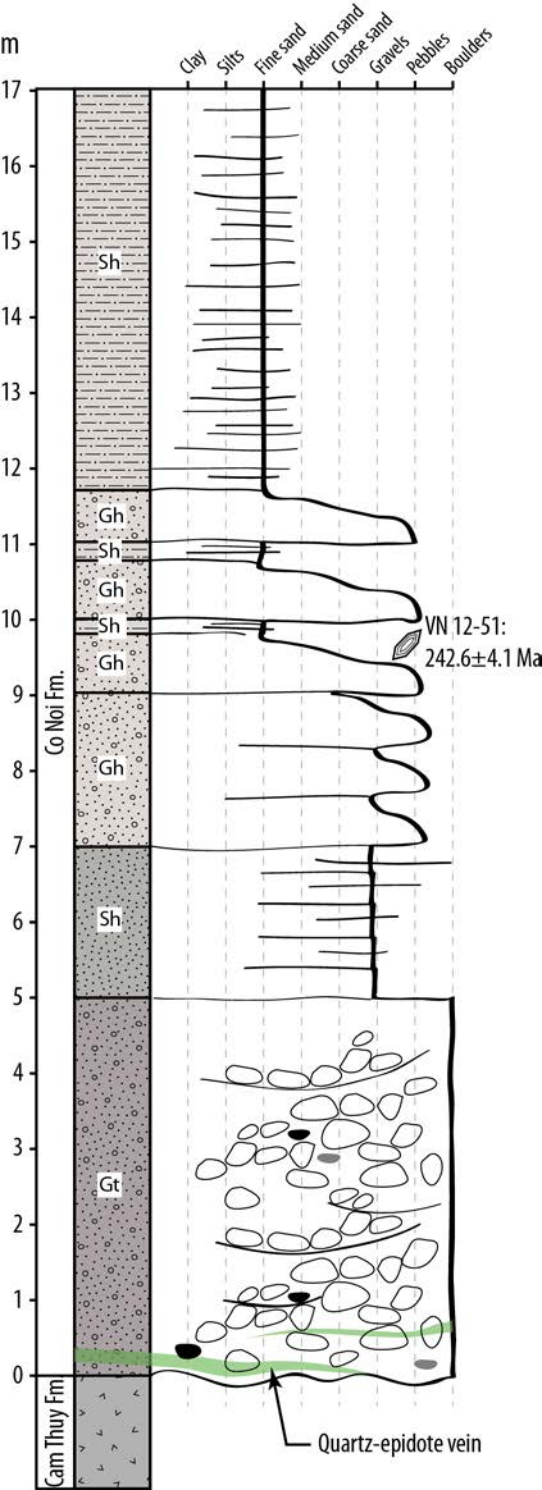
m
Clay
Silts
Fine sand
Medium sand
Coarse sand
Gravels
Pebbles
Boulders
17
16
15
14
13
12
11
10
9
8
7
6
5
4
3
2
1
0
Co Noi Fm.
Cam Thuy Fm
Sh
Gh
Sh
Gh
Sh
Gh
Gh
Sh
Gt
VN 12-51:
242.6±4.1 Ma
Quartz-epidote vein

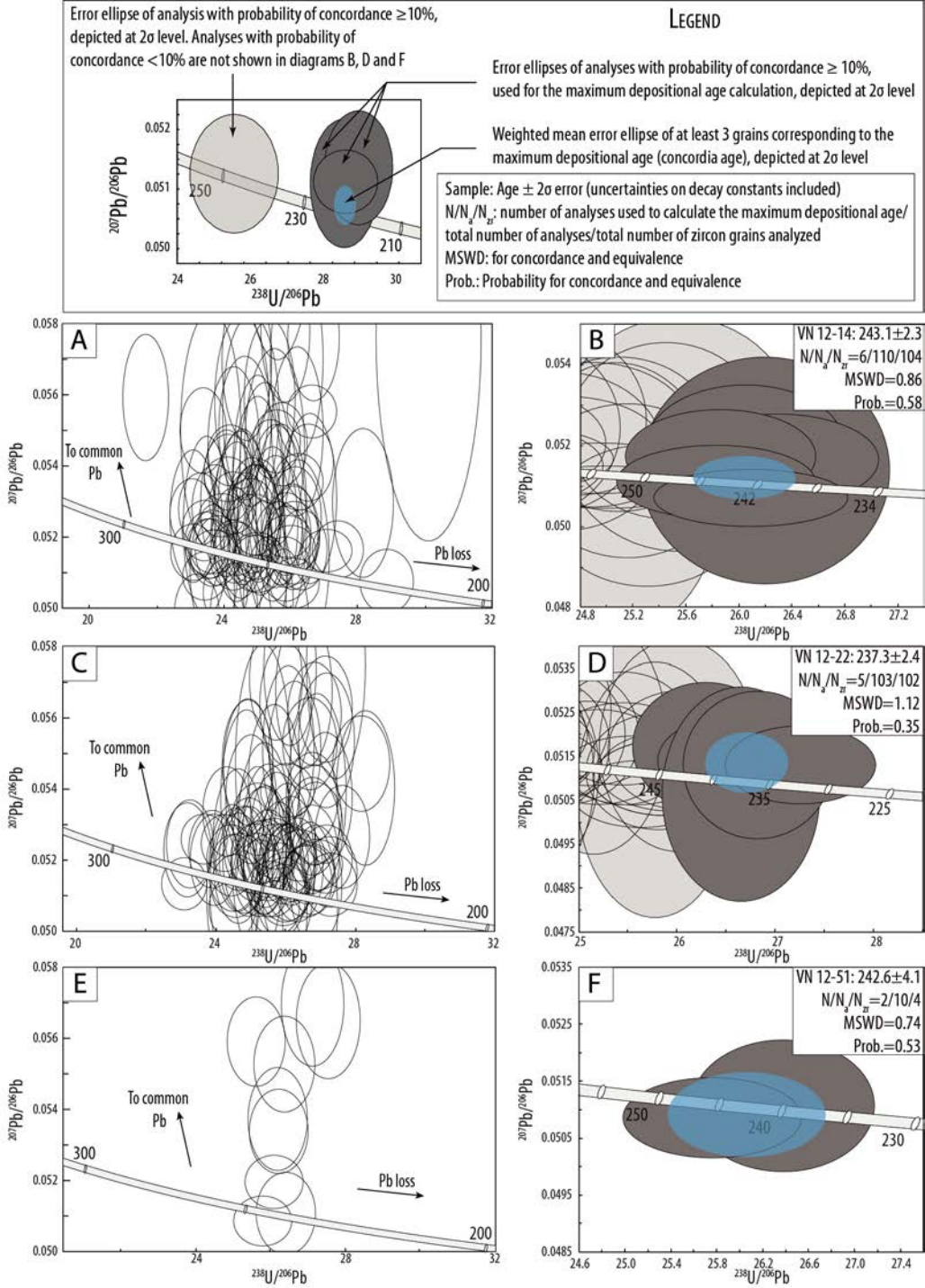
Error ellipse of analysis with probability of concordance ≥10%, depicted at 2σ level. Analyses with probability of concordance <10% are not shown in diagrams B, D and F
LEGEND
Error ellipses of analyses with probability of concordance ≥ 10%, used for the maximum depositional age calculation, depicted at 2σ level
Weighted mean error ellipse of at least 3 grains corresponding to the maximum depositional age (concordia age), depicted at 2σ level
Sample: Age ± 2σ error (uncertainties on decay constants included)
N/N_a/N_zi: number of analyses used to calculate the maximum depositional age/ total number of analyses/total number of zircon grains analyzed
MSWD: for concordance and equivalence
Prob.: Probability for concordance and equivalence
207Pb/206Pb
238U/206Pb
A
To common Pb
Pb loss
300
200
B
VN 12-14: 243.1±2.3
N/N_a/N_zi=6/110/104
MSWD=0.86
Prob.=0.58
250
242
234
C
D
VN 12-22: 237.3±2.4
N/N_a/N_zi=5/103/102
MSWD=1.12
Prob.=0.35
245
235
225
E
F
VN 12-51: 242.6±4.1
N/N_a/N_zi=2/10/4
MSWD=0.74
Prob.=0.53
250
240
230

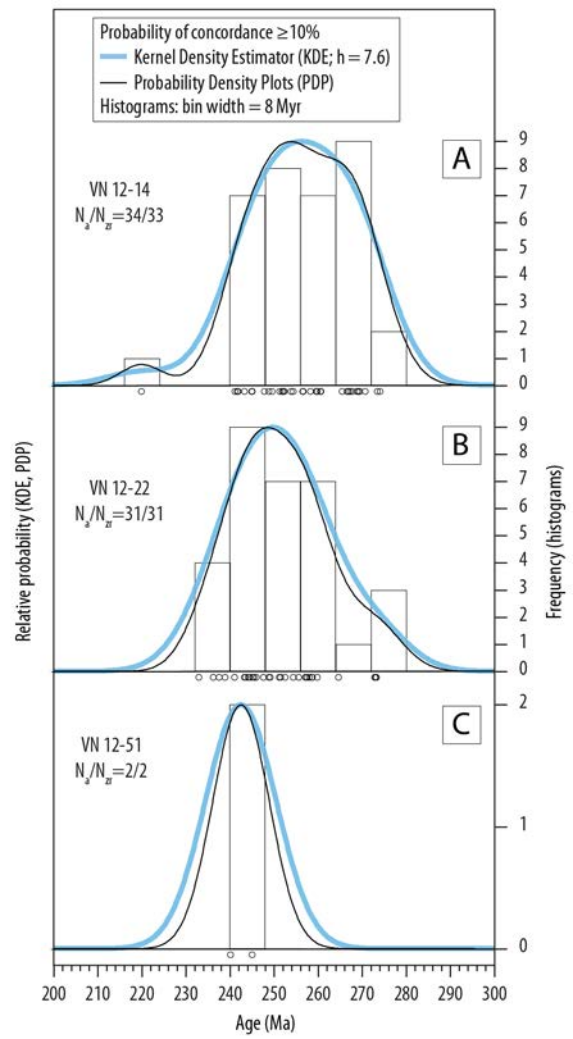
Probability of concordance ≥10%
Kernel Density Estimator (KDE; h = 7.6)
Probability Density Plots (PDP)
Histograms: bin width = 8 Myr
A
VN 12-14
N_a/N_zi=34/33
B
VN 12-22
N_a/N_zi=31/31
C
VN 12-51
N_a/N_zi=2/2
Relative probability (KDE, PDP)
Frequency (histograms)
Age (Ma)
200 210 220 230 240 250 260 270 280 290 300

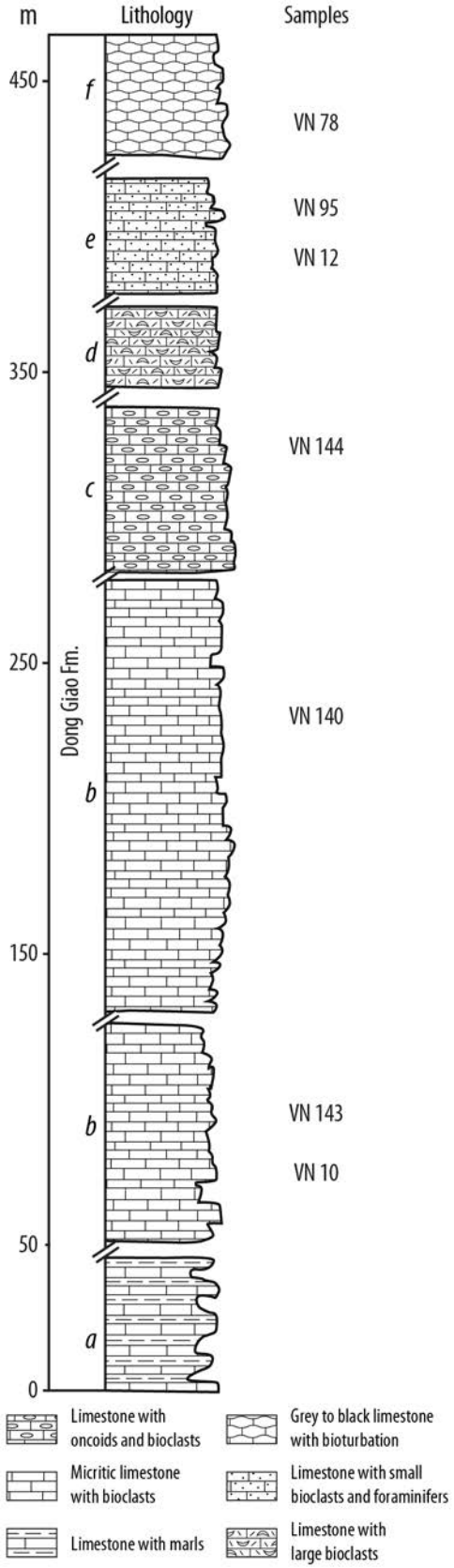
m
Lithology
Samples
450
350
250
150
50
0
f
e
d
c
b
b
a
Dong Giao Fm.
VN 78
VN 95
VN 12
VN 144
VN 140
VN 143
VN 10
Limestone with oncoids and bioclasts
Micritic limestone with bioclasts
Limestone with marls
Grey to black limestone with bioturbation
Limestone with small bioclasts and foraminifers
Limestone with large bioclasts

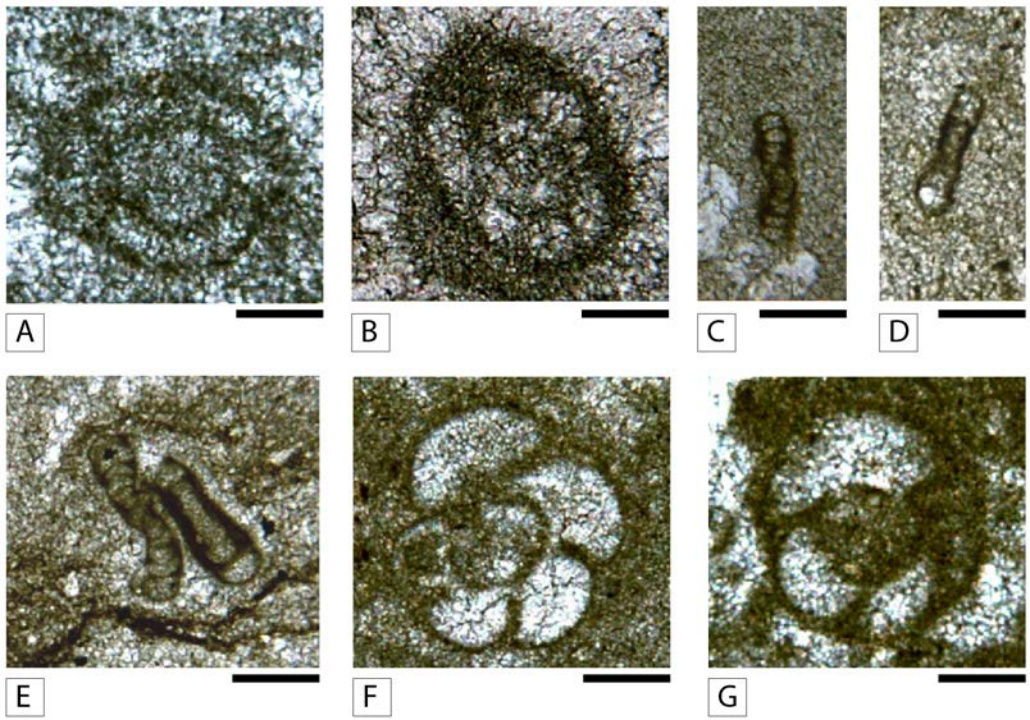
A
B
C
D
E
F
G

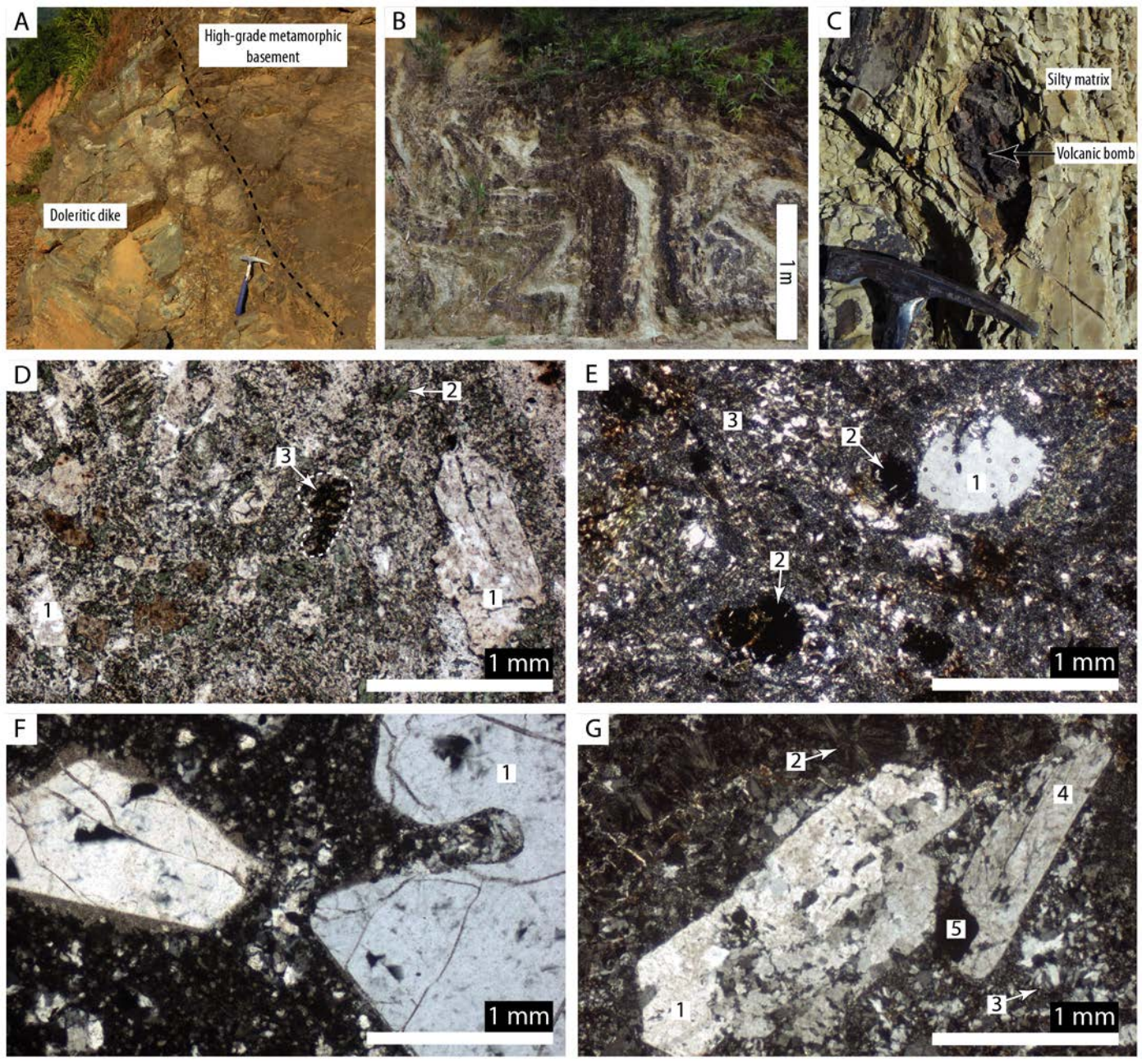
A
High-grade metamorphic basement
Doleritic dike
B
1 m
C
Silty matrix
Volcanic bomb
D
1
2
3
1
1 mm
E
3
2
1
2
1 mm
F
1
1 mm
G
2
4
5
1
3
1 mm

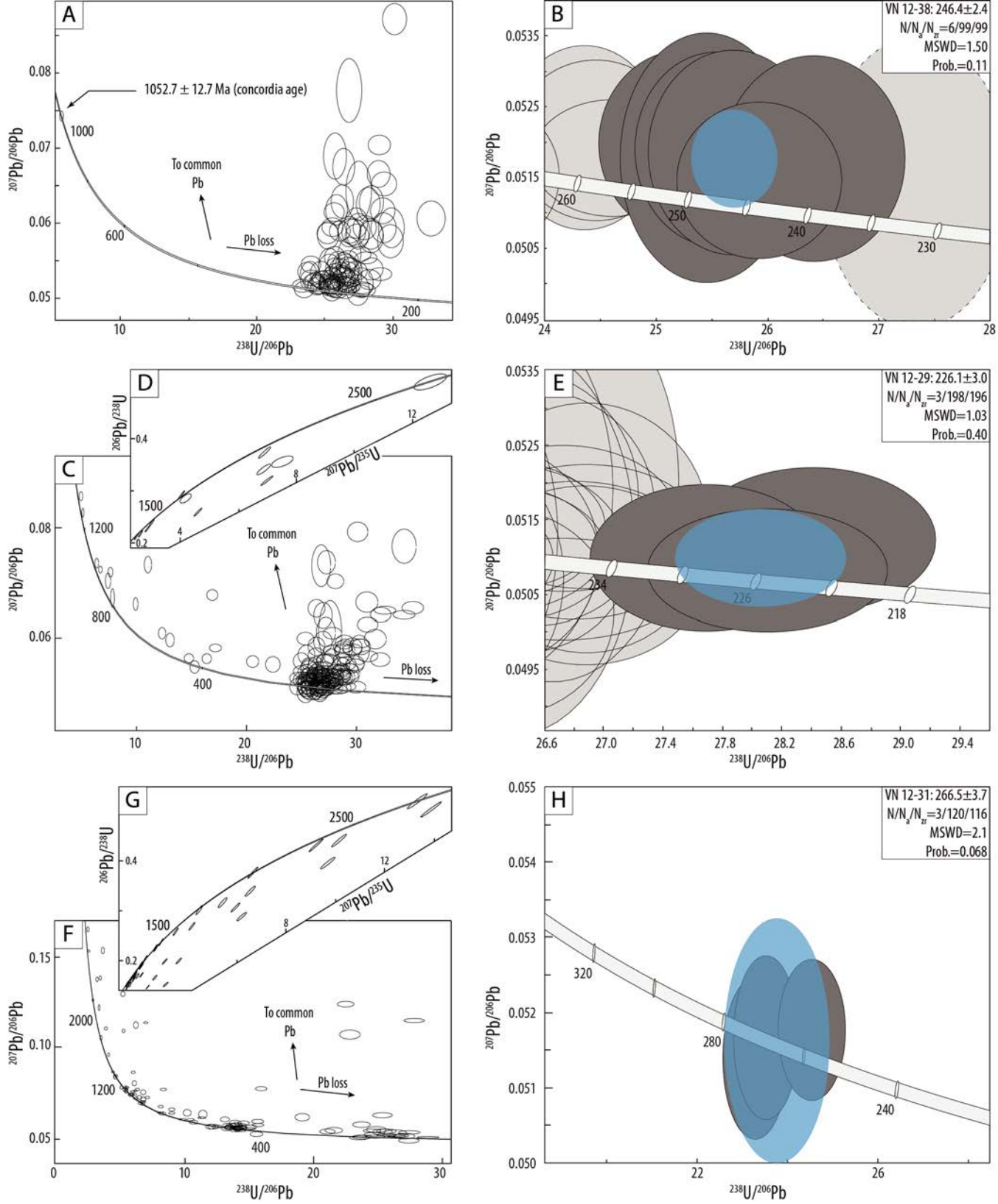
A
1052.7 ± 12.7 Ma (concordia age)
1000
600
200
To common Pb
Pb loss
$^{207}Pb/^{206}Pb$
$^{238}U/^{206}Pb$
B
VN 12-38: 246.4±2.4
$N/N_a/N_{zr}$=6/99/99
MSWD=1.50
Prob.=0.11
260
250
240
230
C
D
1200
800
400
1500
2500
$^{206}Pb/^{238}U$
$^{207}Pb/^{235}U$
E
VN 12-29: 226.1±3.0
$N/N_a/N_{zr}$=3/198/196
MSWD=1.03
Prob.=0.40
234
226
218
F
G
2000
1200
400
1500
2500
H
VN 12-31: 266.5±3.7
$N/N_a/N_{zr}$=3/120/116
MSWD=2.1
Prob.=0.068
320
280
240

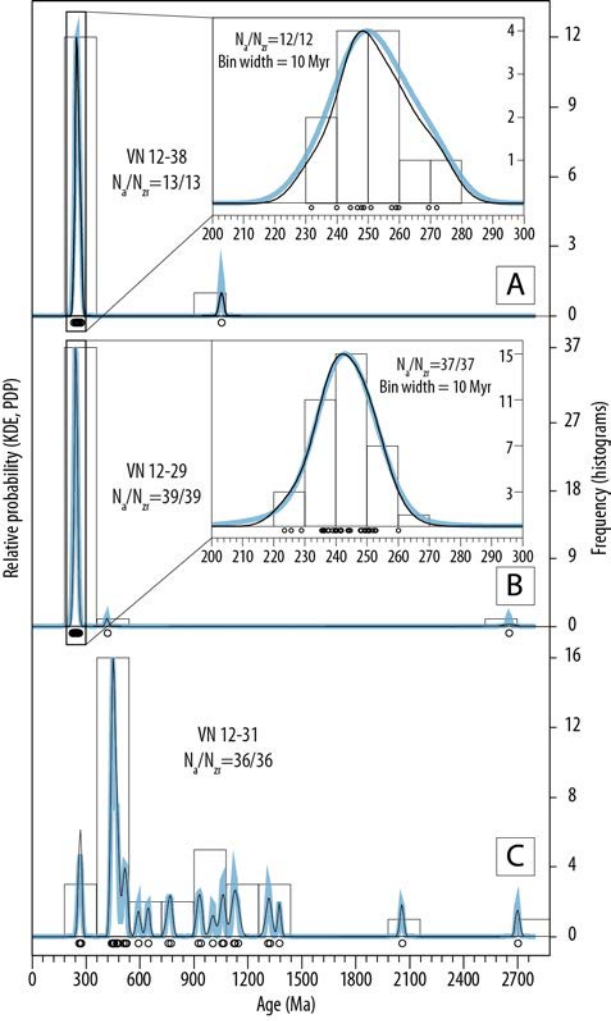

Probability of concordance ≥10%
Kernel Density Estimator (KDE; h = 7.6)
Probability Density Plots (PDP)
Histograms: bin width = 180 Myr

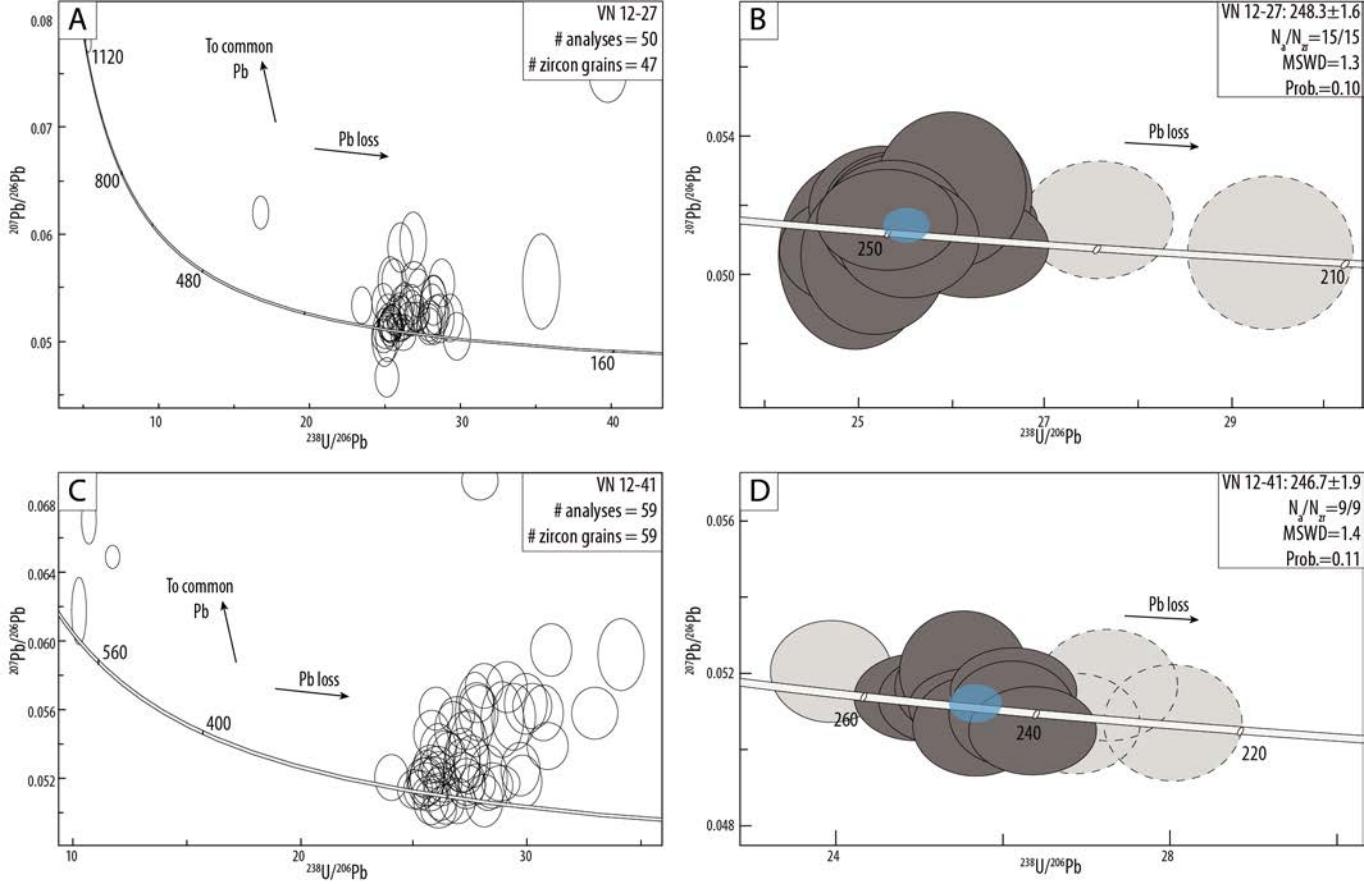
A
VN 12-27
analyses = 50
zircon grains = 47
To common Pb
Pb loss
1120
800
480
160
$^{207}Pb/^{206}Pb$
$^{238}U/^{206}Pb$
B
VN 12-27: 248.3±1.6
N_a/N_{zr}=15/15
MSWD=1.3
Prob.=0.10
Pb loss
250
210
$^{207}Pb/^{206}Pb$
$^{238}U/^{206}Pb$
C
VN 12-41
analyses = 59
zircon grains = 59
To common Pb
Pb loss
560
400
$^{207}Pb/^{206}Pb$
$^{238}U/^{206}Pb$
D
VN 12-41: 246.7±1.9
N_a/N_{zr}=9/9
MSWD=1.4
Prob.=0.11
Pb loss
260
240
220
$^{207}Pb/^{206}Pb$
$^{238}U/^{206}Pb$

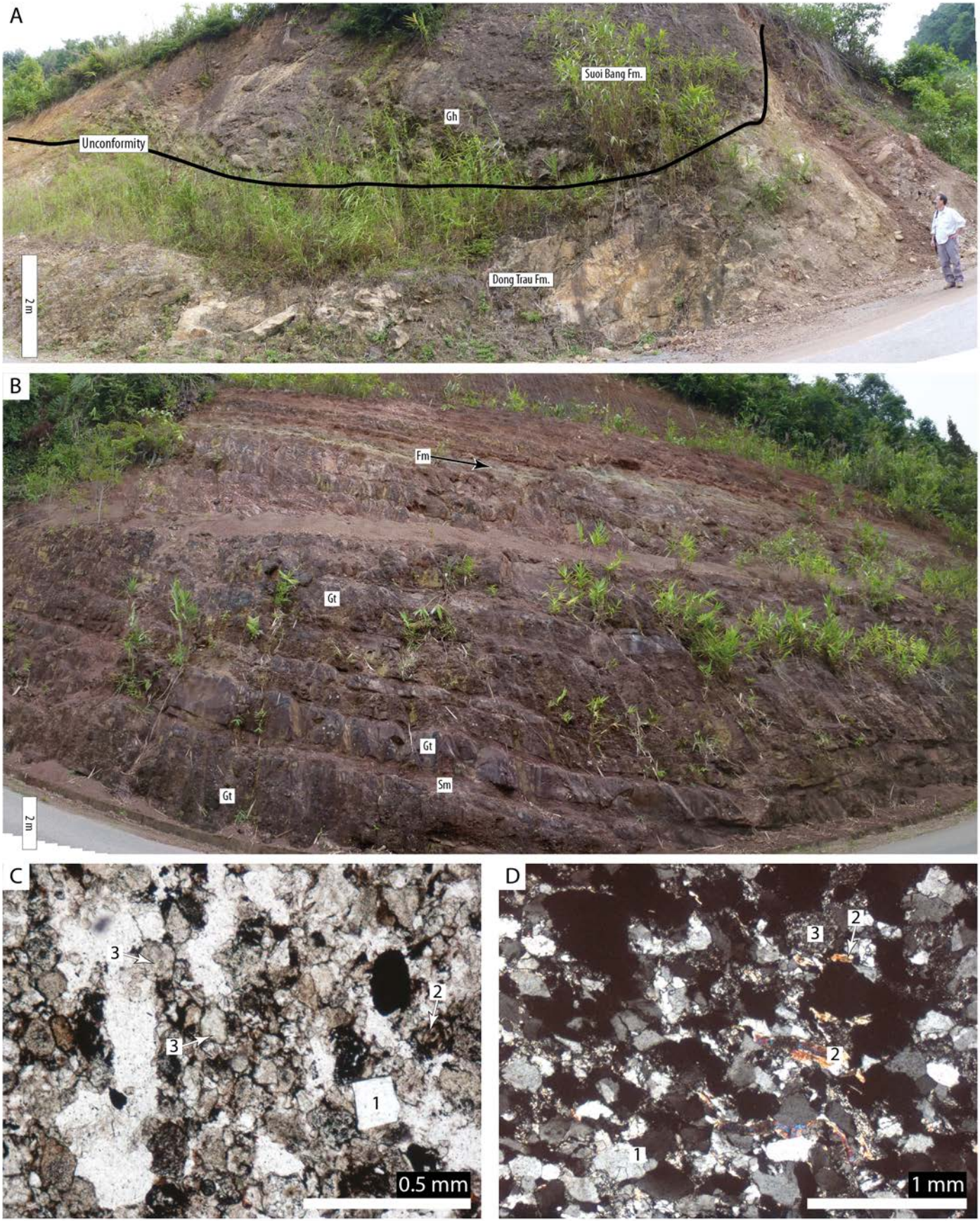
A
Suoi Bang Fm.
Gh
Unconformity
Dong Trau Fm.
2 m
B
Fm
Gt
Gt
Sm
Gt
2 m
C
3
2
3
1
0.5 mm
D
3
2
2
1
1 mm

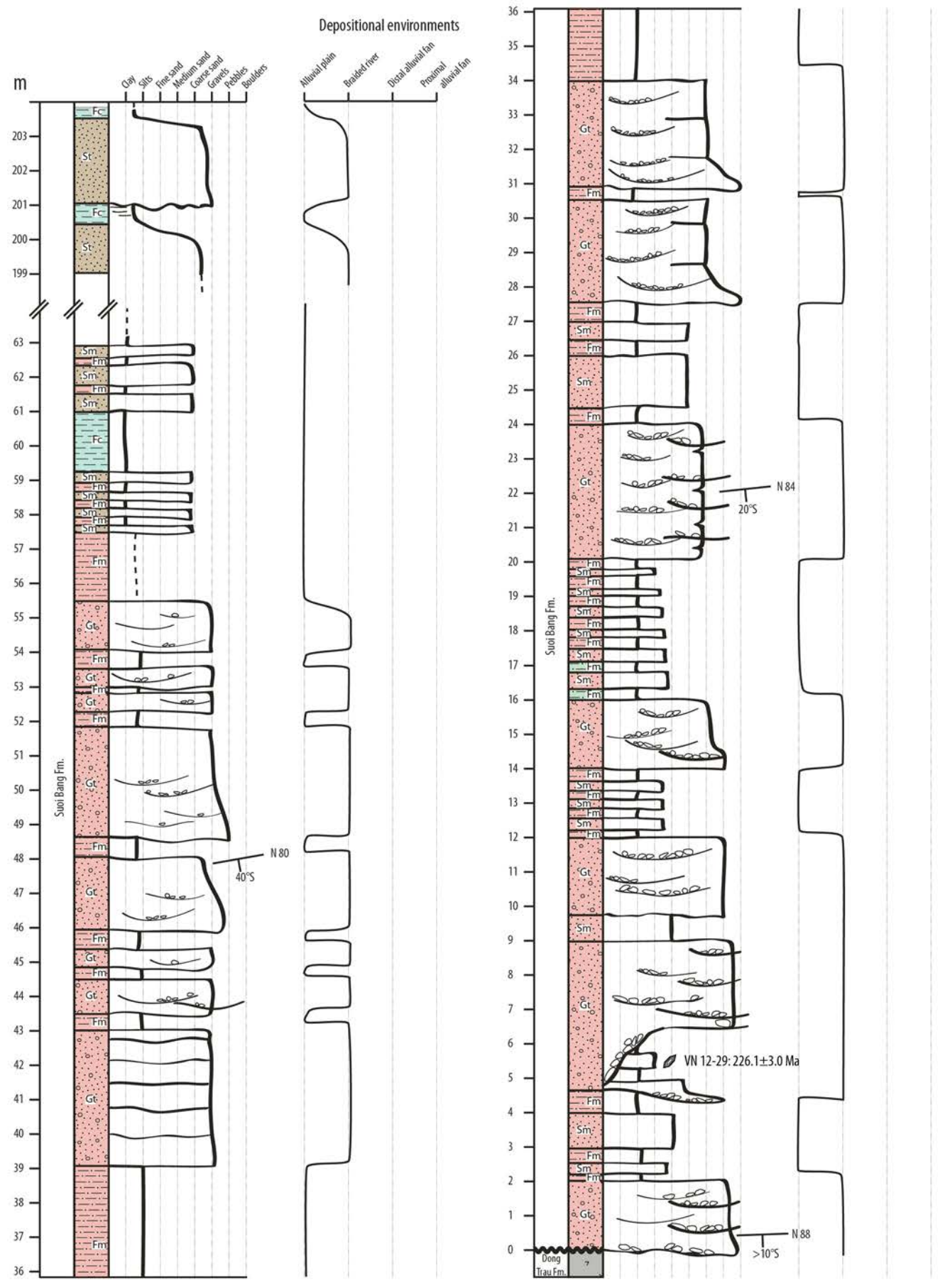
Depositional environments
Clay
Silts
Fine sand
Medium sand
Coarse sand
Gravels
Pebbles
Boulders
Alluvial plain
Braided river
Distal alluvial fan
Proximal alluvial fan
m
Suoi Bang Fm.
Dong Trau Fm.
N 80
40°S
N 84
20°S
N 88
>10°S
VN 12-29: 226.1±3.0 Ma

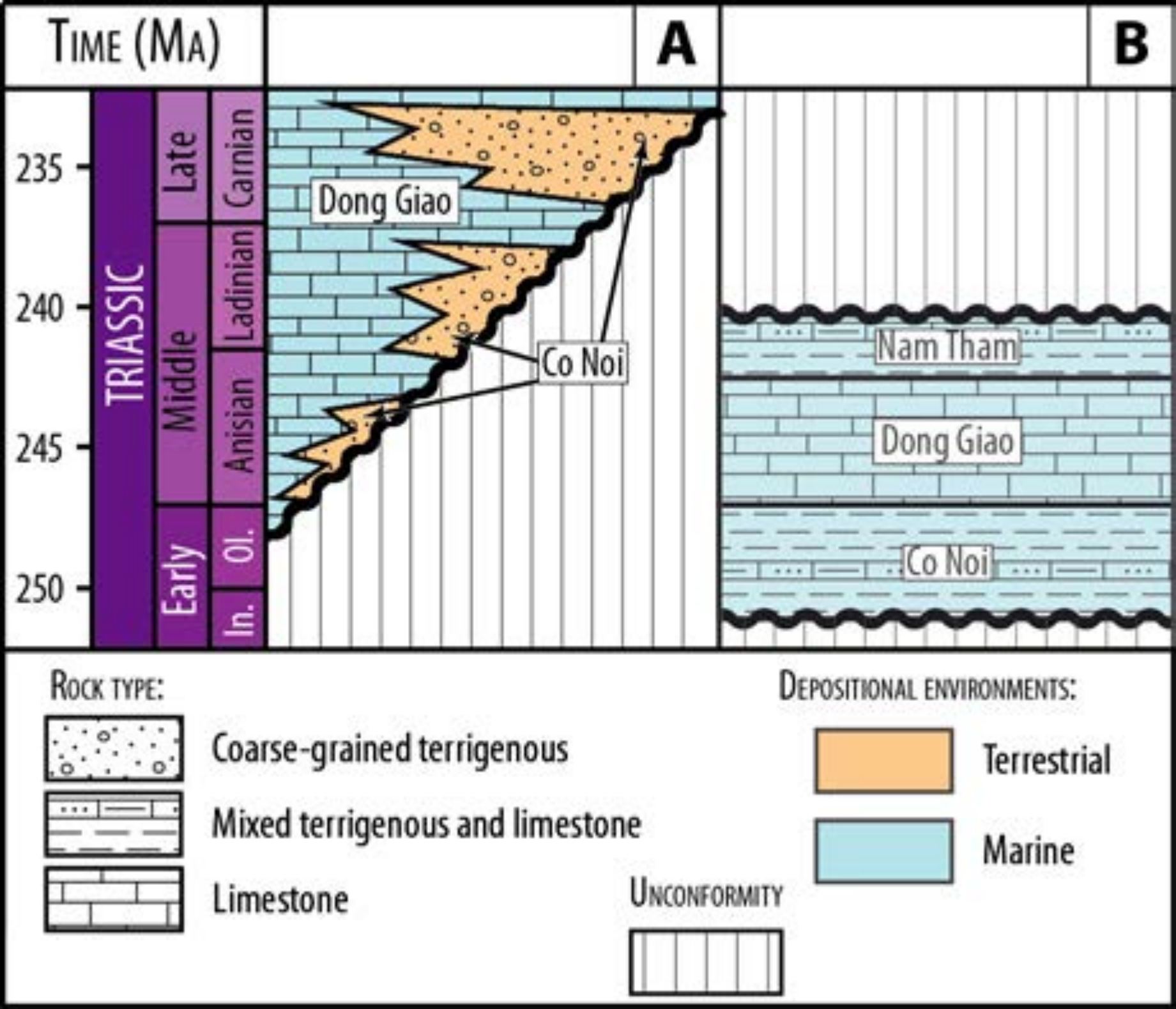
Time (Ma)
A
B
235
240
245
250
TRIASSIC
Late
Middle
Early
Carnian
Ladinian
Anisian
Ol.
In.
Dong Giao
Co Noi
Nam Tham
Dong Giao
Co Noi
Rock type:
Coarse-grained terrigenous
Mixed terrigenous and limestone
Limestone
Unconformity
Depositional environments:
Terrestrial
Marine

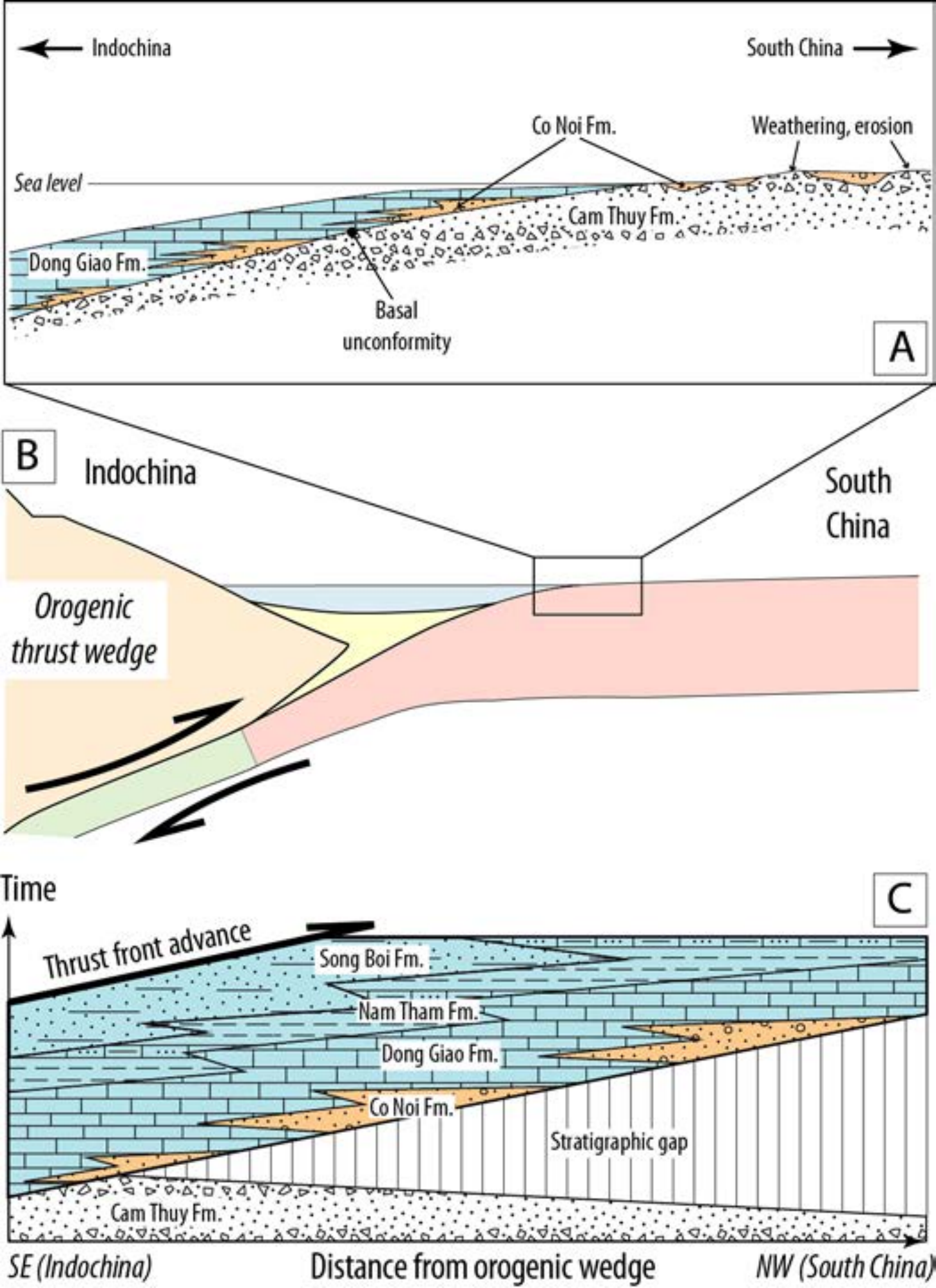
Indochina
South China
Co Noi Fm.
Weathering, erosion
Sea level
Cam Thuy Fm.
Dong Giao Fm.
Basal
unconformity
A
B
Indochina
South
China
Orogenic
thrust wedge
Time
C
Thrust front advance
Song Boi Fm.
Nam Tham Fm.
Dong Giao Fm.
Co Noi Fm.
Stratigraphic gap
Cam Thuy Fm.
SE (Indochina)
Distance from orogenic wedge
NW (South China)

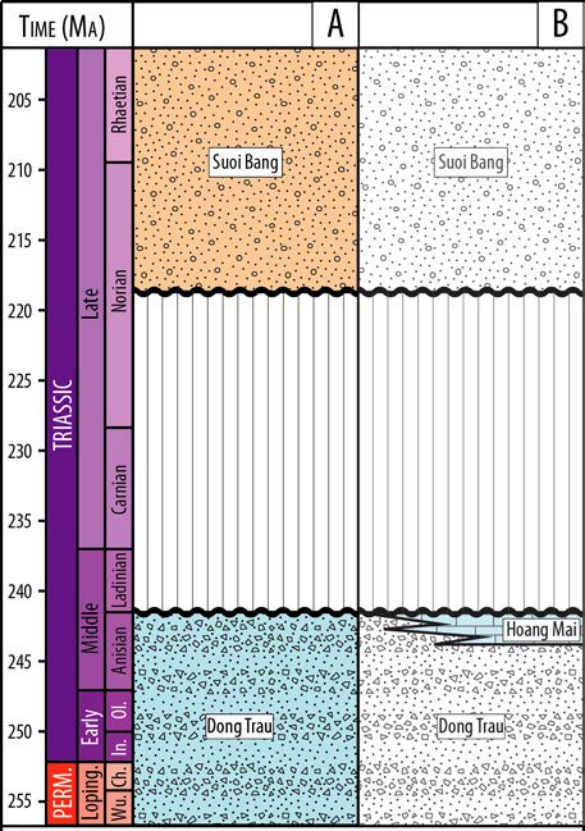
Time (Ma)
A
B
205
210
215
220
225
230
235
240
245
250
255
TRIASSIC
PERM.
Loping.
Wu.
Ch.
Early
In.
Ol.
Middle
Anisian
Ladinian
Late
Carnian
Norian
Rhaetian
Suoi Bang
Suoi Bang
Hoang Mai
Dong Trau
Dong Trau
Rock type:
Coarse-grained terrigenous
Volcaniclastic
Unconformity
Depositional environments:
Terrestrial
Unknown
Marine

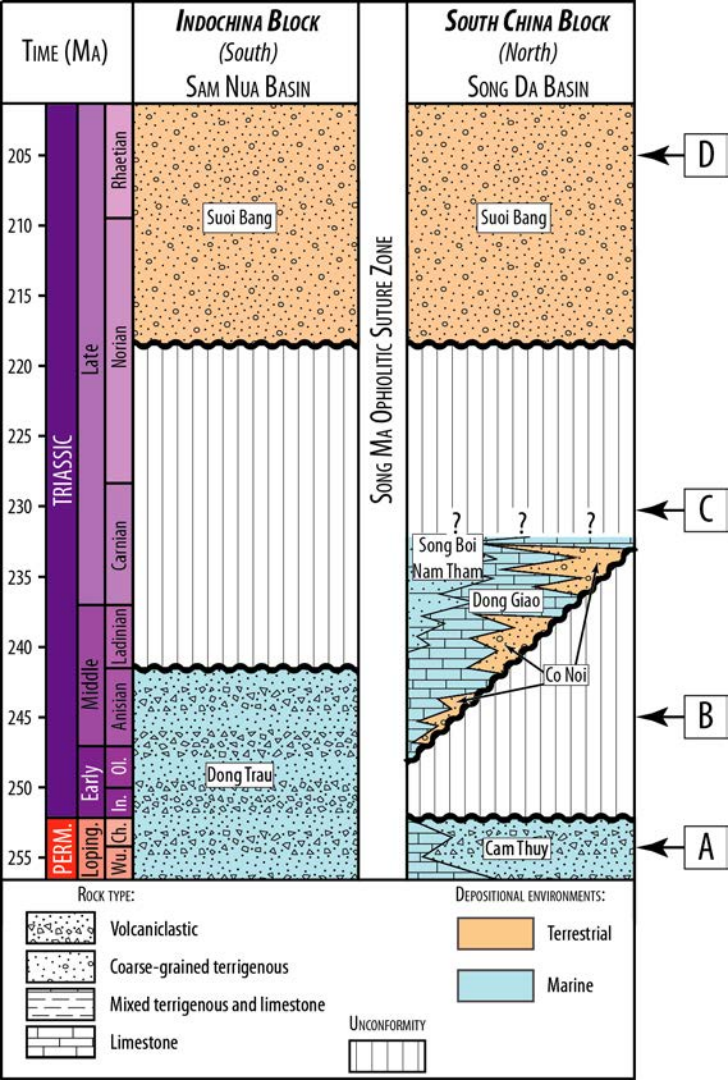
Time (Ma)
Indochina Block
(South)
Sam Nua Basin
South China Block
(North)
Song Da Basin
Song Ma Ophiolitic Suture Zone
TRIASSIC
PERM.
Loping.
Wu.
Ch.
Early
In.
Ol.
Middle
Anisian
Ladinian
Late
Carnian
Norian
Rhaetian
205
210
215
220
225
230
235
240
245
250
255
Suoi Bang
Suoi Bang
Dong Trau
Song Boi
Nam Tham
Dong Giao
Co Noi
Cam Thuy
?
?
?
D
C
B
A
Rock type:
Volcaniclastic
Coarse-grained terrigenous
Mixed terrigenous and limestone
Limestone
Unconformity
Depositional environments:
Terrestrial
Marine

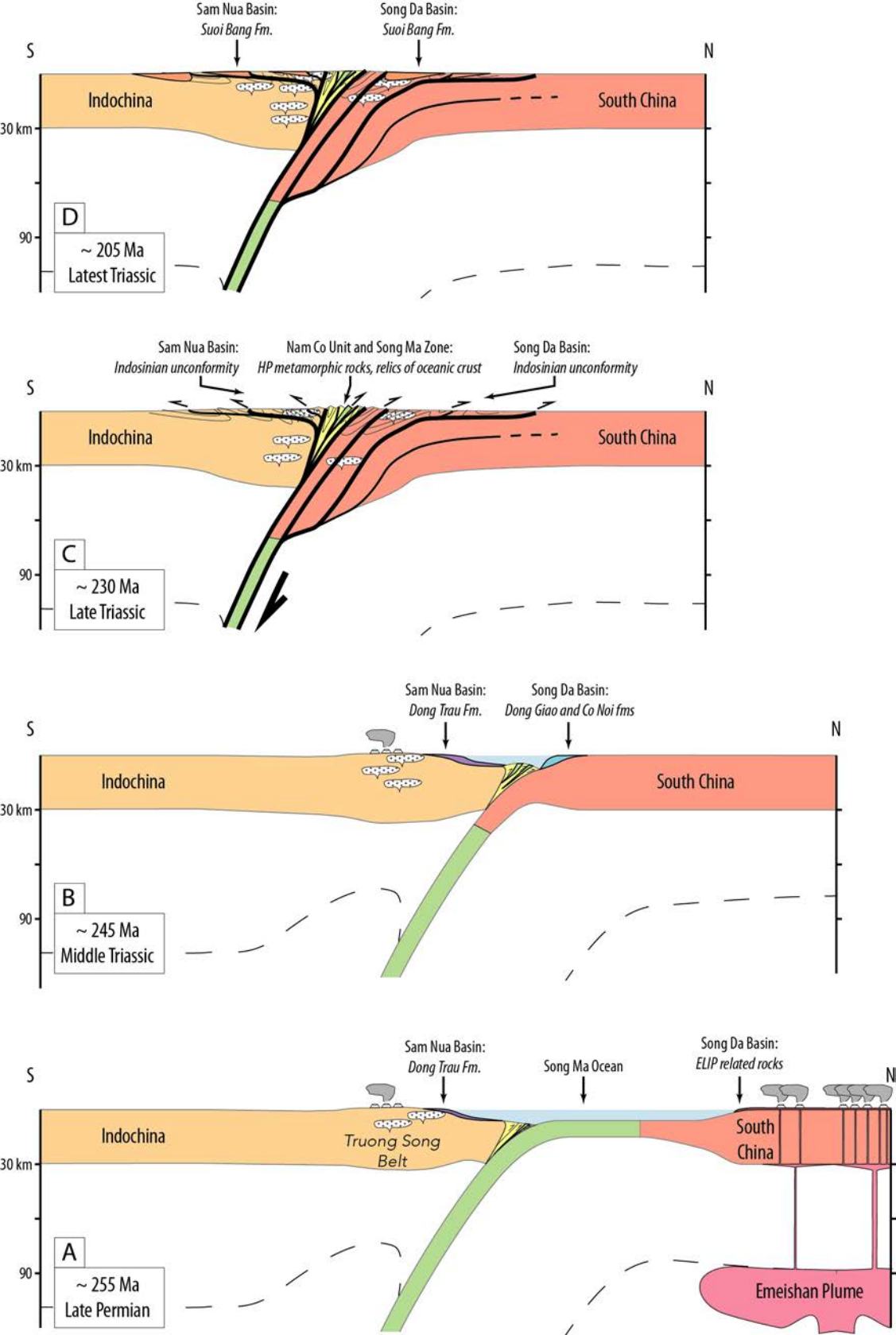
Sam Nua Basin:
Suoi Bang Fm.
Song Da Basin:
Suoi Bang Fm.
S
N
Indochina
South China
30 km
90
D
~ 205 Ma
Latest Triassic
Sam Nua Basin:
Indosinian unconformity
Nam Co Unit and Song Ma Zone:
HP metamorphic rocks, relics of oceanic crust
Song Da Basin:
Indosinian unconformity
S
N
Indochina
South China
30 km
90
C
~ 230 Ma
Late Triassic
Sam Nua Basin:
Dong Trau Fm.
Song Da Basin:
Dong Giao and Co Noi fms
S
N
Indochina
South China
30 km
90
B
~ 245 Ma
Middle Triassic
Sam Nua Basin:
Dong Trau Fm.
Song Ma Ocean
Song Da Basin:
ELIP related rocks
S
N
Indochina
Truong Song
Belt
South
China
30 km
90
A
~ 255 Ma
Late Permian
Emeishan Plume

Highlights

- Revised Triassic stratigraphy for the Song Da and Sam Nua basins
- Song Da and Sam Nua basins: foreland basins during the Triassic
- The Song Da and Sam Nua basins document the South China – Indochina collision